DOCTOR OF PHILOSOPHY

Metabolic regulation in Phosphatase and tensin homologue (PTEN) null T cell lymphoma/leukaemia cells

Grzes, Katarzyna Maria

Award date:
2015

Metabolic regulation in Phosphatase and tensin homologue (PTEN) null T cell lymphoma/leukaemia cells

Katarzyna Maria Grzes

This thesis is submitted
for the degree of
Doctor of Philosophy (Ph.D.)
to the University of Dundee

September 2015

Contents

List of figures

List of tables

Declaration

Candidate:

The candidate is the author of the thesis; that, unless otherwise stated, all references cited have been consulted by the candidate; that the work of which the thesis is a record has been done by the candidate and that it has not been previously accepted for a higher degree. Provided that if the thesis is based upon joint research, the nature and extent of the candidate's individual contribution shall be defined.

…….....

Katarzyna Maria Grzes

Supervisor:

I certify that the conditions of the relevant Ordinance and Regulations have been fulfilled.

…….

Professor Doreen Cantrell

Acknowledgements

First of all, I would like to thank my supervisor, Prof. Doreen Cantrell for giving me the opportunity to do my PhD project in her lab. This project would have not been completed without her guidance, support and encouragement. Thank you.

I am also very grateful to all the wonderful people in Cantrell lab, both present and past. I would like to say a big thank you to:

Liz for all her help with genotyping,

Mahima, Sarah and Laura for their advice and enthusiasm but also for their friendship,

Jens and George for making the hard work a good fun and again Jens for taking me through the mass spec experiment,

Rosie and Arlene for their advice and the long sorts,

but also Linda, Christina, Marcos, Shalini, Aneesa, Ella, Maria, Julia, Marouan and everybody else from the lab and the division.

I am also very grateful to Don Tennant and his co-workers in the Animal Unit.

On the personal note, I would like to thank my parents and my brother for always believing in me and encouraging me to aim high. I would also like to thank Kasia for her friendship and support. And finally I would like to thank Claudia, Giuli, Laura and Fabio for their friendship and Italian lessons, without you my time in Dundee wouldn't be the same. Thanks a lot.

Abstract

Deletion of PTEN selectively in T cell progenitors in the thymus results in the rapid development of aggressive T cell lymphomas in a mouse model for T-ALL. We showed that $PTEN^{-/-}$ T cell lymphoma/leukaemia cells were metabolically active as they readily took up key nutrients. Thus, they had high rates of glucose, glutamine, leucine and transferrin uptake, and expressed constitutively high levels of CD71, the transferrin receptor, and CD98, the System L amino acid transporters. Moreover, $PTEN^{-/-}$ T cell lymphoma/leukaemia cells had high levels of mTORc1 activity. PTEN deletion results in accumulation of $PI(3,4,5)P_3$ and activation of AKT. The present report has addressed whether AKT is the driver of the metabolic changes seen in $PTEN^{-/-}$ T cell lymphoma/leukaemia cells. We showed that PTEN deletion in thymocytes prior to malignant transformation, resulted in a robust activation of AKT but did not cause T cells to increase glucose, glutamine or leucine uptake or activate mTORc1. In this context, we noted that $PTEN^{-/-}$ T cell lymphoma/leukaemia cells but not $PTEN^{-/-}$ non-transformed thymocytes expressed high levels of the transcription factor Hif1α that is required for optimal glucose uptake and glycolysis in normal effector T lymphocytes. We therefore evaluated the importance of Hif1α in T cell lymphomagenesis caused by PTEN deletion. These experiments identified the regulation of Hif1α expression as a critical step in the malignant transformation of $PTEN^{-/-}$ T cell progenitors. They also revealed that the metabolic changes that occur in $PTEN^{-/-}$ T lymphoma/leukaemia cells are not a direct consequence of $PI(3,4,5)P_3$ signalling, but must be mediated by the secondary genetic alterations required for malignant transformation in $PTEN^{-/-}$ T cell progenitors.

Abbreviations

2-DG	2-Deoxyglucose
4E-BP1	eukariotic translation initiation factor4E-binding protein 1
Ab	antibody
AKT/PKB	Protein Kinase B
AKTi	AKT inhibitor VII
ALL	acute lymphoblastic leukaemia
AMPK	5’ Adenosine monophosphate-activated protein kinase
APC	allophycocyanin
APC	antigen presenting cell
APS	ammonium persulfate
ATP	adenosine-5’-triphosphate
BSA	bovine serum albumin
BV	brilliant violet
CD	cluster of differentiation
c.p.m.	counts per minute
CTLs	cytotoxic T lymphocytes
Da	Daltons
DAPI	4’6-diamidino-2-phenylindole
DKO	double knockout
DMEM	Dullbecco’s Modified Eagle’s Medium

DN	double negative
DNA	deoxyribonucleic acid
DP	double positive
DTT	dithiothreitol
ECL	enhanced chemiluminescence
EDTA	ethylenediaminetetraacetic acid
EGTA	ethylene glucol tetraacetic acid
ERK	Extracellular regulated kinase
ES	embryonic stem
FACS	Fluorescence activated cell sorting
FBS	fetal bovine serum
Fc	crystallisable fragment (antibody)
FSC	forward scatter
FITC	fluorescein isothiocyante
Fl	floxed
Foxo	Forkhead domain transcription factor
GAP	GTPase activating protein
GAPDH	glyceraldehyde-3-phosphate dehydrogenase
Glut	glucose transporter
Gly	glycine
GSK3	glycogen synthase kinase

HBSS	Hank’s balanced salt solution
HEPES	4-(2-hydroxyethyl)-1-piperazineethanesulfonic acid
Hif1	hypoxia inducible factor 1
HK	hexokinase
HRP	horseradish peroxidase
IAA	iodoacetamide
IBAQ	intensity based absolute quantification
IL	Interleukin
IMDM	Iscove's Modified Dulbecco's Medium
ImmGen	Immunological Genome project
Itk	Inducible T-cell kinase
JAK	Janus activated kinase
Klf2	Kruppel-like factor 2
KO	knockout
Lck	lymphocyte-specific protein tyrosine kinase
LDH	lactate dehydrogenase
LFQ	label-free quantification
LN	lymph nodes
LNAA	large neutral amino acids
MAPK	Mitogen activated protein kinase

MEMα	Minimum essential medium eagle, α
MEF	mouse embryonic fibroblasts
MHC	major histocompatibility complex
MMAC1	mutated in multiple advanced cancers
mRNA	messenger RNA
MS	mass spectrometry
mTORc	mammalian target of rapamycin complex
myc	myelocytomatosis oncogene
NFAT	nuclear factor of activated T cells
NICD	Notch intracellular domain
p	phospho
PAGE	polyacrylamide gel electrophoresis
PBS	phosphate buffered saline
PBS-T	phosphate buffered saline plus 0.005% (w/v) Tween-20
PCR	polymerase chain reaction
PDK1	3-phosphoisitide-dependent protein kinase 1
PE	phycoerythrin
PFA	paraformaldehyde
PFK	phosphofructokinase
PH	plekstrin homology
PHD	prolyl hydroxylase
PI3K	phosphatidylinositol-3-kinase
PI	phosphatidylinositol

$PI(4,5)P_2$	phosphatidylinositol-4,5-bisphosphate
$PI(3,4,5)P_3$	phosphatidylinositol-3,4,5-trisphosphate
PKM1/2	pyruvate kinase muscle isoform 1/2
pO_2	partial pressure of oxygen
PRAS40	proline rich AKT substrate of 40kDa
PTEN	Phosphatase and tensin homologue
RAG	Recombinase activating gene
Raptor	Regulatory associated protein of mTOR
RHEB	Ras homologue enriched in brain
Rho	Ras homologue gene family
Rictor	Rapamycin-insensitive companion of mTOR
RIPA	radioimmunoprecipitation assay buffer
RNA	Ribonucleic acid
rpm	revolutions per minute
RPMI	Roswell park memorial institute-1640
RT	room temperature
S6	ribosomal protein S6
S6K	p70 S6 Kinase
SAX	strong anion exchange chromatography
SD	standard deviations
SDS	sodium dodecyl sulphate
Ser	serine
SHIP	SH2-domain containing inositol phosphate

SMC1	structural maintenance of chromosome 1
SP	single positive
SSC	side scatter
T-ALL	T cell acute lymphoblastic leukaemia
TBC7	TBC 1 domain protein
TCA	tricarboxylic acid
TCEP	tris(2-carboxyethyl)phosphine
TCR	T cell receptor
TEMED	tetramethylenediamine
TEP1	TGFβ-regulated and epithelial cell-enriched phosphatase
Thr	threonine
Treg	T regulatory cells
Tris	tris(hydroxymethyl)aminomethane
TSC	tuberous sclerosis complex
Val	valine
VHL	von Hippel Lindau
WT	wild type

1 Chapter: Introduction

1.1 PI3K signalling

1.1.1 Lipids as second messengers

The lipids that are present in the plasma membrane and their derivatives have second messenger roles and are crucial for the signal transduction from membrane bound receptors to molecules in cytoplasm and nucleus. One example is the phosphatidylinositol (PI) and its phosphorylated forms that consist around 10% of the total cellular phospholipids. The inositol ring of PI is linked to the lipid via the 1-hydroxyl group. Three out of the five remaining hydroxyl groups on PI can be phosphorylated by kinases to generate at least eight isoforms that differ in the numbers and position of phosphate groups around the inositol ring (Cantley 2002; Vanhaesebroeck & Waterfield 1999).

1.1.2 Introduction to PI3K

Class I phosphoinositide 3-kinases (PI3Ks) are lipid kinases that are activated by different stimuli, i.e. growth factors, hormones, inflammatory stimuli, neurotransmitters or antigens (Hawkins et al. 2006) and their function is to phosphorylate the phosphatidylinositol-(4,5)-bisphosphate ($PI(4,5)P_2$) on its inositol head group to generate phosphatidylinositol-(3,4,5)-trisphosphate ($PI(3,4,5)P_3$). The high levels of $PI(3,4,5)P_3$ can be metabolised to phosphatidylinositol-(4,5)-bisphosphate ($PI(4,5)P_2$) by the Phosphatase and tensin homologue (PTEN) protein or to the phosphatidylinositol-(3,4)-bisphosphate by the pair of phosphatases, SHIP1 and SHIP2 (SH2-domain containing inositol phosphatase) (Vanhaesebroeck et al.

2010). PI(3,4,5)P_3 is an important molecule in cells as it controls cellular growth, cell-cycle entry, cell migration and cell survival (Cantley 2002)

The Class I PI3Ks are heterodimers that are composed of a catalytic subunit, responsible for the lipid kinase activity and an adaptor subunit that links the catalytic subunit to the upstream activating signals (Okkenhaug 2013). They are then subdivided into two groups: class IA and class IB. Class IA is composed of 3 isoforms of the p110 catalytic subunit: α, β, δ that associate with a p85 regulatory subunit. Class IB is composed of p110γ catalytic subunit and the p101 or p87 regulatory subunits. p110δ is expressed selectively in haematopoietic cells (Okkenhaug & Fruman 2010). While class IA enzymes act downstream of kinase receptors, class IB enzymes are regulated by the G-protein-coupled receptors (Vanhaesebroeck et al. 2010).

1.1.3 The importance of PI3K in T cells

In quiescent naïve cells, PI(3,4,5)P_3 intracellular levels are low however they increase rapidly following triggering of the T cell antigen receptor (TCR) with antigenic peptides presented on major histocompatibility complex (MHC) molecules on the surface of antigen presenting cells (APC) (Costello et al. 2002; Harriague & Bismuth 2002). Costello *at al*., showed that T cells can maintain long contacts with antigen loaded APC and during this time they maintain high levels of PI(3,4,5)P_3 (Costello et al. 2002).

The sustained accumulation of PI(3,4,5)P_3 in T cells undergoing immune activation requires constant engagement of the TCR and PI3K activation (Costello et al. 2002;

Huppa et al. 2003). Signals from co-stimulatory molecules, such as CD28, are important during this response, but on their own, do not induce production of $PI(3,4,5)P_3$ in T cells (Garcon et al. 2008). Hence, T cells that encounter activated APC do not generate $PI(3,4,5)P_3$ unless the APC expresses the specific peptide/MHC complex (Costello et al. 2002; Garcon et al. 2008). There are however other physiological stimuli such as cytokines that can directly induce $PI(3,4,5)P_3$ generation in T cells. Interleukin-2 (IL-2) is one such example. Immune activated T cells that are maintained in IL-2 can sustain high cellular levels of $PI(3,4,5)P_3$ over several days (Cornish 2006; Sinclair et al. 2008). Other cytokines such as IL-15 and IL-7 can also induce $PI(3,4,5)P_3$ accumulation, however the relative potency of these different cytokines can vary, e.g. immune activated T cells maintained in IL-15 only have relatively low levels of $PI(3,4,5)P_3$ compared to IL-2 cultured cells (Sinclair et al. 2008). In mature T cells the majority of $PI(3,4,5)P_3$ is produced by the actions of the p110 δ catalytic subunit (Garcon et al. 2008).

What do we know about the role of PI3K in T cell? Deletion of p110δ (Okkenhaug et al. 2002) or p110γ (Sasaki et al. 2000) isoforms in the thymus does not result in major disruption of thymocytes development. However, double deletion of both isoforms has pronounced effects on T cells in the thymus as it leads to the block in early T cell proliferation that is associated with β selection (thymus development is discussed in section 1.3.1) (Swat et al. 2006; Webb et al. 2005). These data, thus, suggest that PI3K activity in thymus is essential for the survival and proliferation of these cells. Studies using conditional deletion of p110δ catalytic subunit of PI3K, loss-of-function mutation in p110δ catalytic subunit (D910A) or selective inhibitor of p110δ, IC87114, contributed to our understanding of the role of PI3K in peripheral T cells.

T cells can be divided by the expression of CD4/CD8 co-stimulatory molecules, into CD4+ and CD8+ cells. Generally, CD4+ cells provide helper function to either immune activated CD8+ T cells or B cells. PI3K regulates CD4+ T helper cells proliferation after stimulation with TCR and also controls CD4+ T cell differentiation into Th subtypes, i.e. Th1 and Th2 cells. Thus, CD4+ expressing PI3K inactive (D910A) mutant or IC87114 treated mice have impaired production of cytokines (Soond et al. 2010; Okkenhaug et al. 2006). Moreover, PI3K is also required for the production of T follicular helper cells in germinal centres, a place where high-affinity antibodies are generated by cooperative work of T and B cells (Rolf et al. 2010). Additionally, PI3K is involved in development and homeostasis of CD4+ T regulatory cells (Treg) and is crucial for full Treg-mediated suppression (Tregs are responsible for limiting the responses of mainly T effector cells to antigen and/or inflammatory stimuli) (Patton et al. 2011). PI3K p110δ is also important in controlling the differentiation of immune activated effector CD8+ T cells, PI3K p110δ signalling thus regulates the production of effector cytokines and controls the expression of adhesion molecules and chemokine receptors that control T cell migration (Macintyre et al. 2011).

1.1.4 PI3K- PI(3,4,5)P_3 signalling in T cells

PI(3,4,5)P_3 in the plasma membrane acts as a tether for proteins that contain plekstrin homology (PH) domains permitting their recruitment to the plasma membrane, and, therefore, their subcellular localisation. PI(3,4,5)P_3 regulated proteins include the serine/threonine protein kinase B (PKB/AKT, here called AKT), phosphoinositide-dependent kinase-1 (PDK1), Tec tyrosine family kinases and guanine-nucleotide-exchange proteins for Rho family GTPases (Okkenhaug & Vanhaesebroeck 2003).

The Tec kinases in T cells comprise Tec and Itk, and these kinases control the release of calcium into the cytoplasm by phosphorylating phospholipase C γ (Scharenberg & Kinet 1998), thus contributing to the sustained calcium signals that are required in the initial phase of T cell activation. One of the mediators of calcium signals in T cells is phosphatase calcineurin. This phosphatase regulates the nuclear localisation of the transcription factor NFAT that mediates expression of cytokines (Winslow et al. 2003; Im & Rao 2004). The Rho family GTPases, in particular RhoA, are important for survival and proliferation of early T cell progenitors in the thymus (Mullin et al. 2007; Cleverley et al. 1999). Moreover, Finlay *at al.,* proposed that proliferation of PTEN null T cell lymphoma/leukaemia cells is dependent on RhoA as inactivation of RhoA in PTEN null T cell progenitors blocks the development of T cell tumours (Finlay et al. 2009).

1.1.5 Downstream effectors of PI3K/ PI(3,4,5)P_3 in T cells: AKT

AKT is the best-studied PI(3,4,5)P_3-regulated kinase. It is a serine/threonine kinase that belongs to the AGC kinase family (L. R. Pearce et al. 2010). The interaction of the PH domain of AKT with PI(3,4,5)P_3 allows AKT to co-localise with the constitutively active PDK1, another PH domain-containing kinase of the AGC kinase family (Calleja et al. 2007). Once in close proximity, PDK1 can phosphorylate AKT on a critical residue, Thr308, localised within the T loop site. In addition, the binding of AKT to PI(3,4,5)P_3 also induces a conformational change in the protein that facilitates this phosphorylation of Thr308 by PDK1 (Mora et al. 2004). While PI(3,4,5)P_3 is an important mechanism for activation of AKT, the co-localisation of AKT and PDK1 can be mediated via a second mechanism. The phosphorylation of AKT on Ser473, mediated by mTORc2, creates a docking site for PDK1. PDK1

contains a PIF-pocket that can bind to the phosphorylated Ser473 on AKT, thus bringing PDK1 in proximity of AKT, permitting the phosphorylation of Thr308 in AKT, and stimulating the activation of AKT (Sarbassov et al. 2005). AKT is the only kinase in AGC family that can be activated via these two independent mechanism, in contrast to other kinases such as protein kinase C or serum-and glucorticoid-induced kinase that can be only activated via the PIF-pocket mechanism (L. R. Pearce et al. 2010). It is not well understood how mTORc2 is regulated and activated in this process, however there is evidence suggesting that PI3K activity is involved, as PI3K inhibitors prevent mTORc2 activation (Sparks & Guertin 2010). Either of these mechanisms is sufficient to stimulate AKT phosphorylation. Thus, T cells that express a knock-in mutant of PDK1 (K465E) that has a PH domain mutation that prevents the binding of $PI(3,4,5)P_3$ shows residual phosphorylation of AKT on Thr308 (Waugh et al. 2009). Similarly, deletion of Rictor, a regulatory component of mTORc2, in immune activated CD8+ T cells (Pollizzi et al. 2015) or in immune activated CD4+ T cells leads to decrease but not ablation of AKT phosphorylation on Thr308 (K. Lee et al. 2010).

1.1.6 Substrates of AKT: Foxo

Important downstream substrates of AKT are the Foxo1 and Foxo3a transcription factors. Phosphorylation of Foxos by AKT leads to their exclusion from nucleus and their sequestration in the cytoplasm by 14-3-3 proteins, thus inhibiting their function as transcription factors (Biggs et al. 1999; Calnan & Brunet 2008). The Foxo transcription factors control a diverse set of genes in T cells (Hedrick et al. 2012). For example, in naïve T cells, one of the target genes of Foxo proteins is the α chain of the IL-7 receptor (Kerdiles et al. 2009; Hedrick et al. 2012). IL-7R signalling is

important in controlling T cell development in the thymus (K. Kim et al. 1998; Rodewald et al. 2001) and maintaining the homeostasis of naïve T cells (Kerdiles et al. 2009), therefore PI3K-AKT-Foxo signalling is important in controlling the development of T cells.

Foxo1/3 transcription factors control also the expression of Kruppel-like factor 2 (KLF2) (Preston et al. 2013) that regulates expression of CD62L, the chemokine receptor CCR7 (Kerdiles et al. 2009) and sphingosine-1-phosphate receptor 1 (Cyster & Schwab 2012). All of these molecules are involved in T cells trafficking. Thus, PI3K activity in effector CD8+ T cells, by causing the exclusion of Foxo proteins from the nucleus, leads to downregulation of expression of these genes and to changes of T cell trafficking (Sinclair et al. 2008; Finlay et al. 2009). The AKT-Foxo pathway is also important for immune activated CD8+ T cells. Hence the inhibition of AKT leads to the re-expression of Foxo target genes, such as IL-7 receptor, Klf2 and to the loss of Foxo repressed genes such as Interferon γ, a cytokine critical for effector function of immune activated CD8+ cells (Macintyre et al. 2011).

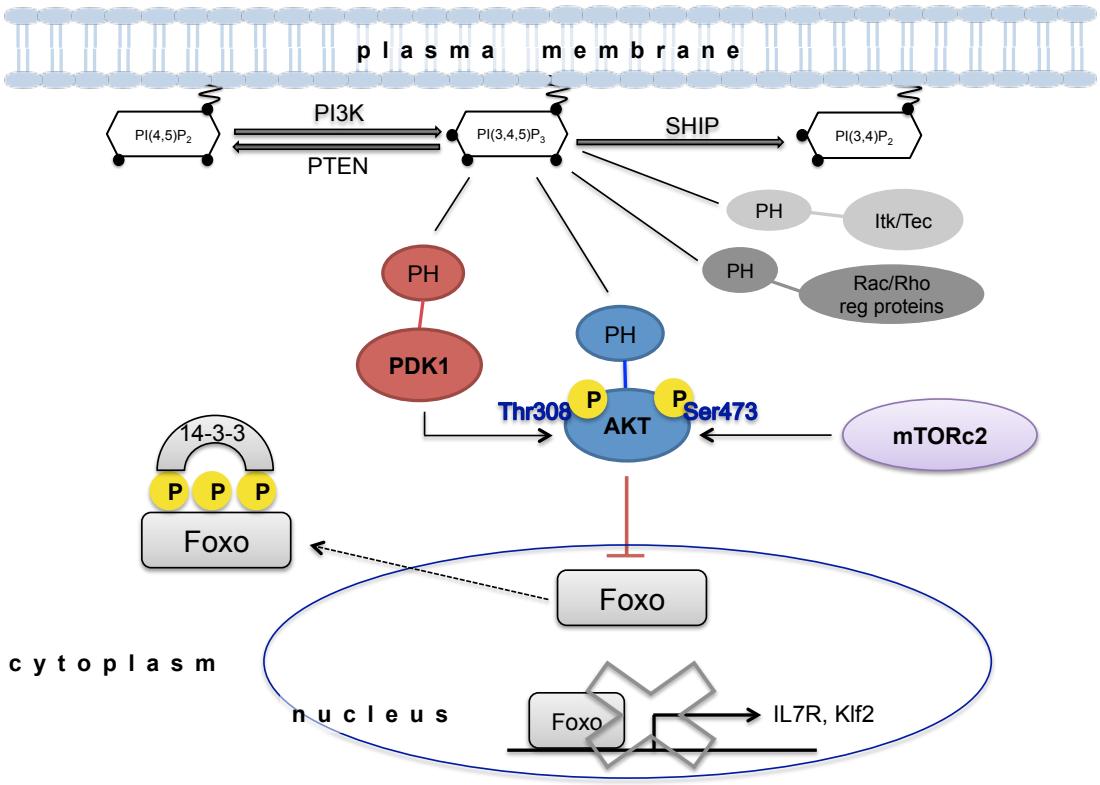

Figure 1-1 **PI3K- PI(3,4,5)P_3-AKT activation in T cells.**

PI(3,4,5)P_3 is produced from PI(4,5)P_2 by PI3K. PI(3,4,5)P_3 is dephosphorylated by PTEN to PI(4,5)P_2 or by SHIP to PI(3,4)P_2. Following T cell antigen receptor stimulation of cytokine signalling, PI(3,4,5)P_3 accumulates in the plasma membrane and this leads to recruitment of proteins containing PH domains. One of them is AKT. Binding of the PH domain of AKT to PI(3,4,5)P_3 in the membrane leads to conformational change that allows for the phosphorylation of AKT on Thr308 by PDK1 and Ser473 by mTORc2. Active AKT phosphorylates Foxo transcription factors and this leads to Foxos exclusion from the nucleus to the cytoplasm where they are captured by 14-3-3 proteins. Phosphorylated Foxos are no longer able to initiate transcription of their target genes, such as IL-7 or Klf2.

1.2 The negative regulator of PI3K: PTEN

1.2.1 PTEN as a tumour suppressor

PTEN, also known as mutated in multiple advanced cancers (MMAC1) or TGFβ-regulated and epithelial cell-enriched phosphatase (TEP1), was identified in 1997 by three independent research groups (J. Li et al. 1997; Steck et al. 1997; D. M. Li & Sun 1997) as a result of experiments to map a region of chromosome 10q23 that was frequently mutated in cancers. The PTEN protein was found to share similarity to the

catalytic domain of members of the protein tyrosine phosphatase family and to the cytoskeletal proteins tensin and auxillin.

The proper activity of protein phosphatases is critical for the controlled phosphorylation of substrates and any deregulation in their activity can contribute to diseases such as cancer (Tonks 2006). As the *Pten* gene was identified through its association with mutations in cancers and because of its homology to a phosphatase, it was suggested that PTEN was a tumour suppressor. Screening of multiple cell lines, xenografts, and primary tissues revealed that PTEN function can be lost due to both genetic mutations and posttranslational modifications (Ali et al. 1999; Bonneau & Longy 2000; Teng et al. 1997). Importantly, mutation or loss in only one of the PTEN alleles is sufficient to cause tumour formation (Suzuki et al. 1998; Di Cristofano et al. 1998; Podsypanina et al. 1999). Somatic deletions or mutations of PTEN are most often found in glioblastoma and endometrial cancers and to lesser extend in prostate, breast, colon and lung (Bonneau & Longy 2000).

The importance of PTEN function is also highlighted by the findings that germline mutations in PTEN cause hereditary disorders called PTEN hamartoma tumour syndromes (Bonneau & Longy 2000), such as Cowden syndrome and Bannayan-Riley-Ruvalcaba syndrome. These are autosomal dominant diseases characterised by cellular overgrowth and the formation of benign hamartomas. 80% of Cowden syndrome and 60% of Bannayan-Riley-Ruvalcaba syndrome are caused by PTEN mutations (Eng 2003).

PTEN function is not just important for preventing aberrant growth of cells, it is also essential for development. While homozygous loss of PTEN in mice leads to early embryonic lethality (Suzuki et al. 1998; Di Cristofano et al. 1998; Podsypanina et al.

1999), loss of one PTEN allele results in high susceptibility to tumours, such as teratocarcinoma and prostatic cancer but also to high frequency of T cell lymphomas (Suzuki et al. 2008; Xue et al. 2008). The conditional deletion of PTEN in the haematopoietic cells (HSC) compartment in mice results in development of myeloproliferative disorders which give rise to acute myeloid/T cell lymphoid leukaemia (Jiwang Zhang et al. 2006; Guo et al. 2008). Moreover, tissue-specific deletion of PTEN in haematopoietic stem cells or thymocytes using Cre-loxP strategies results in T leukaemogenesis or lymphomagenesis (Guo et al. 2008; Hagenbeek & Spits 2007; X. Liu et al. 2010).

1.2.2 Other functions of PTEN

The role of PTEN is to dephosphorylate $PI(3,4,5)P_3$ to $PI(4,5)P_2$. It is well established that PTEN null cells have increased levels of AKT activity due to increased levels of $PI(3,4,5)P_3$ in the plasma membrane (Maehama & Dixon 1998; Myers et al. 1998), and this process can be reversed by re-expression of PTEN (Dahia et al. 1999; Stambolic et al. 1998). This ability of PTEN to antagonise the AKT activity is conserved in *Drosophila* (Jingxiang Huang & Manning 2009) and *C. elegans* (Ogg & Ruvkun 1998). The loss of PTEN, and hence activation of PI3K/$PI(3,4,5)P_3$ signalling, was reported to stimulate cell migration in MEFs or leukocytes for example (Lacalle et al. 2004; Leslie et al. 2007; Liliental et al. 2000) and re-expression of PTEN can rescue this phenotype (Liliental et al. 2000). Additionally, deletion of PTEN specifically in muscle tissues has been shown to protect mice from long-term insulin resistance and diabetes caused by a high-fat diet (Wijesekara et al. 2005). However, loss of PTEN in the liver had the opposite effect and leads to increased insulin sensitivity and glucose tolerance (Stiles et al. 2004). Therefore,

these data argue that PTEN, depending on the environment, can assume different roles.

1.2.3 The structure of PTEN protein

The PTEN gene encodes a 403 amino acid protein (Leslie & Downes 2004). The N-terminal domain contains the protein tyrosine phosphatase catalytic domain and the C-terminal region contains the C2 domain that is involved in membrane interaction. The phosphatase domain of PTEN contains the highly conserved active site motif (CX_5R) that is a signature motif found in all protein tyrosine phosphatases and dual specific phosphatases. This motif contains the residues essential for catalysis (Vazquez & Sellers 2000). The active site pocket of PTEN is positively charged and larger than other protein tyrosine phosphatases. The phosphatase activity of PTEN is involved in its tumour suppression function as point mutations in the catalytically active region of PTEN disrupts this function (Myers et al. 1997; Papa et al. 2014).

Furthermore, PTEN contains a short regulatory N-terminal region that mediates PTEN recruitment to the membrane (Das et al. 2003; Walker et al. 2004). On the C-terminal tail, PTEN contains a cluster of Ser/Thr phosphorylation residues, a PEST sequence and a PDZ protein binding site that mediates protein-protein interactions (Leslie & Downes 2004).

1.2.4 PTEN as protein and lipid phosphatase

The catalytic activity of PTEN is dependent on the cysteine 124 within the CX_5R signature motif. The sulfhydryl group of the cysteine functions as a nucleophile that

attacks the phosphorous atom of its substrate, with the formation of a thiophosphate-enzyme intermediate (Myers et al. 1997; Zhou et al. 1994). Point mutation of cysteine 124 to serine leads to complete loss of phosphatase activity with loss of PTEN ability to control cellular growth (Furnari et al. 1998). Identification of potential physiological substrates for PTEN performed by Myers and co-workers, revealed that PTEN was preferentially active against acidic substrates, such as the highly acidic and artificial random copolymer of glutamate and tyrosine ($polyGly_4,Tyr_1$) (Myers et al. 1997). Additionally, they showed that PTEN was able to dephosphorylate proteins phosphorylated on serine and threonine residues, albeit to much lower degree. While it was clear that PTEN exhibited phosphatase activity towards proteins, the activity towards these substrates was low, suggesting that there were other non-protein substrates.

Indeed, further studies showed that PTEN had a strong phosphoinositide 3-phosphatase activity both *in vitro* and *in vivo*. Expression of the catalytically inactive mutant, C124S, resulted in the accumulation of $PI(3,4,5)P_3$ in the plasma membrane despite the lack of insulin stimulation (Maehama & Dixon 1998). Moreover, characterisation of the lipid phosphatase activity of PTEN demonstrated that it can hydrolyse PI(3)P, $PI(3,4)P_2$ and $PI(3,4,5)P_3$, showing high specificity for the latter even when compared with its water-soluble head group IP_4 (McConnachie et al. 2003; Myers et al. 1998). The large and positively charged active site of PTEN is, therefore, adapted to the high negative charge and large size of the phosphorylated inositol head group of $PI(3,4,5)P_3$ (J. O. Lee et al. 1999). These data thus confirms that $PI(3,4,5)P_3$ is a physiological lipid substrate for PTEN.

While the role of PTEN as lipid phosphatase is well described, its role as a protein phosphatase is less clear. However, it is known that via its protein phosphatase activity PTEN can regulate migration and invasion of glioma cells (Leslie et al. 2009). Thus cells expressing mutated PTEN G129E, that retains only the protein phosphatase activity, have impaired migration compared to cells expressing PTEN WT. Additionally, a recent report showed that protein phosphatase activity of PTEN can autodephosphorylate itself and thus regulates lipid phosphatase activity (Tibarewal et al. 2012).

1.3 Introduction to T cell development

In the previous section we mentioned that heterozygous loss of PTEN leads to development of tumours in different tissues with high frequency of T cell lymphoma. Therefore, in this section T cell development will be discussed.

1.3.1 Development of αβ T cells

T cell development allows for the generation of T cells that express functional and mature T cell antigen receptor complexes (TCR) and either CD4 or CD8, the co-receptors of major histocompatibility complex (MHC) (Boehmer et al. 1999). There are two classes of TCR receptors expressed on T cells: αβ (here we will discuss their development) and γδ. The TCR is composed of two highly variable chains: αβ or γδ linked to invariant chains: CD3γ, δ, ε and ζ. There is a great variability in the specificity of the TCR for the processed antigens and it is dependent on the structure of the antigen-binding site. The variability of the structure of TCRα and β chains is achieved via the gene rearrangement processes of the genes that encode these proteins

(described below). The αβ TCRs can recognise antigens presented to them by MHC class I (if the CD8 co-receptor is expressed) or MHC class II (if the CD4 co-receptor is expressed).

T cells are generated from bone marrow progenitors (Shah & Zuniga-Pflucker 2014). T cell progenitors in the thymus do not express CD4 or CD8 co-receptors and hence are called double negative (DN). As CD4/CD8 DNs progress through their development they are characterised by different expression of CD25, the α chain of the cytokine receptor for IL-2, and CD44. T cell progenitors are thus CD25-CD44+ (DN1). In the next, DN2 phase, cells become CD25+CD44+ and start to rearrange the TCRβ loci, a process that is mediated by RAG1 and RAG2 genes, and DNA-modifying proteins that are involved in the repair of DNA double-strand breaks. TCRβ rearrangements are required for the assembly of the functional TCR and production of mature T cells, progressing through the DN3 stage where thymocytes are CD25+CD44-. Once the β chain of TCR has been rearranged successfully, thymocytes start to express the pre-TCR complex that is composed of β chain, pre-Tα and CD3 molecule (Michie & Zúñiga-Pflücker 2002). The pre-TCR then promotes the survival and induces proliferation of thymocytes and their progression into DN4 stage (CD25-CD44-). It is a crucial step during thymus development and it is called β selection, because only thymocytes with properly rearranged β chain can proliferate and become CD4/CD8 double positive (DP) cells. Thus, T cells in mice deficient for RAG genes expression are not able to properly assemble pre-TCR and hence their development is stopped at the DN3 stage (Shinkai et al. 1992).

The differentiation through the DN1 to DN3 stage is promoted by the signals that are derived from thymic epithelial cells. In particular, Notch-mediated signals delivered by binding to Delta ligand (Radtke et al. 1999) and signals delivered by Interleukin-7 (IL-7) (Peschon et al. 1994; Maki et al. 1996) are crucial for thymocytes development. In this context, Notch1 is essential for specification and commitment of the developing thymocytes to the T cell lineage (Ciofani & Zúñiga-Pflücker 2007) by inducing the expression of transcription factors, including Gata3, Tcf1 and Hes1. An absence of Notch signals in haematopoietic cells, abrogates the development of T cells, and instead allows for the accumulation of immature B cells and DC in the thymus (Feyerabend et al. 2009). Additionally, Notch1 has been shown to be essential for the β selection in αβ T cells, as it promotes the survival of DN pre-T cells by maintaining their size, glucose uptake and metabolism (Ciofani & Zúñiga-Pflücker 2005).

During the next step of T cell differentiation, DN thymocytes up-regulate the expression of the CD4 and CD8 co-receptors, becoming so called double positive cells (Germain 2002; Mariathasan et al. 1999). CD4/CD8 DP cells initiate TCRα rearrangements, a process that is again controlled by the RAG1 and RAG2 genes. The rearrangement of the α chain locus occurs in repeated cycles to allow higher number of cells to produce functional T cell receptor. The newly formed TCR expressed on surface of CD4/CD8 DP cells then interacts with MHC molecules (expressed on the surface of thymic epithelial cells) to become either CD4+ or CD8+ single positive (SP) mature T cells. Moreover, depending on the strength and duration of the interaction between TCR and self-peptide MHC complex thymocytes are either positively or negatively selected. Thus if TCR has an intermediate affinity/avidity for

self-peptide-MHC complexes, thymocytes will be positively selected and survive. When TCR has high affinity for self-antigens, thymocytes will undergo death by apoptosis (negative selection). If TCR fails to engage in the interaction with self-peptide-MHC complexes this will lead to their death by neglect (Germain 2002). Positive selection allows for survival of these thymocytes that have some potential to recognize self-antigens and that will be able to activate when encounter self-MHC loaded with 'foreign' antigen.

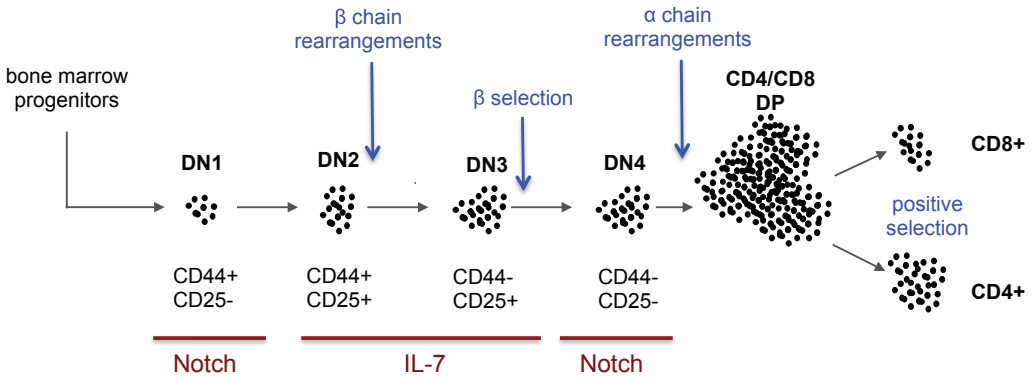

Figure 1-2 **αβ T cell development in the thymus.**

The main function of the thymus is to generate a repertoire of T cells capable of recognizing a variety of antigens without significant self-reactivity. Rearrangements of the TCRα and TCRβ genes allow for the production of diverse range of TCR receptors. Thymocytes that successfully rearranged TCRβ chain survive and proliferate (β selection) and start to rearrange TCRα chain. Expression of mature TCR on thymocytes surfaces trigger positive or negative selection. Positive selection leads to production of CD4+ or CD8+ T cells. Notch signals support the commitment of DN1 cells to become T cells and later supports survival of cells during β selection. Il-7 signalling is an important factor in supporting survival and proliferation of early T cell progenitors.

1.4 T cell acute lymphoblastic leukeamia

1.4.1 What is T cell acute lymphoblastic leukaemia (T-ALL)?

T cell development in the thymus is a crucial step for the production and maintenance of mature T cells that function in peripheral organs as part of the adaptive immune

system. However, any abnormalities that arise during this stage may have serious consequences and can lead to development of diseases, such as T-ALL. T-ALL is a severe, hematological disorder that originates in T cell progenitors in the thymus (Armstrong et al. 2009; Bressanin et al. 2012). It affects both adults and children but has peak prevalence in children between the ages of 2 and 5 years old (Pui et al. 2008). This disease is still not fully curable with the mortality rate higher in adults (40-50%) than it is in children (20%). The genetic mutations that underpin the development of T-ALL are still not fully determined, but it is thought that multiple genetic events contribute to its formation rather than a single mutation (Jinghui Zhang et al. 2012).

1.4.2 Notch mutations in T-ALL

Aberrant activation of Notch1 signalling is found in 60% of T-ALL cases (González-García et al. 2012). As already mentioned, during T cell fate determination, the interaction between Notch1 and Delta-like ligands mediates T cell specification. Activating mutations in Notch can arise from a number of different types of mutations. A relatively infrequent chromosomal translocation (7;9) between *Notch1* and *Tcrb* gene were identified in T-ALL (Weng et al. 2004). The most common mutations that contribute to around 50% of all T-ALL are activating mutations that are located within the PEST and HD domains, both involved in stability of Notch1 (Andersson et al. 2011). These mutations regulate the stability of Notch1 and are associated with increased expression of the intracellular domain of Notch1 (NICD), which can then translocate to the nucleus and can induce expression of target genes (Sulis et al. 2008). Additionally, constitutively active Notch1 was found to be necessary to sustain the growth and activity of self-renewing T-ALL initiating cells

(or leukaemia initiating cells, LIC) that are capable of transforming into leukaemic cells. These cells are maintained by signals from the Notch1 pathway and blocking Notch1 activity can efficiently inhibit LIC activity (Armstrong et al. 2009).

1.4.3 IL-7R mutations in T-ALL

IL-7 is an important cytokine during the early thymus development and also in maintaining homeostasis, differentiation and activity of peripheral T cells (Ribeiro et al. 2013). *In vivo* studies have shown that IL-7 is important for the progression of T-ALL (Silva et al. 2011). Human T-ALL cells transplanted into immunodeficient mice that lacked the ability to express IL-7, initiated leukaemia more slowly that human T-ALL transplanted into immunodeficient mice expressing IL-7. Mice that overexpress IL-7Rα spontaneously develop T cell lymphomas. Indeed, the analysis of human T-ALL samples shows that mutations in the IL-7R are associated with tumourigenesis (Zenatti et al. 2011) and deregulated signalling of IL-7/IL-7R was shown to contribute to 10% of all T-ALL (Shochat et al. 2011; Zenatti et al. 2011; Ribeiro et al. 2013). Heterozygous somatic mutations in the *Il-7R* gene resulting in gain-of-function, lead to the promotion of T cell growth regardless of the availability of IL-7. The canonical IL-7 signalling assumes that upon IL-7 binding to IL-7Rα, the receptor dimerises with the common γ chain and initiate activation of the tyrosine kinases JAK1 and JAK3 (Walsh 2012). In contrast, the most common mutation of the IL-7R in T-ALL creates an unpaired cysteine residue in the extracellular juxtamembrane-transmembrane interface region that enables the homodimerization of IL-7Rα chains and the subsequent activation of the tyrosine kinase JAK1 phosphorylation irrespective of IL-7 availability, common γ chain or JAK3 (Ribeiro et al. 2013).

1.4.4 PTEN mutations in T-ALL

Changes in the expression or activity of PTEN have been linked to the formation of human T-ALL. Different mechanisms of PTEN inactivation have been described in the literature. Genetic mutations contribute to about 20% of T-ALL cases (Zenatti et al. 2011). There is a subset of T-ALL that develops due to *Pten* mutations that lead to its inactivation. Approximately 30% of these mutations can be found in exon 7 and result in C-terminal protein truncation (Jotta et al. 2010; Gutierrez et al. 2009) and truncated PTEN is targeted for the degradation (Georgescu et al. 1999). Moreover, sequence alterations in PI3K and AKT genes were identified in approximately 20% of human T-ALL samples (Gutierrez et al. 2009). In addition to genetic loss or mutations of PTEN, data indicates that inactivation of the PTEN protein can contribute to T-ALL progression. In this respect, analysis of human T-ALL samples revealed that in some cases, while mRNA of *Pten* was intact and the PTEN protein was expressed, the activity of PTEN was diminished and this inversely correlated with hyperactivation of PI3K and AKT. The authors proposed that the posttranslational modification of PTEN, by either phosphorylation mediated by the serine/threonine protein kinase caseine kinase 2 or by the catalytic inactivation of the protein by reactive oxygen species can directly downregulate the activity of PTEN (Silva et al. 2008).

1.4.5 PTEN null mouse model of T-ALL

Cre-loxP mediated deletion of PTEN specifically in early T cell progenitors in the thymus of mice has allowed a direct study of the role of PTEN in T cells (Hagenbeek & Spits 2007; Hagenbeek et al. 2004). It was shown that initially loss of PTEN in T

cells is associated with the normal development of thymocytes and that other tumour-initiating events must occur to promote tumour development (Xue et al. 2008). This lag period is characterised by several features. First, PTEN loss in T cells leads to an increased survival of PTEN null thymocytes. While development of normal early thymocytes requires IL-7 signalling and pre-TCR signals, PTEN null T cell progenitors are able to survive and proliferate at normal rates without pre-TCR and/or IL-7 signalling (Hagenbeek et al. 2004). Secondly, mature PTEN null T cells that develop in the thymus have decreased ability to home to secondary lymphoid organs, which leads to decreased number of T cells in the periphery, known as lymphopenia (Finlay et al. 2009). In normal thymocytes Klf2 induces expression of chemokine CCR7 and adhesion molecule CD62L, molecules that are involved in migration from blood vessels to secondary lymphoid organs (Carlson et al. 2006). In PTEN null thymocytes, as a result of AKT phosphorylation and exclusion of Foxo transcription factors from the nucleus, there is a reduction of *Klf2* mRNA, that leads to downregulation of expression of CCR7 and CD62L at both message and protein level (Finlay et al. 2009). Thus, PTEN null thymocytes fail to normally express CCR7 and CD62L and fail to properly home to lymph nodes and spleen. Thirdly, PTEN null thymocytes, in particular CD4+ T cells are hyperproliferative, autoreactive and have increased production of cytokines compared to normal thymocytes (Suzuki et al. 2001).

After a lag period of around 10-12 weeks after birth, mice with PTEN null T cell progenitors will develop tumours (Hagenbeek & Spits 2007). Why do mice with thymocytes specific PTEN deletion develop tumours? It was proposed that PTEN is critical in maintenance of genomic integrity and the disruption of PTEN leads to chromosomal translocations and centromere breakage (Shen et al. 2007). Thus,

secondary mutations are necessary to induce tumour development in mice with thymocyte specific PTEN deletion (Hagenbeek & Spits 2007; Xue et al. 2008). It was proposed that premalignant changes that occur in thymocytes make them susceptible to *c-Myc* translocations that are the main secondary mutation in PTEN null T cell lymphoma/leukaemias (Guo et al. 2011; Xue et al. 2008). Some of the studies proposed that one group that is particularly susceptible to translocations are CD4/CD8 double positive thymocytes (Guo et al. 2008; Guo et al. 2011). However, as mice with T cell specific deletion not only develop tumours that are of CD4/CD8 DPs origin, other thymic populations, like CD4 and CD8 or CD4/CD8 double negative thymocytes must also be able to acquire secondary mutations. The tumours that develop in mice with PTEN specific deletion are mainly monoclonal and disseminate into peripheral organs such as spleen or lymph nodes. A common method to examine if the T cell lymphomas are monoclonal or polyclonal is to analyse the TCRβ variable region. This analysis revealed that PTEN null T cell tumours are composed of relatively mature, clonally expanded post β-selected thymocytes (Hagenbeek & Spits 2007). Importantly, only deletion of PTEN in early T cell progenitors allows for the tumour development. If PTEN is deleted in naïve T cells in the periphery, these mice remain tumour free (Soond et al. 2012).

1.5 Metabolic regulation in T-ALL and normal T cells

Analysis of primary T cell lymphoma/leukaemia cells from mice where PTEN had been deleted showed that these cells are big, blast-like cells, implying that they might be metabolically active (Finlay et al. 2009). In this context, activation of naïve T cells (small, metabolically quiescent cells) by TCR stimulation is associated with a striking change in T cell growth, size and proliferation that needs to be matched by a

metabolic reprogramming (Finlay 2012). In particular, activated T cells up-regulate expression of glucose transporters (Glut1 and Glut3), glucose uptake and switch from metabolising glucose primarily through oxidative phosphorylation to using the glycolytic pathway despite no limitation in the availability of oxygen (aerobic glycolysis) (Maciver et al. 2008; Fox et al. 2005). Glycolysis is regulated by rate limiting glycolytic enzymes, such as hexokinase, phosphofructokinase, pyruvate kinase and lactate dehydrogenase (Lunt & Vander Heiden 2011). This switch, known as the Warburg effect (Vander Heiden et al. 2009), mirrors the situation seen in many solid tumours and allows for the production of biosynthetic precursors, such as pyruvate, than then are used for the production of lipids, nucleic acids and proteins. It is recognised that acute leukaemia cells also undergo a glycolytic switch and have high rates of glucose uptake and lactate output (Boag et al. 2006; Akers et al. 2011; W.-L. Chen et al. 2014; Hulleman et al. 2009).

Not much is known about the uptake of amino acids by PTEN null T-ALL cells, however, in normal T cells it is known that immune activation is associated with massive increase in amino acid uptake due to upregulation of expression of amino acid transporters (Sinclair et al. 2013; R. Wang et al. 2011a; Cornish 2006; Preston et al. 2015). Thus regulated uptake of amino acids is also important for proliferating cells for the production of biosynthetic precursors and fuelling translation. In particular, large neutral amino acids (LNAA), such as leucine, are important for these processes (Sinclair et al. 2013). Intracellular leucine is also sensed by the lumen of the lysosome (Zoncu et al. 2011), and is a potent activator of mammalian target of rapamycin complex 1 (mTORc1), a kinase that plays a central role in regulation of metabolism via phosphorylation of components of translational machinery (discussed

in section 1.5.2) (BEUGNET et al. 2003; Proud 2007; Sinclair et al. 2013). Another important essential amino acid for many cells is glutamine (Carr et al. 2010). Glutamine cooperates with leucine to induce mTORc1 activation. On one hand, transport of glutamine into the cell is followed by its efflux and simultaneous import of leucine. Thus, glutamine availability is rate limiting for uptake of leucine by the cell (Nicklin et al. 2009). On the other hand, it was proposed that production of α-ketoglutarate from glutamine via glutaminolysis is facilitated by leucine (Duran et al. 2012). α-Ketoglutarate then can stimulate the recruitment of mTORc1 to the lysosome where RHEB can activate it.

One other important protein for rapidly proliferating cells is transferrin, as transferrin transports iron inside the cell (Ponka & Lok 1999). Iron acts as a cofactor for a number of cellular enzymes, including ribonucleotide reductase, a rate-limiting enzyme for DNA synthesis (Richardson & Ponka 1997). The importance of iron in cellular proliferation has been demonstrated by the findings that the treatment of cells with iron chelators halts DNA synthesis (Robbins & Pederson 1970; White et al. 1990; Kemp et al. 1995). Recent studies have shown that c-Myc, a critical oncogene, controls transferrin receptor expression in normal T cells (Preston et al. 2015). Also expression of transferrin receptor is used as marker for tumour cells (Daniels et al. 2012).

1.5.1 Regulation of metabolism in T cells and T-ALL cells

In certain cell systems, such as skeletal muscles or adipocytes, the serine/threonine kinase AKT plays a key role in maintaining cellular metabolism by regulating glucose homeostasis (Hajduch et al. 2001; C. J. Green et al. 2008; Mahfouz et al.

2014). In the thymus, PI3K-induced activation of AKT was proposed to support the metabolism of developing early T cell progenitors (Juntilla & Koretzky 2008). During the CD4/CD8 double negative stage, thymocytes enter β selection, a process that requires an increase in metabolism to sustain rapid cell proliferation. T cell progenitors that lack the expression of the two AKT isoforms expressed in thymus have reduced glucose uptake and fail to develop beyond the CD4/CD8 DN stage (Juntilla et al. 2007). This phenotype can be rescued by the expression of a constitutively active mutant of AKT that restores the viability and glycolytic rates of early T cell progenitors (Ciofani & Zúñiga-Pflücker 2005). Additionally, $PI(3,4,5)P_3$-PDK1-mediated activation of AKT in T cell progenitors is required for the expression of nutrient receptors, such as CD71 and CD98 (Kelly et al. 2007), that are important to support the growth and proliferation of these cells.

PI3K-AKT activation has been also proposed to play a role in controlling glucose metabolism in immune activated peripheral T cells. Early studies showed that the inhibition of PI3K signalling caused reduction in the expression of the glucose transporter, Glut1, and a reduction in the uptake of glucose in antigen receptor activated T cells (Frauwirth et al. 2002). However, these experiments used LY294002, a PI3K inhibitor that has many off target effects (Bain et al. 2007; Gharbi et al. 2007). Further studies that have used selective inhibitors of AKT (AKTi), or PI3K – p110δ (IC87114) in TCR activated effector CD8+ T cells, found that PI3K-AKT signalling is dispensable for the glucose uptake and proliferation of immune activated T cells (Macintyre et al. 2011). There is therefore contradictory data regarding the role of AKT in controlling metabolism of mature T cells.

In this thesis we wanted to ask whether AKT activation plays a role in controlling the metabolism of T leukaemic cells. There are two studies that have suggested that activation of PI3K-AKT signalling regulates glucose uptake and proliferation in T-ALL populations (Barata 2004; Hagenbeek et al. 2014). However, these studies used LY294002 as a pharmacological tool to inhibit PI3K-AKT activation and therefore should be interpreted with caution. In contrast to the above reports, a study performed by Finlay *at al*., suggested that that the upstream activator of AKT, PDK1 is not necessary to sustain metabolism and proliferation in PTEN-induced T-ALL (Finlay et al. 2009). In normal T cell progenitors, PDK1 is essential for the proliferation and survival of these cells (Hinton et al. 2004). However, PTEN can bypass the PI3K-PDK1-AKT-mediated control of metabolic checkpoint and PTENxPDK1 null T cell progenitors can survive and proliferate normally (Finlay et al. 2009). Therefore, we wished to further dissect the role of AKT in controlling the metabolism and nutrient transport in T-ALL cells. We also wanted to understand if there are other pathways through which the metabolism of T cell progenitors/T-ALL cells can be regulated.

One kinase that is important in immune activated T cell metabolism is the mTORc1 kinase. This kinase could potentially also plays a role in controlling the metabolism of T-ALL tumours. In this respect the loss or the genetic deletion mTORc1 function can delay the development of T cell tumours in a mouse model of PTEN deletion in haematopoietic cells (Tandon et al. 2011; Kalaitzidis et al. 2012). In addition, it is known that mTOR catalytic inhibitors can be cytotoxic for T-ALL (Evangelisti et al. 2011). Furthermore, administration of a mTORc1 specific inhibitor, rapamycin, leads to a depletion of the leukaemia initiating T cells that are able to produce tumours (Yilmaz et al. 2006).

1.5.2 mTORc1

1.5.2.1 Overview

mTOR is a serine/threonine kinase that belongs to the PI3K-related kinase family (Lempiainen & Halazonetis 2009; Schmelzle & Hall 2000) and is the catalytic component of two complexes, mTORc1 and mTORc2. mTORc1 consists of the scaffolding protein Raptor (regulatory-associated protein of mTOR), PRAS40 (the proline-rich AKT substrate 40kDa), Deptor (DEP-domain containing mTOR-interacting protein) and mLST8 (mammalian lethal with Sec13 protein 8) (Laplante & Sabatini 2013). mTORc2 consists of the scaffolding protein Rictor (raptor-independent companion of TOR), mLST8, mSIN1 and Proctor (Protein observed with rictor) (Guertin & Sabatini 2007). mTORc1, in contrast to mTORc2, is sensitive to the drug rapamycin that is used as an immunosuppressant, mainly in transplantation procedures (Saunders et al. 2001). Rapamycin, by binding to the FKBP12 domain on mTOR, can block the association of Raptor with mTOR and hence prevent mTORc1 activity (Brown et al. 1994).

1.5.2.2 Signalling up-stream of mTORc1

As an environmental sensor, mTORc1 integrates signals from amino acids, growth factors, oxygen, stress and energy status to regulate intracellular processes involved in protein translation, lipid biosynthesis and autophagy (Laplante & Sabatini 2012). The activation of mTORc1 is promoted by the availability of amino acids and is decreased when there is shortage of nutrients, leading to a decrease in cellular biosynthesis and an increase in autophagy (Yu et al. 2010; Korolchuk et al. 2011; Boya et al. 2013). How is mTORc1 activity regulated? Recent studies showed that

activation of mTORc1 takes place on lysosomes (Sancak et al. 2010; E. Kim et al. 2008). mTORc1 is directly activated by the Ras homologue enriched in brain (RHEB) GTPase (Yee & Worley 1997; Saucedo et al. 2003). RHEB activity is regulated by the tuberous sclerosis complex (TSC) that consists of TSC1, TSC2 and TBC1D7 (Saucedo et al. 2003; Manning & Cantley 2003). TSC2 is localised on the lysosome and inhibits mTORc1 activity by suppressing the activity of RHEB. However, insulin receptor driven activation of AKT (Yecies & Manning 2011) leads to the phosphorylation of TSC2 on several sites, out of which Ser939 and Thr1262 are highly conserved (Menon et al. 2014; Demetriades et al. 2014). This phosphorylation leads to the inhibition of the GAP activity of the TSC1-TSC2-TBC7 complex towards RHEB (Menon et al. 2014; Dibble et al. 2012). Additionally, phosphorylation of TSC2 facilitates its binding to 14-3-3 proteins and this further sequesters TSC away from the lysosomally bound RHEB (Cai et al. 2006). Therefore, phosphorylation of TSC2 by AKT allows for RHEB-GTP loading and, potentially, mTORc1 activation (Menon et al. 2014). MAPK signalling, via ERK1/2 mediates the phosphorylation of TSC2 on Ser660 and Ser540 and this leads to the disintegration of the TSC2 complex and hence mTORc1 activation (L. Ma et al. 2005). In contrast to AKT and ERK, phosphorylation of TSC2 by AMPK on Ser1388 leads to an increased activity of TSC2 and further inhibition of mTORc1 (Inoki et al. 2002). Additionally, AKT can directly contribute to mTORc1 activation by phosphorylating and inactivating PRAS40, a negative regulator of mTORc1 signalling (Sancak et al. 2007).

Full activation of mTORc1 requires signals from growth factors and from amino acids, in particular leucine (Menon et al. 2014). The amino acid sensing of mTORc1 functions through a mechanism that is independent of TSC2. Amino acids are sensed

on the lysosome by an unknown mechanism that is dependent on Rag GTPases and involves the vATPase (Zoncu et al. 2011) that can activate the GEF activity of the Ragulator complex (Bar-Peled et al. 2012) towards the heterodimer of RagA/B and RagC/D (RagA/B^{GTP}-RagC/D^{GDP}). Then, the active RagA recruits mTORc1 to the lysosome (Sancak et al. 2010), which can be activated by RHEB that is constitutively present on the lysosome. Also glutamine availability is important for mTORc1 activity (described in section 1.5).

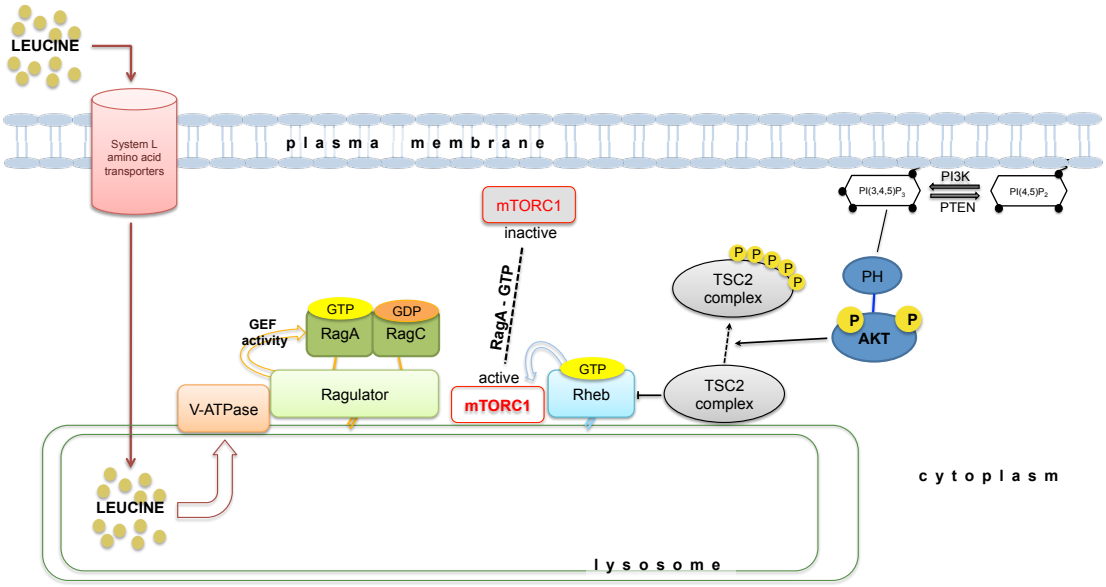

Figure 1-3 **Model of mTORc1 activation.**

Amino acids, e.g. leucine are crucial for mTORc1 activation. Leucine levels are sensed on the lysosome to initiate the cascade of events involving vATPase, Ragulator complex and RagA that recruits mTORc1 from the cytosol to the lysosome. Activation of PI3K e.g. by growth factors, initiate AKT activation that phosphorylates and inhibits TSC2 function, allowing GTP-loading of RHEB and RHEB activates mTORc1. Figure based on (Bar-Peled & Sabatini 2012; Menon et al. 2014).

What is known about mTORc1 activation in T cells? While naïve T cells present only low mTORc1 activation, consistent with the fact that they are quiescent cells, activated T cells show high levels of mTORc1 activity (Waickman & Powell 2012). Amino acid-driven mTORc1-regulating pathways are crucial for the maintenance of

mTORc1 activity in T cells (Sinclair et al. 2013). Additionally, TCR induced calcium-calcineurin signalling leads to the upregulation of the expression of System L amino transporters that transport large neutral amino acids, such as leucine, into the cell (Sinclair et al. 2013). Leucine is an mTORc1 activator (BEUGNET et al. 2003; Proud 2007). In T cells, Slc7a5 plays a crucial role (Sinclair et al. 2013). While Slc7a5 expression is not important for the development of T cells and maintenance of naïve T cells, it is crucial for the differentiation of effector CD8+ cells. Slc7a5 null T cells, thus, are not able to perform the metabolic switch that is required for their activation.

The contribution of the AKT-TSC2 signalling to the activation of mTORc1 is still not fully understood in T cells. A study by Shrestha *at al*., proposed that the deletion of TSC1 in T cells leads to increased mTORc1 activity only seen in TCR stimulated, but not in quiescent T cells (Shrestha et al. 2014). Similarly, deletion of TSC2 in T cells leads to only a slight upregulation of mTORc1 activity in quiescent T cells (Pollizzi et al. 2015). However, there are no studies addressing if active AKT promotes the re-localisation, or decrease in GAP activity, of TSC2 in T cells. Our laboratory has shown that inhibition of the PI3K-AKT pathway with specific inhibitors does not inhibit mTORc1 activity (Macintyre et al. 2011), but instead has found that PDK1 is the major regulator of mTORc1 activity in T cells (Finlay et al. 2012). Moreover, mTORc1, rather than AKT, controls metabolism in normal T cells by regulating the expression of Hypoxia-inducible factor 1α (Hif1α) (Finlay et al. 2009).

1.5.2.3 Downstream targets of mTORc1

mTORc1 has two main substrates: initiation factor 4E binding protein 1 (4E-BP1) and the p70 S6 ribosomal kinase1 (S6K1) (Laplante & Sabatini 2012). Phosphorylated 4E-BP1 enables the eIF4E-promoted cap methylation of mRNAs characterised by a 5' terminal oligopyrimidine (TOP) motif (Thoreen et al. 2012). Similarly, phosphorylation of S6K by mTORc1 leads to an increase in mRNA biogenesis, cap-dependent translation, elongation and translation of ribosomal proteins (X. M. Ma & Blenis 2009). Additionally, mTORc1 is a positive regulator of transcription factors, such as sterol regulatory element binding protein (Porstmann et al. 2008) and peroxisome proliferator-activated receptor γ (J. E. Kim & J. Chen 2004) that control expression of genes involved in lipid and cholesterol homeostasis. Moreover, mTORc1 is involved in repressing autophagy, by phosphorylating and inhibiting ULK1 and autophagy-related gene (ATG13), proteins that are required for the generation and activation of autophagy specific activity (Ganley et al. 2009; Hosokawa et al. 2009).

1.5.3 Hypoxia inducible factor α (Hif1α)

1.5.3.1 Overview

mTORc1 controls the expression of glucose transporters and glycolytic enzymes in T cells. It has been proposed that mTORc1 exerts these functions by regulating Hif1α expression (Finlay et al. 2012). Hif1α was identified at the enhancer of the erythropoietin gene under hypoxic conditions (Semenza & G. L. Wang 1992; R. Wang & D. R. Green 2012). There are three isoforms of Hifα: Hif1α, Hif2α and Hif3α. Whereas Hif1α is ubiquitously expressed, expression of Hif2α is

predominantly confined to tissues such as brain, heart, lung or kidney (Wiesener et al. 2003). In this section we will focus on Hif1α, as lymphocytes exclusively express Hif1α isoform.

Hif1α and its binding partner Hif1β are members of the basic-helix-loop-helix Per/ARNT/Sim (bHLH-PAS) family of transcription factors (G. L. Wang et al. 1995). In order to induce expression of target genes Hif1α must dimerise with Hif1β (Salceda et al. 1996) via the bHLH and part of the PAS domain and then with DNA via the bHLH domain (Jiang et al. 1996; Sang et al. 2002). Hif1α function is critical during embryogenesis as mice with Hif1α deletion die prematurely mainly due to a lack of blood vessel formation (Ryan et al. 1998; Iyer et al. 1998; Kotch et al. 1999). In contrast, deletion of one allele of Hif1α rescues mice from death but impairs their physiological responses when challenged by hypoxia (Kline et al. 2002). Initially, the primary function of Hif1α was considered to be in the processes involved in erythropoiesis and angiogenesis (Josko et al. 2000). Subsequently, it was discovered that Hif1α also stimulates expression of glycolytic enzymes. Hypoxic cells, due to expression of Hif1α and its transcriptional activity, are able to upregulate the expression of glucose transporters and rate-limiting glycolytic enzymes (C. Chen et al. 2001; Wenger 2002).

1.5.3.2 Hif1α regulation

The expression of Hif1α under 21% O_2 is prevented because Hif1α protein is ubiquitinated and subjected to proteasomal degradation by the von Hippel Lindau protein (pHVL) (Maxwell et al. 1999). This is in contrast to hypoxic conditions that allow for the stabilization and accumulation of Hif1α protein expression due to

reduced degradation by the pVHL. The degradation of Hif1α under normoxic conditions is mediated by prolyl hydroxylase domain-containing proteins 1, 2 and 3 (PHD1, PHD2, PHD3) that catalyse hydroxylation of conserved proline residues (Pro402 and Pro564). PHD2 has the highest affinity for Hif1α. The hydroxylated Hif1α is then targeted for degradation by the E3 ubiquitin ligase containing pVHL (Ivan et al. 2001; Kenneth & Rocha 2008).

The mechanism by which Hif1α translation is regulated is still not fully understood. It has been proposed that mTORc1 (Hudson et al. 2002) and MAPK (Fukuda et al. 2002) signalling pathways are involved in Hif1α translation. The translational repressor 4E-BP1 can be phosphorylated by mTORc1 and MAPK and, thus, allows eIF4E to promote cap-dependent translation of mRNA (Thoreen et al. 2012). However, the discovery that Hif1α mRNA does not contain the 5' TOP motif rejected this hypothesis and left the question open. Nonetheless, mTORc1 does play a role in Hif1α T cells regulation because treatment with rapamycin abolishes Hif1α translation and not mRNA expression (Finlay et al. 2012).

1.5.3.3 The role of Hif1α in T cells and T-ALL cells

What is known about Hif1α signalling in T cells? The Hif1α protein is absent in naïve T cells and mRNA is only expressed after TCR mediated activation under hypoxic conditions and this expression of Hif1α is needed for the repression of activation-induced death in T cells that promotes their survival (Lukashev et al. 2001; Makino et al. 2003). However, it was shown that Hif1α ablation in TCR activated T cells does not have a detrimental effect on the T cells, but instead leads to the overproduction of pro-inflammatory cytokines, i.e. IFNγ, TNFα, IL-2, IL4 and IL13 under normoxic

and hypoxic conditions (Lukashev et al. 2006). The data, thus, argue that Hif1α is important for the negative regulation of T cells and may have an anti-inflammatory function; however, it is not fully understood how this function is regulated. The most recent work performed in different types of lymphocytes, i.e. effector CD8+ cells or effector CD4+ (Th17 cells) cells showed that Hif1α directly contributes to the glycolytic behaviour of these cells by promoting expression of glucose transporters and rate-limiting glycolytic enzymes (Shi et al. 2011; E. V. Dang et al. 2011; Finlay et al. 2012). There is not much known about the Hif1α role in T-ALL. However, the current data imply that pharmacological inhibition or deletion of Hif1α in leukaemia inducing cells, that are capable of promoting tumours, leads to their elimination (Y. Wang et al. 2011b; Giambra et al. 2015).

1.5.4 c-Myc in T cells and T-ALL

mTORc1 is an important metabolic regulator in normal T cells and could be important in controlling metabolism in T-ALL cells. However T-ALLs also express c-Myc and this molecule is also a key regulator of metabolism in many cell systems including T cells (Schubbert et al. 2014; Roderick et al. 2014; Weng et al. 2006; Bonnet et al. 2011; Wise et al. 2008). Expression of c-Myc is crucial for T cell activation as it induces glucose and glutamine metabolism (R. Wang et al. 2011a). Additionally, levels of c-Myc protein are tightly controlled in immune activated T cells by the T cell antigen receptor and the key pro-inflammatory cytokine, IL-2 (Preston et al. 2015). Importantly, c-Myc is constantly phosphorylated by GSK3 on Thr58 and targeted for degradation, therefore it can only accumulate in cells that are metabolically active and have high rates of protein synthesis.

The importance of c-Myc as a proto-oncogene in lymphomas was first noticed in Burkitt's lymphomas, where *c-Myc* was mutated due to translocations of the gene (Taub et al. 1982; Dalla-Favera et al. 1982). *c-Myc* translocations t(8;14)(q24;q11) between *c-Myc* and *Tcra* chain are relatively infrequent in human T-ALL (less than 1%) (Shima et al. 1986; Erikson et al. 1986), however the overexpression of c-Myc protein is commonly observed in T-ALL. One mechanism by which *c-Myc* mRNA is overexpressed is via Notch1 activation (Palomero et al. 2006; Weng et al. 2006). Another mechanism by which malignant cells increase the expression of c-Myc protein is by preventing its proteasomal degradation. c-Myc can be phosphorylated on Thr58 and this phosphorylation targets c-Myc for degradation (Welcker, Orian, Jin, et al. 2004b) Thus, inactivating mutations or deletions in E3 ubiquitin ligase, Fbw7, contributes to the formation of T-ALL (O'Neil et al. 2007). Also, in Burkitt's lymphoma, the Thr58 site on c-Myc is frequently found to be mutated leading to stabilization of c-Myc protein (Bhatia et al. 1993). Due to the frequent c-Myc mutations in T cell leukaemia, its role in tumourigenesis was already studied. It was shown that the inhibition of bromodomain (a potent regulator of c-Myc expression) that downregulate *c-Myc* transcription or deletion of c-Myc by shRNA in leukaemia initiating cells led to impaired proliferation of malignant cells (Schubbert et al. 2014; Roderick et al. 2014). Moreover, genetic ablation of *c-Myc* in PTEN null haematopoietic cells prevents tumourigenesis, arguing for the critical role of c-Myc (J Zhang et al. 2011).

1.6 Aims of thesis

Deletion of PTEN selectively in T cell progenitors in the thymus results in the rapid development of aggressive T cell lymphomas in a mouse model for T-ALL. In the present thesis we will use this mouse model of T-ALL to explore the signaling pathways that control metabolism in T-ALL. Normal T cells precisely regulate expression of key nutrient receptors, in particular they tightly regulate expression of LNAA (e.g. leucine), glutamine and glucose transporters as well as transferrin receptor. The aim of the present study was to examine the regulation of the nutrient uptake in PTEN null T-ALL and to address the relative contributions of PI3K/AKT, mTORc1 and Hif1α in the metabolism of these cells.

In the first part we will explore what is the capacity of PTEN null T-ALL to take up leucine, glutamine, glucose and transferrin. Once we have established the metabolic status of the PTEN T-ALL, we will examine whether PTEN deletion is sufficient to initiate uptake of key nutrients. For this question, we will utilise leukaemic T cells isolated from tumour bearing $PTEN^{fl/fl}$ x Lck^{Cre+} mice and non-transformed thymocytes isolated from tumour free $PTEN^{fl/fl}$ x Lck^{Cre+} mice.

A key question is the role of mTORc1 and Hif1α in controlling T-ALL metabolism. Therefore in the second part of this thesis we want to understand if mTORc1 is active in PTEN null leukaemic T cells. Furthermore, we will evaluate if mTORc1 can drive the metabolism in PTEN null T-ALL cells and also, if and when Hif1α is expressed and whether its expression is mTORc1-dependent.

Finally, given the importance of Hif1α in regulating glucose metabolism and glycolysis and the fact that the increased glucose uptake is the hallmark of increased metabolism, we will examine how deletion of Hif1α in $PTEN^{fl/fl}$ x Lck^{Cre+} mice contributes to the development of T cell leukaemia/lymphoma cells.

2 Chapter: Materials and Methods

2.1 Transgenic mice

2.1.1 PTEN$^{fl/fl}$ x Lck$^{Cre+/-}$ mice

PTEN$^{fl/fl}$ mice, in which LoxP sites flank exon 5 of the *Pten* gene, were generated and described by Hagenbeek at al. (Hagenbeek et al. 2004). To delete PTEN, PTEN$^{fl/fl}$ mice were backcrossed with mice expressing Cre recombinase under the control of the proximal Lck promoter. This allows for deletion of flanked PTEN in early T cell progenitors in the thymus (the deletion is completed by the DN3 stage of thymus development). Mice used in experiments: PTEN$^{-/-}$ non-transformed thymocytes were obtained from PTEN$^{fl/fl}$ x Lck^{Cre+} mice culled before 6th week of age and hence before development or symptoms of tumours. PTEN$^{-/-}$ T cell lymphoma/leukaemia cells were isolated from PTEN$^{fl/fl}$ x Lck^{Cre+} mice culled when the signs of tumour occurred and typically included hunched posture, rough coat, lack of mobility and/or swollen abdomen/neck. As controls, mice with the genotypes PTEN$^{fl/fl}$ x Lck^{Cre-} or PTEN$^{wt/wt}$ x Lck^{Cre+} (WT) were used.

2.1.2 Hif1α$^{fl/fl}$ x Lck$^{Cre+/-}$ mice

Hif1α$^{fl/fl}$ mice, in which LoxP sites flank exon 2 of the *Hif1α* gene, were purchased from the Jackson Laboratory™. Hif1α$^{fl/fl}$ mice were backcrossed with mice expressing Cre recombinase under the control of the proximal Lck promoter, which allows for deletion of flanked Hif1α in early T cell progenitors. To examine the role of Hif1α in T cells, Hif1α$^{fl/fl}$ x Lck^{Cre+} mice were compared to Hif1α$^{wt/wt}$ x Lck^{Cre+} or Hif1α$^{fl/fl}$ x Lck^{Cre-} (WT).

2.1.3 PTEN$^{fl/fl}$ x Hif1α$^{fl/fl}$ x Lck$^{Cre+/-}$ mice

PTEN$^{fl/fl}$ x Hif1α$^{fl/fl}$ x Lck$^{Cre+/-}$ mice were generated by crossing mice with floxed PTEN alleles, floxed Hif1α alleles, and mice expressing Cre recombinase under the control of the proximal Lck promoter. To establish the role of Hif1α in PTEN null mice, PTEN$^{-/-}$ x Hif1α$^{-/-}$ T cell lymphoma/leukaemia cells from PTEN$^{fl/fl}$ x Hif1α$^{fl/fl}$ x Lck^{Cre+} mice were compared to WT thymocytes from PTEN$^{fl/fl}$ x Hif1α$^{fl/fl}$ x Lck^{Cre-} mice (WT). PTEN$^{fl/fl}$ x Hif1α$^{fl/fl}$ x Lck^{Cre+} mice were culled when the signs of tumour occurred and typically included hunched posture, rough coat, lack of mobility and/or swollen abdomen/neck.

2.1.4 Mice maintenance

All mice in this study were bred and maintained in the Wellcome Trust Biocentre Transgenic Resource Unit, University of Dundee in compliance with UK Home Office Animals (Scientific Procedures) Act 1986 guidelines.

2.2 Cell culture

2.2.1 Reagents

- Hamster-anti-mouse CD3 (2C11), R&D Systems/CRUK hybridoma unit
- anti-CD28 antibody, Life technologies
- β-mercaptoethanol, Sigma
- Fetal bovine serum, Life Technologies
- Penicilin/Streptomycin, Life Technologies
- Recombinant human IL-2 (Proleukine®), Novartis

- RPMI (Rosewell Park Memorial Institute) 1640 (+L-glutamine, +glucose), Life Technologies
- RPMI (Rosewell Park Memorial Institute) 1640 (-glutamine, +glucose), Life technologies
- DMEM (Dullbecco's Modified Eagle's Medium), Life Technologies
- α-MEM (Minimum Essential Medium eagle-α), Life Technologies
- IMEM (Iscove's Modified Dulbecco's Medium), Life Technologies
- HBSS (Hank's Balanced Salt Solution), Life Technologies

2.2.2 Cell culture media and solutions

T-ALL medium: IMEM with 10% (v/v) FBS, 100 U/ml penicillin-G and 100 μg/ml streptomycin.

Thymocyte medium: DMEM, 10% (v/v) FBS, 100 μM β-mercaptoethanol, 100 U/ml penicillin-G, 100 μg/ml streptomycin.

OP9 medium: α-MEM, 20% (v/v) FBS, 100 μM β-mercaptoethanol.

Glutamine free medium: RPMI 1640 pre-supplemented with 25 mM glucose, 10% (v/v) FBS, 100 U/ml penicillin-G, 100 μg/ml streptomycin.

Amino acid free medium: HBSS, 10% (v/v) FBS, 100 U/ml penicillin-G, 100 μg/ml streptomycin.

CTLs medium: RPMI 1640 pre-supplemented with 25 mM glucose and 300 mg/mL L-glutamine, 10% (v/v) FBS, 100 μM β-mercaptoethanol, 100 U/ml penicillin-G, 100 μg/ml streptomycin.

ACK (Ammonium-Chloride-Potassium) buffer, to lyse red blood cells: 155 mM ammonium chloride, 10mM potassium bicarbonate, 0.1 mM ethelenedieaminetetraacetic acid (EDTA). The buffer was adjusted to pH 7.8 and autoclaved.

2.2.3 *In vitro* T-ALL cell culture

The $PTEN^{-/-}$ T leukemic cell lines, F04, F07 and F15, were maintained at $0.3x10^6$ cells/ml in T-ALL medium incubated at 37°C with 5% CO_2. To investigate nutrient deprivation, cells were switched to Glutamine-free medium or Amino acid-free medium and incubated at 37°C with 5% CO_2. To subject cells to hypoxic conditions, cells were cultured at 37°C with 5% CO_2 and 1% O_2.

2.2.4 *In vitro* thymocytes cell culture

Thymi were obtained from age- and sex- matched WT and $PTEN^{fl/fl}$ x Lck^{Cre+}, $Hif1\alpha^{fl/fl}$ x Lck^{Cre+} or $PTEN^{fl/fl}$ x $Hif1\alpha^{fl/fl}$ Lck^{Cre+} mice. To obtain a single cell suspension, the thymi were passed through a 70μm cell strainer. Thymocytes were maintained at $10x10^6$ in Thymocyte medium at 37°C with 5% CO_2. To subject the thymocytes to hypoxic conditions, cells were cultured at 37°C with 5% CO_2 and 1% O_2.

2.2.5 *In vitro* OP9 cultures generation

OP9-DL1 system allows the assessment of Notch responsiveness in pre-T cells *in vitro*. OP9 bone marrow stromal cells expressing the Notch ligand OP9-DL1 (Schmitt et al, 2004b) and control OP9 cells were a gift from Juan Carlos Zuniga- Pflucker (Toronto, Canada). OP9 cells were maintained in the OP9 medium. DN thymocytes were purified using CD4+ and CD8+ T cell isolation kits (Miltynei Biotec) and were co-cultured on OP9 and OP9-DL1 monolayers for the required duration of culture. On the day of harvest, thymocytes were filtered through 50 μm filters to remove OP9 cells.

2.2.6 *In vitro* cytotoxic T cell generation

Spleens and lymph nodes were obtained from age and sex matched WT and $PTEN^{fl/fl}$ x Lck^{Cre+}, $Hif1\alpha^{fl/fl}$ x Lck^{Cre+} or $PTEN^{fl/fl}$ x $Hif1\alpha^{fl/fl}$ Lck^{Cre+} mice and passed through a 70μm cell strainer to disaggregate the cells. Red blood cells were lysed by treating the cell suspension with 5 ml of ACK buffer for less than a minute. Cells were then washed and resuspended in CTLs medium. T cells were activated by addition of 500 ng/mL 2C11 and 4 ng/mL αCD28 in the presence of 20 ng/mL IL-2. After 48 hours, cells were washed and resuspended in CTLs medium with 20 ng/mL IL-2. The following day, CD8+ cells were purified using a CD8+ T cell isolation kit (Miltynei Biotec). Following purification the cells were washed and resuspended in CTLs medium and maintained in exponential growth with 20 ng/mL IL-2 for a further 4 days.

2.2.7 Auto MACS purification of CD8+ T cells

CD8+ T cells or DN thymocytes were isolated from a spleen or thymus cell suspension using an auto MACS CD8+ T cell isolation kit or CD8+ and CD4+ isolation kit, respectively. The cells of interest were isolated by depletion of non-labelled cells (negative selection). The cell suspension was indirectly labelled with a cocktail of biotin-conjugated monoclonal antibodies binding to the unwanted cells. Following incubation with the antibodies, the cells to be deleted were magnetically labelled with streptavidin-beads. Then, using MACS columns and a MACS separator, magnetic separation was performed. During the separation the magnetically labelled non-CD4+/CD8+ T cells were depleted by their retention on a MACS column in the magnetic field of a MACS separator, while the unlabelled T cells pass through the column. The non-labelled cells were collected and the purity was tested by flow cytometry analysis.

2.2.8 Inhibitor treatments and stimulations

Where indicated cells were treated with inhibitors at the following concentrations:

- Rapamycin at 20 nM
- AKT inhibitor VIII (AKTi) at 1μM
- Phorbol ester at 25 ng/ml
- Pervanadate at 100 μM

2.3 Assessment of Hif1α^{fl} and PTEN^{fl} deletion

2.3.1 DNA extraction

DNA was extracted from 1-5x10^6 WT thymocytes or tumours isolated from PTEN$^{fl/fl}$ x Hif1α$^{fl/fl}$ x Lck^{Cre+} mice using the Ultra Clean® Tissue & Cells DNA isolation kit, as per the manufacturer's instructions. The concentration of the extracted DNA was determined using a Nanodrop spectrophotometer (Thermo Scientific).

2.3.2 Assessment of deletion by PCR

Deletion of exon 2 in Hif1α and exon 5 in PTEN was assessed by PCR of 50 ng DNA using the following primers:

- Hif1α loxP F: GCCTTACCTAGTAAAGCAAG
- Hif1α loxP R: GCAAAGAATCTTGGTGTTAC
- Hif1α R: GCGCTGCTGGAAACAATCACAAGAA
- PTEN loxP F: GGTGCTGGTGTCCAAAATGT
- PTEN loxP R: GGGCAGTACTGGAAAGATGG
- PTEN R: ATAGCTATTAGTGTCTTAACCTGCCC

2.4 Flow cytometric analysis

Flow cytometric data were obtained using a FACS Verse or a FACS LSRII Fortessa. The collected events were stored without gates and the data were analysed using FlowJo version 9.6.4 data analysis software (Tree star inc.).

2.4.1 Reagents for flow cytometry

- HBSS, Life Technologies
- Phosphate buffered saline (PBS) tablets, Sigma
- Fetal bovine serum, Life Technologies
- Methanol, VWR International
- Paraformaldehyde, Sigma
- DMEM, Life technologies
- Bovine serum albumine (BSA), Sigma
- Transferrin, Alexa Fluor conjugate, Invitrogen
- Holo-transferrin, Sigma
- DAPI, Invitrogen

2.4.2 Solutions for flow cytometry

FACS buffer: 0.5% (v/v) FBS in HBSS

Fixing buffer: 1% (w/v) paraformaldehyde in water

Permeabilization buffer: 90% (v/v) methanol in water

Transferrin free medium: DMEM with 5% (w/v) BSA, 100 μM β-mercaptoethanol, 100 U/ml penicillin-G, 100 μg/ml streptomycin

Acid wash: 150mM NaCl, 20 mM citric acid, adjusted to pH 5.0

2.4.3 Cell counting by flow cytometry

Cells were resuspended in PBS and counted using the Verse Flow cytometer. The number of cells per 1 ml was calculated as follows: cells/volume x dilution x 10^6.

2.4.4 Antibodies for flow cytometry

Antibodies recognising specific targets (see Table 1.1) were directly conjugated to the flurophores: Fluorescein Isothiocyanate (FITC), R-Phycoerythrin (PE), Allophycocyan (APC), Peridinin-chlorophyll proteins (PerCP), Briliant Violet (BV), Horizon V450 (HV450).

Antibodies and working dilution	**Clone/ catalogue number**	**Company**
Thy1.1 (FITC) 1:200, (APC) 1:400, (BV510) 1:200	53-2.1, HIS51	Pharmingen, eBioscience, Biolegend
Thy1.2 (APC) 1:400	HIS51	eBioscience
CD8α (FITC, PE, PerCP-Cy5.5, APC, HV450, BV510) 1:200	53-6.7	Pharmingen, Biologened
CD4 (PECy7, BV605) 1:200	RM 4-5	Pharmingen, Biolegend
B220 (HV500) 1:200	RA3-682	BD Horizon
TCRβ (PerCP Cy5.5, APC ef 780) 1:200	H57-597	eBioscience
CD25 (FITC, PECy7) 1:200	7D4, PC61	Pharmingen
CD44 (APC ef780) 1:200	IM7	Pharmingen
CD71 (PE, APC) 1:200	C2, R17217	eBioscience Pharmingen
CD98 (PE) 1:200	RL388	eBioscience
CD24 (PerCP Cy5.5) 1:200	M1/69	eBioscience
Alexa-647 conjugated transferrin 1:100	T23366	Invitrogen
pS6 (Ser235/236) 1:100	#4558	Cell Signaling Technology
Alexa-647 conjugated anti-rabbit 1:5000	711605152	Jackson ImmunoReaserach
FITC conjugated anti-rabbit 1:100	111095003	Jackson ImmunoReaserach

Table 1 Flow cytometry antibodies and their conjugates

2.4.5 Live cell staining

Cells (1-3x10^6) were stained at previously determined saturating concentrations of antibody at 4ºC for a minimum of 5 minutes in FACS buffer. Cells were washed and resuspended in FACS buffer prior to acquisition. A minimum of 20000 relevant events was collected. Live cells were gated according to their forward scatter (FCS) and side scatter (SSC) profiles or, when analysing transferrin uptake or cell cycle, the live cells were identified as DAPI negative populations (1µg/ml of DAPI).

2.4.6 Analysis of intracellular phospho-S6 staining/levels in fixed cells

Ex vivo isolated thymocytes were either left untreated or stimulated with 20 nM rapamycin or 25 ng/ml Phorbol ester at 37ºC for 30 minutes prior to staining. Cells were stained for the cell surface markers Thy1, CD4 and CD8 for 5 minutes, before being fixed in fixing buffer at 37ºC for 15 minutes and permeabilised with permeabilization buffer at -20º C for at least 60 minutes. Cells were washed twice after permeabilization and incubated with primary antibody against pS6 (Ser235/236) at RT for 30 minutes. Cells were again washed twice and incubated with secondary antibody: either FITC conjugated anti-rabbit or Alexa -647 conjugated anti-rabbit secondary antibodies at RT for another 30 minutes. Cells were washed twice, resuspended in FACS buffer prior to acquisition. A minimum of 20000 relevant events was collected.

2.4.7 Transferrin uptake assays

Ex vivo isolated thymocytes (1x10^6 cells) were incubated in filtered, pre-warmed Transferrin free medium at 37º C for 2 hours. Next, cells were resuspended in 100 µl

of 0.5% (w/v) BSA/DMEM and treated as follows: left untreated at 37° C, treated with 5 μg/ml transferrin with or without 500 μg/ml holo-transferrin, or treated with 5 μg/ml transferrin on ice. Transferrin uptake was measured over a 10 minutes period. Uptake of transferrin was stopped by placing cells on ice, after which they were washed twice with acid wash to strip surface-bound transferrin. The cells were then resuspended in FACS buffer. Cell surface staining for the Thy1, CD4, CD8, and CD71 was then performed and transferrin uptake was quantified from the fluorescence emission at 647 nm.

2.4.8 Cell cycle analysis

Ex vivo isolated thymocytes ($5x10^6$ cells) were incubated with 10 μg/ml Hoechst-33342 (Molecular probes) in DMEM with 1% (v/v) FBS at 37º C for 30 minutes. Next, cells were stained for the surface markers Thy1, CD4 and CD8 as described before. Immediately before analysis, cells were resuspended in FACS buffer containing 1μg/ml DAPI. Data were analysed using doublet discrimination module and fitted to the Watson-pragmatic model (Watson et al. 1987).

2.4.9 Fluorescence Activated Cell Sorting (FACS)

FACS was performed on a BD Influx™ Cell Sorter by Dr Rosemary Clarke or Arlene Wigham, University of Dundee. *Ex vivo* isolated thymocytes were stained for the surface markers Thy1, CD4, CD8 as described and prior to sorting cells were resuspended in FACS buffer containing 1μg/ml DAPI. Double positive thymocytes were sorted.

2.5 Metabolic assays

2.5.1 Measurements of glucose, glutamine or leucine uptake.

2.5.1.1 Reagents

- RPMI 1640 (+glutamine, -glucose), Life technologies
- RPMI 1640 (-glutamine, +glucose), Life technologies
- HBSS, Life technologies
- Deoxy-D-glucose, 2-[1,2-^{3}H(N)]-, Perkin Elmer
- L-[3,4-^{3}H(N)]-Glutamine, Perkin Elmer
- L-[3,4,5-^{3}H(N)]-Leucine, Perkin Elmer

1.5.1.2 Glucose analogue/glutamine/leucine uptake assay

Glucose, glutamine and leucine uptakes were performed in the same manner, with the uptake of nutrients being measured over 4 minute periods. A total of $4x10^{6}$ of *ex vivo* isolated thymocytes were washed and re-suspended in 800 µl of glucose-free, FCS-free medium (glucose uptake) or FCS-free HBSS (glutamine/leucine uptake) as appropriate. Then, $1x10^{6}$ thymocytes, in 200 µl of the appropriate medium, were loaded on top of 500 µl phthalatediisononylester oil (Sigma-Aldrich) mixed in 1:1 ratio with poly(dimethyloiloxane-co-methyl-phenylsiloxane) oil (Sigma-Aldrich) containing 200 µl of 0.5 µCi/ml deoxy-D-glucose, 2-[1,2-^{3}H(N)]- in glucose-free medium or 0.5 µCi/ml L-[3,4-^{3}H(N)]-Glutamine in HBSS or 0.5 µCi/ml L-[3,4,5-^{3}H(N)]-Leucine in HBSS. After 4 minutes of exposure to the radiolabelled nutrients, cells were spun at 8000 rpm for 3 minutes and washed twice with deionised water to remove the excess of oil. Cell pellets were lysed with 200 µl of 1M NaOH, and the

incorporated ^{3}H radioactivity was quantified via liquid scintillation counting using a Beckman LS 6500 Scintillation Counter. Each condition was performed in triplicate.

2.5.2 Measurement of lactate production

2.5.2.1 Reagents

- Glycine, Sigma-Aldrich
- Hydrazine monohydrate, Sigma-Aldrich
- β- Nicotinamide adenine dinucleotide hydrate (NAD+), Sigma-Aldrich
- Rabbit muscle lactate dehydrogenase VII (LDH), Sigma-Aldrich
- L- Lactate, Sigma-Aldrich

1.5.2.2 Lactate production assay

The lactate assay is based on a colorimetric reaction in which L(+)-lactate is oxidised by lactate dehydrogenase (LDH) that exhibits a maximum absorbance at 450 nm. For measuring lactate output, $1x10^{6}$ *ex vivo* isolated thymocytes were washed, resuspended in DMEM medium containing 10% (v/v) dialysed FCS and cultured for 4 hours. After this time, cells were pelleted down and supernatant collected and stored at -80ºC. For the lactate standard curve, sodium lactate at concentration of 40 mM was used to make 2-fold serial dilutions. 100 µl of cell supernatants and standards were added in triplicates into a 96-well plate and mixed with 100 µl of a master-mix reaction containing: 320 mM glycine, 320 mM hydrazine, 2.4 mM NAD+ and 3U/ml LDH. The plate was then incubated at 25ºC for 10 minutes and the absorbance was read in a cytofluor II Fluorescence Multi-Well Plate Reader (Perceptive BioSystems), excitation 360 nm, emission 460 nm, gain 45x. Lactate

content was determined by subtracting the background signal from all readings and then constructing a standard curve of log[lactate] versus absorbance, fitted using a sigmoidal model.

2.6 SDS-PAGE and Western blotting

2.6.1 Reagents

- 4x LDS sample buffer, Life Technologies
- cOmplete protease inhibitor cocktail, Roche
- Powdered non-fat milk, Marvel
- TCEP (tris(2-carboxyethyl)phosphine), Thermo

2.6.2 Solutions

RIPA lysis buffer: 50 mM HEPES pH 7.4, 150 mM NaCl, 1% (w/v) NP-40, 0.5% (w/v) sodium deoxycholate, 0.1% (w/v) SDS, 10% (w/v) glycerol, 1 mM EDTA, 1 mM EGTA, 50 mM NaF, 5 mM sodium pyrophosphate, 10 mM sodium β-Phosphoglycerate, 0.5 mM sodium orthovanadate, 1 mM neutralised TCEP, with 1 tablet cOmplete Protease inhibitor Cocktail tablet per 10 ml

Tris lysis buffer: 50 mM NaCl, 10 mM Tris-HCl pH 7.05, 30 mM sodium pyrophosphate, 50 mM NaF, 5 μM $ZnCl_2$, 10% (w/v) glycerol, 0.5% (w/v) Triton, 1 mM neutralised TCEP, with 1 tablet cOmplete Protease inhibitor Cocktail tablet per 10 ml

SDS-PAGE gel (resolving): 8 or 10% acrylamide, 0.1% (w/v) SDS, 0.375 M Tris-HCL pH 8.8

SDS PAGE gel (stacking): 4% acrylamide, 0.1% (w/v) SDS, 0.125 M Tris-HCl pH 6.8

Transfer buffer: 48 mM Tris, 39 mM glycine in 20% (v/v) methanol

PBS-T: phosphate buffered saline (PBS), 0.05% (w/v) Tween-20

Ponceau S: 0.1% Ponceau S, 0.5% (v/v) acetic acid

2.6.3 Antibodies

Antibodies (see Table 2) were diluted in 5% (w/v) non-fat milk in PBS-T or in 5% (w/v) BSA.

Antigen	catalogue number	Company
PTEN	sc-7974	Santa Cruz Biotechnology, Inc.
pAkt (T308)	#4056	Cell Signalling Technology
pAkt (S473)	#4058	Cell Signalling Technology
pan Akt	#9272	Cell Signalling Technology
S6K (T389)	#9239	Cell Signalling Technology
pan S6K	#9202	Cell Signalling Technology
Hif1 alpha	241809	R&D Systems
Hif1 beta	sc-8076	Santa Cruz Biotechnology, Inc.
c-myc	#9402	Cell Signalling Technology
pan S6	#2317	Cell Signalling Technology
Smc1	A300-055A	Bethyl Laboratries, Inc.
pPRAS40 (T246)	#13175	Cell Signalling Technology
pan PRAS40	#2691	Cell Signalling Technology
pTSC2 (T1462)	#3611	Cell Signalling Technology
pan TSC2	#4308	Cell Signalling Technology
cleaved Notch1 (Val1744)	#4147	Cell Signalling Technology

Table 2 Western blot antibodies

2.6.4 Sample preparation, SDS-PAGE and Western blotting

Cells were washed with ice cold PBS and lysed in Tris buffer or RIPA buffer at $40x10^6$ cells/ml (for thymocytes) or $20x10^6$/ml (for CTLs) on ice for 15 minutes and then sonicated with a Branson Digital Sonicator to shear DNA. The lysates were then spun down in a refrigerated bench mini centrifuge at 14000 rpm for 15 minutes to remove non-soluble proteins. Samples were then mixed with 4x LDS buffer and TCEP, and incubated in 95ºC for 5 minutes to denature and reduce the proteins. Samples were loaded on a SDS-PAGE gel with a fixed acrylamide concentration of 8 to 12% depending on the molecular weight of the proteins to be analysed. A Mini-

Protean system (Bio-Rad) was used for electrophoresis and blotting of proteins. Samples were run at a fixed voltage of 100 V for 120 minutes or until the running dye from the sample buffer had left the gel. The proteins were then transferred onto Hybond-N membranes (GE Healthcare) on ice for 90 minutes. Transfer and equal loading was confirmed with Ponceau S staining. The membrane was washed with water and was then blocked with 5% (w/v) milk in PBS-T or 5% (w/v) BSA in PBS-T at RT for 60 minutes. Blots were probed with primary antibodies, at optimised concentrations (1 μg/ml in most cases), diluted in 5% (w/v) milk in PBS-T or 5% (w/v) BSA in PBS-T at 4ºC overnight. Membranes were then washed three times with PBS-T at RT for 10 minutes then incubated with HRP tagged secondary antibody diluted in 5% (w/v) milk in PBS-T or 5% (w/v) BSA in PBS-T (1:5000) for 60 minutes. Membranes were washed three times with PBS-T at RT for 20 minutes before detected proteins were visualised using ECL.

2.7 Quantitative Mass Spectrometry

2.7.1 Reagents

- Deepwell Plate 96/500, Lo Bind, Eppendorf
- Deepwell Plate 96/1000, Lo Bind, Eppendorf
- Pierce Detergent Removal Spin Plates, Thermo
- Sep-Pak C18 SPE cartridges, Waters
- Sep-Pak tC18 96-well μElution plate, Waters

2.7.2 Solutions

Urea buffer lysis: 8 M urea, 100 mM Tris-HCl, pH 8.0 with 2x cOmplete protease inhibitor tablet and 1x PhosStop phosphatase inhibitor tablet per 10 ml.

Digest buffer: 100 mM Tris-HCl pH 8.0, 0.1 mM $CaCl_2$

Desalting wash buffer: 0.1% (v/v) TFA

Desalting elution buffer: 0.1% (v/v) TFA, 50% (v/v) acetonitrile

SAX buffer: 10 mM sodium borate, pH 9.3, 20% (v/v) acetonitrile

2.7.3 Sample lysis and in solution digest

Ex vivo isolated thymocytes from $PTEN^{fl/fl}$ x Lck^{Cre-} (WT) mice and tumour cells from $PTEN^{fl/fl}$ x Lck^{Cre+} mice were purified using Dead cell removal kit (Miltynei, Biotec) according to manufacturer's protocol. $20x10^6$ isolated cells were washed three times with cold HBSS and transferred into a 2.0 ml Lo Bind Eppendorf tube. Cells were lysed in 0.2 ml of urea lysis buffer and vigorously mixed at RT for 15 minutes. The samples were then sonicated with a Branson Digital Sonicator and mixed for another 15 minutes. The protein concentration was determined by BCA assay as per manufacturer's instructions. DTT, at a working concentration of 10 mM, was added to reduce cysteines and the samples were incubated at 30ºC for 30 min. Then, IAA was added, at a working concentration of 50 mM, and lysates were incubated in the dark at RT for 45 minutes to alkylate the sulfhydryl groups of the cysteines. Lysates were diluted with digest buffer to 4 M urea. LysC was added to the samples in a 50:1 (protein:LysC) ratio, and the samples were incubated at 30ºC overnight. The samples were then diluted to 0.8 M urea with digest buffer and trypsin

was added in a 50:1 (protein:trypsin) ratio to the samples. The samples were then incubated for further 8 hours at 30ºC before the resulting peptides were desalted.

2.7.4 Sample desalting using Sep-Pak cartridges

Samples were adjusted to 1% (v/v) TFA using 10% (v/v) TFA. The Sep-Pak cartridges were washed twice with 1 ml elution buffer and equilibrated twice with 1 ml wash buffer before the acidified peptide samples were loaded. The flow through was loaded again to ensure maximal peptide binding. The peptide-loaded cartridges were washed three times with 1 ml washing buffer. Peptides were eluted into 2.0 ml Eppendorf tubes by two elutions of 600 µl elution buffer. The eluted peptides were reduced to dryness in a vacuum concentrator.

2.7.5 Strong anion exchange chromatography

The dried peptides were resuspended in 210 µl SAX buffer and the pH was readjusted to 9.3 with 1 M NaOH if necessary. Samples were injected and peptides separated by a Dionex Ultimate 3000 HPLC system equipped with an AS24 strong anion exchange column, using a similar protocol to the hSAX method described previously (Ly et al. 2014). Peptides were chromatographed using a borate buffer system, namely 10 mM sodium borate, pH 9.3 (Buffer A) and 10 mM sodium borate, pH 9.3 + 0.5 M sodium chloride (Buffer B) and eluted using an exponential elution gradient into 12 fractions of 750 µl.

2.7.6 Desalting with tC18 Sep-Pak 96-well plate

Fractions from the strong anion exchange chromatography were adjusted to 1% (v/v) TFA with 10% (v/v) TFA. Each well of the desalting plate was washed with 0.2 ml acetonitrile and equilibrated with 0.2 ml desalting buffer. The samples were then slowly applied onto the columns and washed first with 0.8 ml and then with 0.2 ml of the desalting wash buffer. The samples were then eluted into an Eppendorf 1000µl 96-well plate with 0.2 ml desalting elution buffer. Samples were reduced to dryness in a vacuum concentrator.

2.7.7 Liquid chromatography mass spectrometry (LC-MS/MS)

Samples from desalting were resuspended at a concentration 0.066 µg/µl in 5% formic acid and 15 µl was used for analysis. Peptide chromatography was performed using Dionex RSLCnano HPLC. Peptides were loaded onto a 0.3 mm id x 5 mm Pep-Map-C18 column using the following mobile phases: 2% acetonitrile + 0.1% formic acid (Solvent A) and 80% acetonitrile + 0.1% formic acid (Solvent B). The linear gradient began with 5% B to 35% B over 156 minutes with a constant flow of 300 nl/min. The peptide eluent flowed into nanoelectrospray emitter at the front end of a Velos Orbitrap mass spectrometer (Thermo Fisher, San Jose, CA). A typical ‘Top15’ acquisition method was preformed. Briefly, the primary mass spectrometry scan (MS1) was performed in the Orbitrap at 60000 resolution. Then, the top 10 most abundant m/z signals were chosen from the primary scan for collision-induced dissociation and MS2 analysis in the Orbitrap mass analyser at 17500 resolution. Precursor ion charge state screening was enabled and all unassigned charge states, as well as singly charged species, were rejected.

2.7.8 Mass spectrometric data analysis by MaxQuant

The data were processed, searched and quantified using the MaxQuant software package version 1.4.1.2 as described previously (Cox & Mann 2008), using the default settings and employing the mouse Uniprot database from October 2013 and the contaminants database supplied by MaxQuant. The following settings were used to assign peptides to masses: two miscleavages were allowed; carbamidomethylation on cysteine was treated as a fixed modification; enzymes were specified as Trypsin and LysC; variable modifications included in the analysis were methionine oxidation, deamination of glutamine and aspargine, N-terminal pyroglutamic acid formation, and protein N-terminal acetylation. Default MaxQuant settings included a mass tolerance of 7 ppm was for precursor ions, and a tolerance of 0.5 Da for fragment ions. A reverse database was used to apply a maximum false positive rate of 1% for both peptide and protein identification. This cut-off was applied to individual spectra and whole proteins in the MaxQuant output. The match between runs feature was activated with an allowed time window of 2 minutes. All proteins were quantified on the basis of unique proteins with the requantification enabled.

Further downstream analysis was performed using the proteomic ruler in Persues software (Wisniewski et al. 2014) to calculate the copy numbers of each protein and Microsoft Excel. Student's t-test was performed to determine statistical significance of recurring ratios.

2.8 Data analysis and statistical evaluation

All quantified data were processed in Microsoft Excel. Statistical evaluation was performed using Prism version 6 for Macintosh. Prism was used to generate bar and

line graphs, dot plots, column and survival graphs. Statistical tests used to determine significant differences were two-tailed t-tests for the experiments where the mean of at least 3 biological replicates were included and for the survival kinetics: Log-rank (Mentel-Cox) and Gehan-Breslow-Wilcoxon. Differences were considered significant when $p<0.05$. In figure legends, biological replicate assumes the use of single mouse and independent experiment assumes a replicate of an experiment performed on a different day.

3 Chapter: Nutrient uptake in primary PTEN$^{-/-}$ T cell lymphoma/leukaemia cells

3.1 Introduction

The objective of this study was to study the regulation of nutrient uptake in a mouse model of T-ALL. The model of choice was to use the mice with specific PTEN deletion in T cell progenitors in thymus generated and described by Hagenbeek *at al*., (Suzuki et al. 2001; Hagenbeek et al. 2004; Hagenbeek & Spits 2007). Mice with PTEN alleles floxed with LoxP Cre excision sites were backcrossed with mice that express Lck-cre transgene. The completion of deletion of floxed alleles is finished early during thymocytes development, at the CD4/CD8 double negative (DN3/DN4) stage (Gu et al. 1994). Initially, PTEN null mice show normal thymus development but around 8-10 weeks of age they develop aggressive T cell lymphoma/leukaemias that model T-ALL (Hagenbeek & Spits 2007; Hagenbeek et al. 2004). The PTEN null T cell lymphoma/leukaemia cells disseminate into peripheral lymph nodes and spleen. PTEN$^{fl/fl}$ x Lck^{Cre+} mice die around 17 weeks of age (Finlay et al. 2009; Hagenbeek & Spits 2007). Importantly, T-ALLs have additional, secondary mutations, such as *c-Myc* translocations, IL-7R mutations or Notch activation, which occur around the transformation time making them a good model of human T-ALL (Bonnet et al. 2011; J Zhang et al. 2011; Shochat et al. 2011; Weng et al. 2004; Zenatti et al. 2011).

In this chapter we will explore the nutrient uptake of PTEN$^{-/-}$ T cell lymphoma/leukaemia cells from the PTEN$^{fl/fl}$ x Lck^{Cre+} mice. It is well established

that tumour cells switch to aerobic glycolysis to metabolise glucose and increase glucose uptake to meet their metabolic demands (Hanahan & Weinberg 2011; Vander Heiden et al. 2009). However, change in the uptake of other nutrients is equally important for rapidly proliferating cells. For example elevated glutamine uptake and subsequent glutaminolysis is frequently observed in tumour cells which are considered to be glutamine addicted (Duran et al. 2012; Wise & Thompson 2010). It is known that T cell lymphoma/leukaemia cells have high levels of glucose uptake (Boag et al. 2006; Akers et al. 2011) but very little is known about whether they also increase uptake of other key nutrients such as amino acids and transferrin. Accordingly, we have explored patterns of nutrient uptake in primary $PTEN^{-/-}$ T cell lymphoma/leukaemia cells that develop in $PTEN^{fl/fl}$ x Lck^{Cre+} mice. The control population used was WT thymocytes as these are the best-matched normal, non-transformed T cells for the $PTEN^{-/-}$ T cell lymphoma/leukaemia cells.

3.2 Results

3.2.1 PTEN$^{-/-}$ T cell lymphoma/leukaemia cells

PTEN$^{fl/fl}$ x Lck^{Cre+} mice developed aggressive T cell lymphoma/leukaemias and mice typically became sick and culled once the symptoms occurred, such as hunched posture, rough coat, lack of mobility and/or swollen abdomen/neck. WT mice remained healthy during the course of experiment. The median survival for PTEN$^{fl/fl}$ x Lck^{Cre+} mice was 68 days (Fig. 3-1).

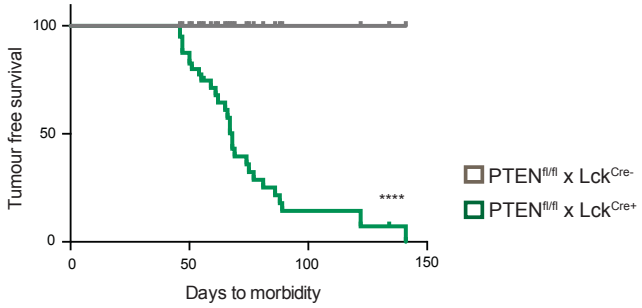

Figure 3-1 **PTEN$^{fl/fl}$ x Lck^{Cre+} mice develop tumours and die prematurely.**

Graph showing the Kaplan-Meier curve for PTEN$^{fl/fl}$ x Lck^{Cre+} and WT mice (PTEN$^{fl/fl}$ x Lck^{Cre-}). In the experiment 40 mice of each genotype were used. Once tumour development was observed in PTEN$^{fl/fl}$ x Lck^{Cre+} mice, they were sacrificed along with age-matched controls (PTEN$^{fl/fl}$ x Lck^{Cre-} mice). If PTEN$^{fl/fl}$ x Lck^{Cre-} mice were tumour free at the time of sacrifice, they were marked as live. **** $p < 0.0001$ was calculated by Log-rank (Mantel-Cox) test and by Gehan-Breslow-Wilcoxon test.

Flow cytometric analysis of forward and side scatter of *ex vivo* isolated PTEN$^{-/-}$ T cell lymphoma/leukaemia cells showed that these cells are large, blast-like cells in comparison to WT thymocytes (Fig. 3-2a). WT thymus typically contained around 120 to 130 million cells whereas the T cell tumours isolated from the PTEN$^{fl/fl}$ x Lck^{Cre+} mice had 3-fold higher cell numbers (Fig. 3-2b).

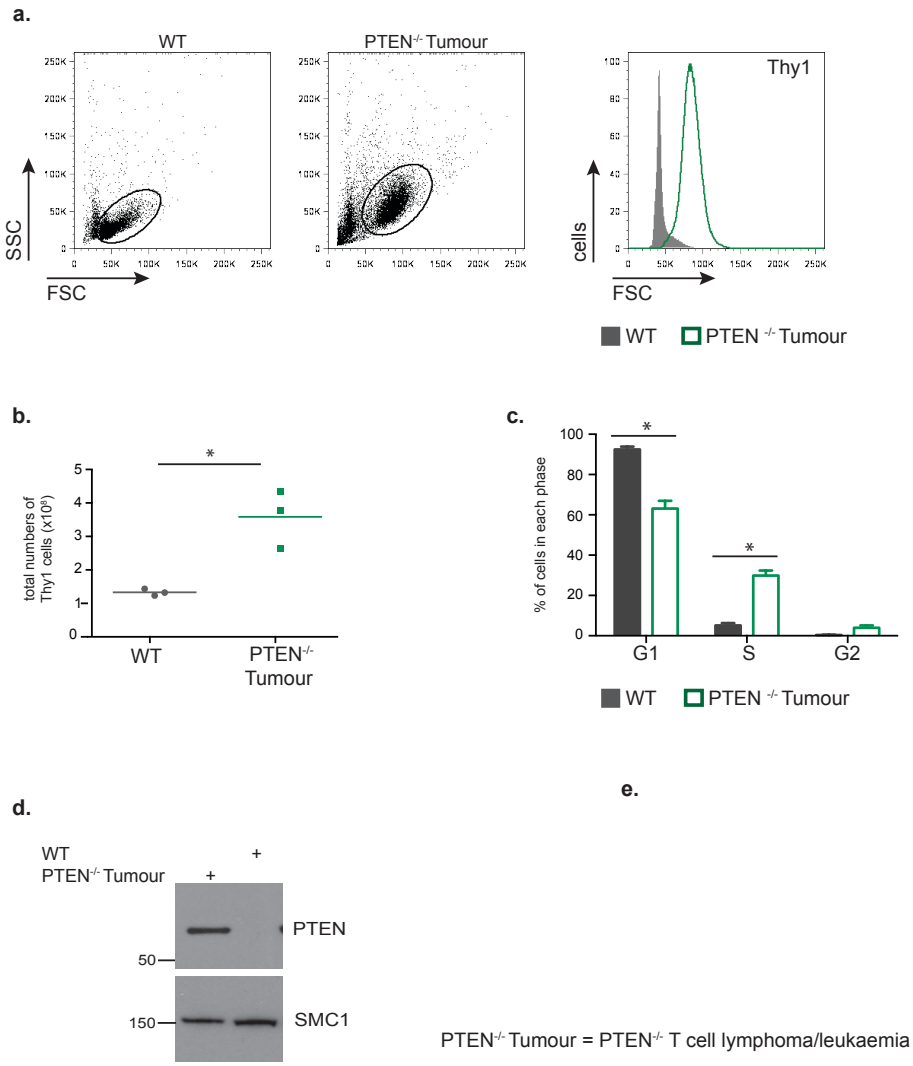

Figure 3-2 **A comparison of the size and cellularity of PTEN$^{-/-}$ T cell lymphoma/leukaemia cells and WT thymocytes.**

a. Flow cytometric analysis of WT thymocytes and PTEN$^{-/-}$ T cell lymphoma/leukaemia cells presented as dot plot graph (left) and histogram of Thy1 positive cells (right) showing their size. **b.** Total numbers of Thy1 positive cells for WT thymocytes and PTEN$^{-/-}$ T cell lymphoma/leukaemia cells. Data are shown as mean from 3 biological replicates from 3 independent experiments; * $p<0.05$ was calculated by t-test. **c.** Graph bar showing the percentage of viable cells in each stage of cell cycle of WT thymocytes and PTEN$^{-/-}$ T cell lymphoma/leukaemia cells. DNA was stained with Hoechst 33342 and non-viable cells excluded with DAPI. Cell cycle populations were determined by fitting the data to the Watson-pragmatic model. Data are shown as mean +/- SD from 3 biological replicates from 3 independent experiments; *$p<0.0001$ was calculated by multiple t-test. **d.** Western blot analysis of WT thymocytes and PTEN$^{-/-}$ T cell lymphoma/leukaemia cells was performed with antibodies against PTEN and SMC1. SMC1 was used as a loading control. Equal numbers of cells were lysed. Numbers represent molecular weights markers and are given in kDa. Data are representative of at least 3 biological replicates.

We also examined the cell cycle status of the *ex vivo* $PTEN^{-/-}$ T cell lymphoma/leukaemia cells. To analyse this, the percentage of cells in each cell cycle phase was assayed by staining with the intracellular DNA of viable WT thymocytes and $PTEN^{-/-}$ T cell lymphoma/leukaemia cells with Hoechst 33342 and then fitted to the Watson-pragmatic model (Watson et al. 1987). This cell cycle analysis showed that the majority of WT thymocytes (approximately 90%) were in G1 phase, around 5% was in S phase and less than 1% were in G2 phase of cell cycle (Fig. 3-2c). In contrast, $PTEN^{-/-}$ T cell lymphoma/leukaemia cells had significantly lower percentage of cells in G1 phase – on average 62% whereas approximately 30% of cells were in S phase and 4% were in G2 phase of cell cycle. Therefore, there was a nearly 6-fold increase in cells in S phase in $PTEN^{-/-}$ T cell lymphoma/leukaemia cells compared to WT thymocytes. These data were consistent with a high proliferative capacity for the $PTEN^{-/-}$ T cell lymphoma/leukaemia cells.

The Western blot analysis in Fig. 3-2d shows that the T cell lymphoma/leukaemia cells from the $PTEN^{fl/fl}$ x Lck^{Cre+} mice failed to express PTEN consistent with the fact that were generated from PTEN null T cell progenitors (Hagenbeek & Spits 2007).

3.2.2 Primary $PTEN^{-/-}$ T cell lymphoma/leukaemia cells show increased glucose uptake compared to WT thymocytes

The increase in cell size of $PTEN^{-/-}$ T cell lymphoma/leukaemia cells could indicate that these cells are more metabolically active than quiescent thymocytes and naïve peripheral T cells. We therefore monitored the cellular uptake of ^{3}[H]-2-Deoxyglucose ([^{3}H] 2-DG) to assess glucose transport in primary *ex vivo* T cell lymphoma/leukaemia cells isolated from the $PTEN^{fl/fl}$ x Lck^{Cre+} mice. As negative

control, we monitored the glucose transport capacity in WT thymocytes that comprise predominantly quiescent CD4/CD8 DPs and SP populations. For a positive control, we monitored glucose uptake in IL-2 maintained cytotoxic T cells (CTLs). Previous studies have shown that these cells have high rates of glucose uptake and high rates of glycolysis (Macintyre et al. 2011; Finlay et al. 2012).

The data showed that *ex vivo* WT thymocytes had very low rates of glucose uptake compared to CTLs. The T cell lymphoma/leukaemia cells from the $PTEN^{fl/fl}$ x Lck^{Cre+} mice had higher rates of glucose uptake compared to WT thymocytes (Fig. 3-3a). The rates of glucose uptake by the $PTEN^{-/-}$ T cell lymphoma/leukaemia cells were almost 2-fold lower than in the CTLs. Similar results were obtained when the ability of $PTEN^{-/-}$ T cell lymphoma/leukaemia cells to take up glucose was expressed per mass of cellular protein rather than per cell number. The analysis showed that T cell lymphoma/leukaemia cells isolated from $PTEN^{fl/fl}$ x Lck^{Cre+} mice increased this process 4 to 8-fold when compared to WT thymocytes.

The high rates of glucose transport by CTLs reflect that these cells upregulate expression of the glucose transporters, Glut1 and Glut3, and are expressed in the range of $6.2x10^4$ molecules of Glut1 and $7.3x10^4$ molecules of Glut3 (Hukelmann et al. 2015). To explore whether increased expression of glucose transporters could explain the increased glucose uptake seen in the T cell lymphoma/leukaemia cells from $PTEN^{fl/fl}$ x Lck^{Cre+} mice we performed an unbiased label-free quantitative (LFQ) mass spectrometry based proteomics analysis of the $PTEN^{-/-}$ T cell lymphoma/leukaemia cells and WT thymocytes. In this experiment we analysed 3 $PTEN^{-/-}$ T cell lymphoma/leukaemia cells and 3 WT biological controls and the

experiment was performed in collaboration with Dr Jens Hukelmann. Full details of the protocols are in the materials and methods.

An average of 6509 proteins were identified in the WT controls and an average of 6552 proteins were identified in PTEN$^{-/-}$ T cell lymphoma/leukaemia cells (Fig. 3-3c). Intensity based absolute quantification (IBAQ) values were used to estimate the abundance of proteins in the cell and the protein copy numbers (Wisniewski et al. 2014). The IBAQ values are derived from the sum of intensities for all MS peaks of all peptides matching one protein and then divided by the number of theoretically observable peptides (Ly et al. 2014). The proteomic analysis did not detect expression of Glut1 in either WT thymocytes or the PTEN$^{-/-}$ T cell lymphoma/leukaemia cells. However expression of Glut3 was detected in both samples. This was a relatively low abundant protein in both the WT and the PTEN$^{-/-}$ T cell lymphoma/leukaemia cell samples but on average the abundance of Glut3 in PTEN$^{-/-}$ T cell lymphoma/leukaemia cells was increased 2-fold compared to WT thymocytes (Fig. 3-3d). In terms of the abundance of Glut3 in the PTEN$^{-/-}$ T cell lymphoma/leukaemia cells compared to the CTL controls, this is difficult to estimate, as the experiments were not carried out at the same time. However, it could be beneficial to perform the Western blot analysis and test the levels of Glut1 and Glut3 expression in WT thymocytes, PTEN$^{-/-}$ T cell lymphoma/leukaemia cells and CTLs.

a.

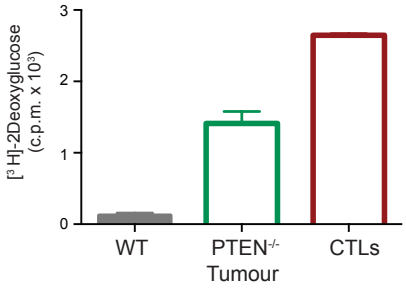

PTEN$^{-/-}$ Tumour = PTEN$^{-/-}$ T cell lymphoma/leukaemia

b.

	size (averaged)	glucose uptake
fold change (normalised to WT)	1.67	7.2 - 15.1
	protein content (averaged)	**glucose uptake**
fold change (normalised to WT)	1.73	4.2 - 8.8

c.

Biological replicate	Proteins detected
WT1	6403
WT2	6562
WT3	6561
KO1	6430
KO2	6668
KO3	6556

KO = PTEN$^{-/-}$ T cell lymphoma/leukaemia

d.

Protein name	Gene name	WT protein abundance	KO protein abundance	fold change
Glut3	Slc2a3	67,275	136,951	2.04

KO = PTEN$^{-/-}$ T cell lymphoma/leukaemia

Figure 3-3 **A comparison of glucose uptake and expression of glucose transporters by PTEN$^{-/-}$ T cell lymphoma/leukaemia cells and WT thymocytes.**

a. *Ex vivo* isolated WT thymocytes and PTEN$^{-/-}$ T cell lymphoma/leukaemia cells and IL-2-maintained CTLs were assayed for ^{3}[H]-2-Deoxyglucose uptake. Units show counts per minute per 1x10^{6} cells. Error bars show SD of 1 biological replicate. Data are representative of 3 biological replicates from 3 independent experiments. **b.** Fold change of glucose uptake by WT thymocytes and PTEN$^{-/-}$ T cell lymphoma/leukaemia cells in units per mass of cellular protein (1mg/ml) normalised to WT thymocytes. The analysis was performed on 3 biological replicates from 3 independent experiments. **c.** The numbers of protein identified in LFQ-MS experiment for WT thymocytes and PTEN$^{-/-}$ T cell lymphoma/leukaemia cells. **d.** Glut3 abundance (IBAQ) identified by LFQ-MS experiment for WT thymocytes and PTEN$^{-/-}$ T cell lymphoma/leukaemia cells (3 biological replicates from 1 experiment).

One way of comparing the tumour data with the historical CTLs data is to say that in CTLs we detected 6792 proteins in total and Glut1 and Glut3 were ranked at 1621 and 1483, respectively (Hukelmann et al. 2015). In the PTEN$^{-/-}$ T cell

lymphoma/leukaemia cells samples we detected 6552 proteins and Glut3 was ranked as the 5410th most abundant protein.

Together, these data argue that the increased glucose transport in the PTEN$^{-/-}$ T cell lymphoma/leukaemia cells was explained by increased expression of Glut3. The fact that rates of glucose transport in the T cell lymphoma were lower than in CTLs could be because the CTLs had high levels of expression of both Glut1 and Glut3 (Hukelmann et al. 2015) whereas the PTEN$^{-/-}$ T cell lymphoma/leukaemia cells had only expressed Glut3.

In CTLs, high rates of glucose uptake fuel glycolysis. In this respect the proteomic data showed that the T leukaemic cells had increased expression of multiple glycolytic enzymes including hexokinase 2, pyruvate kinases, and lactate dehydrogenase compared to the WT thymocytes (Table 3) and their expression was increased by 2 to 7 fold.

Protein name	Gene name	KO1 fold change	KO2 fold change	KO3 fold change
Hexokinase-2	Hk2	3.60	6.67	4.56
Glucose-6-phosphate isomerase	Gpi	2.54	1.28	2.56
6-phosphofructokinase type C	Pfkp	3.37	1.22	1.99
Fructose-bisphosphate aldolase A	Aldoa	4.94	1.94	3.50
Triosephosphate isomerase	Tpi1	2.32	1.68	2.02
Glyceraldehyde-3-phosphate dehydrogenase	Gapdh	1.53	1.89	2.57
Alpha-enolase	Eno1	2.88	1.58	2.54
Pyruvate kinase PKM2	PKM2	2.72	2.15	3.65
Pyruvate kinase PKM1	PKM1	2.54	4.61	2.55
L-lactate dehydrogenase A chain	Ldha	2.58	1.50	2.05

KO = PTEN$^{-/-}$ T cell lymphoma/leukaemia

Table 3 **The expression of glycolytic enzymes by PTEN$^{-/-}$ T cell lymphoma/leukaemia cells compared to WT thymocytes.**

Fold change of the abundance (IBAQ) of enzymes involved in glycolysis identified in LFQ-MS experiment for PTEN$^{-/-}$ T cell lymphoma/leukaemia cells. Data based on 3 biological replicates from 1 experiment. Enzymes are ordered according to their appearance in glycolytic pathway.

The first rate-limiting enzyme in glycolysis is hexokinase 2. We assessed its expression and noted that it was the most upregulated enzyme among the glycolytic enzymes in T cell lymphoma/leukaemia cells isolated from PTEN$^{fl/fl}$ x Lck^{Cre+} mice (Table 3). The other interesting rate-limiting enzyme is pyruvate kinase M2 (PKM2). Overexpression of PKM2 isoform is a hallmark of cancer and other rapidly proliferating cells (Mazurek et al. 2005). We detected expression of PKM2 and PKM1 isoforms. Interestingly, expression of both isoforms was increased in PTEN$^{-/-}$ T cell lymphoma/leukaemia cells compared to WT thymocytes (2 and 3 fold increase, Table 3). However, the PKM2 isoform was much more abundant and ranked as 33rd most expressed protein compared to PKM1 ranked as 3727th most expressed protein in PTEN$^{-/-}$ T cell lymphoma/leukaemia cells. PKM2 was also the most abundant isoform in CTLs and its expression was increased by approximately 60 times over the PKM1 expression (Hukelmann et al. 2015). To validate these data we will test the

expression of rate-limiting enzymes such as PKM1 and PKM2 and HK2 in WT thymocytes, $PTEN^{-/-}$ T cell lymphoma/leukaemia cells and CTLs.

The increased expression of glycolytic enzymes in the $PTEN^{-/-}$ T cell lymphoma/leukaemia cells prompted us to assess their glycolytic capacity and compared it to WT thymocytes and IL-2 maintained CTLs. To do this, we measured how much lactate was produced by the different cells. Figure 3-4a shows that WT thymocytes produced only approximately 60 nmoles of lactate per hour per 10^6 cells in contrast to CTLs, which upregulated this process by 10-fold. $PTEN^{-/-}$ T cell lymphoma/leukaemia cells increased the lactate production by 2-fold compared to WT thymocytes, however, they were not as glycolytic as CTLs that produced approximately 4 times more lactate. The analysis of lactate production expressed per mass of cellular protein of $PTEN^{-/-}$ T cell lymphoma/leukaemia cells in Fig. 3-4b shows an increase of 1.3 fold compared to WT thymocytes. Since both the size and protein fold change of $PTEN^{-/-}$ T cell lymphoma/leukaemia cells compared to WT thymocytes were similar, these data, then, suggested that primary T cell lymphoma/leukaemia cells isolated from $PTEN^{fl/fl}$ x Lck^{Cre+} had increased glycolysis although not as high as CTLs.

a.

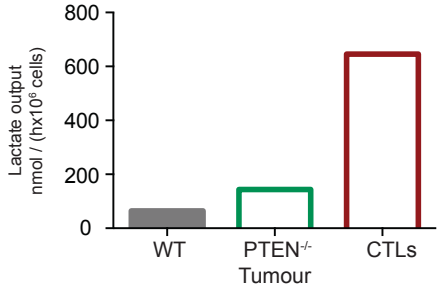

b.

	size (averaged)	lactate output
fold change (normalised to WT)	1.67	2.2
	protein content (averaged)	**lactate output**
fold change (normalised to WT)	1.73	1.3

PTEN$^{-/-}$ Tumour = PTEN$^{-/-}$ T cell lymphoma/leukaemia

Figure 3-4 **A comparison of lactate production by PTEN$^{-/-}$ T cell lymphoma/leukaemia cells and WT thymocytes.**

a. Lactate production by *ex vivo* isolated WT thymocytes, PTEN$^{-/-}$ T cell lymphoma/leukaemia cells and IL-2 maintained CTLs was measured over a period of 4 hours. One million of cells was used. The data are shown as mean from 2 biological replicates from 2 independent experiments. **b.** Fold change of lactate production by WT thymocytes and PTEN$^{-/-}$ T cell lymphoma/leukaemia cells in units per mass of cellular protein (1mg/ml) normalised to WT thymocytes. The analysis was performed on 3 biological replicates from 3 independent experiments.

3.2.3 PTEN$^{-/-}$ T cell lymphoma/leukaemia cells increased glutamine uptake compared to WT thymocytes

The amino acid glutamine is required for protein synthesis and can also be diverted into metabolic intermediates such as pyruvate and lactate or for catabolic processes known as glutaminolysis (R. Wang et al. 2011a; Nakaya et al. 2014; Carr et al. 2010). We then analysed the proteomic data for the PTEN$^{-/-}$ T cell lymphoma/leukaemia cells for expression of glutamine transporters i.e. Slc38a1, Slc38a2 and Slc1a5. The data show that Slc38a1 was increased in abundance in PTEN$^{-/-}$ T cell lymphoma/leukaemia cells (5 to 14-fold) compared to WT thymocytes. There was also an increase in the abundance of Slc1a5 in PTEN$^{-/-}$ T cell lymphoma/leukaemia cells compared to WT thymocytes (2 to 4-fold). In contrast, the expression of Slc38a2 was only increased in one of the PTEN$^{-/-}$ T cell lymphoma/leukaemia cells samples

compared to WT thymocytes. Therefore, it is probable that $PTEN^{-/-}$ T cell lymphoma/leukaemia cells preferentially upregulated expression of Slc38a1 over Slc1a5 or Slc38a2.

We then examined the glutamine transport capacity of $PTEN^{-/-}$ T cell lymphoma/leukaemia cells and compared to WT thymocytes. We used CTLs as positive controls in these experiments. Figure 3-5b shows that e*x vivo* isolated WT thymocytes had low level of ^{3}[H]-Glutamine uptake in contrast to CTLs that showed high rates of glutamine uptake. Primary $PTEN^{-/-}$ T cell lymphoma/leukaemia cells also strikingly increased rates of glutamine uptake compared to WT thymocytes (Fig. 3-5b). Similarly when the ability of $PTEN^{-/-}$ T cell lymphoma/leukaemia cells to take up glutamine was expressed per mass of cellular protein, T cell lymphoma/leukaemia cells isolated from $PTEN^{fl/fl}$ x Lck^{Cre+} mice increased this process 4 to 20-fold when compared to WT thymocytes (Fig. 3-5c).

a.

Protein name	Gene name	WT copy numbers	KO1 copy numbers	KO1 fold change	KO2 copy numbers	KO2 fold change	KO3 copy numbers	KO3 fold change
Snat1	Slc38a1	346	4,920	**14.24**	2,084	**6.03**	1,725	**4.99**
Snat2	Slc38a2	1,155	3,902	**3.38**	2,186	**1.89**	1,785	**1.55**
Asct2	Slc1a5	1,155	4,281	**3.71**	2,347	**2.03**	2,467	**2.14**

KO = PTEN$^{-/-}$ T cell lymphoma/leukaemia

b.

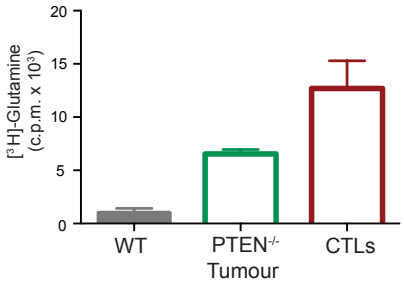

PTEN$^{-/-}$ Tumour = PTEN$^{-/-}$ T cell lymphoma/leukaemia

c.

	size (averaged)	glutamine uptake
fold change (normalised to WT)	1.67	6.6 - 70.6
	protein content (averaged)	**glutamine uptake**
fold change (normalised to WT)	1.73	3.8 - 19.7

Figure 3-5 **A comparison of expression of glutamine transporters and glutamine uptake by PTEN$^{-/-}$ T cell lymphoma/leukaemia cells and WT thymocytes.**

a. Protein copy numbers estimated from IBAQ values identified in LFQ-MS experiment for WT thymocytes and PTEN$^{-/-}$ T cell lymphoma/leukaemia cells and their fold change. Data calculated for 3 biological replicates from 1 experiment. **b.** *Ex vivo* isolated WT thymocytes, PTEN$^{-/-}$ T cell lymphoma/leukaemia cells and IL-2 maintained CTLs were assayed for ^{3}[H]-glucose uptake. Units show counts per minute per 1x10^{6} cells. Error bars show SD of 1 biological replicate. Data are representative of 3 biological replicates from 3 independent experiments. **c.** Fold change of glutamine uptake by WT thymocytes and PTEN$^{-/-}$ T cell lymphoma/leukaemia cells in units per mass of cellular protein (1mg/ml) normalised to WT thymocytes. The analysis was performed on 3 biological replicates from 3 independent experiments.

How important is high glutamine uptake for PTEN$^{-/-}$ T cell lymphoma/leukaemia cells? The primary T cell lymphoma/leukaemia cells from PTEN$^{fl/fl}$ x Lck^{Cre+} mice could not be maintained in culture. However, Hagenbeek *at al.,* have previously derived a PTEN null murine T leukaemic cell line (F15) from T cell lymphoma/leukaemia cells that develop in PTEN$^{fl/fl}$ x Lck^{Cre+} mice (Hagenbeek et al. 2014). We, therefore, assessed the impact of glutamine deprivation on this F15 PTEN$^{-/-}$ T leukaemic cell line. The data (Fig. 3-5a) show that F15 cells cultured in full media showed a 6-fold increase in cell number after 2 days in the culture. In

contrast F15 cells deprived of glutamine did not proliferate during the course of experiment; rather their numbers decreased. In addition, while the majority of F15 cells kept in full media were alive, more than 90% of F15 cells deprived of glutamine were dead, as judged by DAPI stain, after 2 days of culture (Fig. 3-6b). Therefore, we showed that survival of PTEN$^{-/-}$ T leukaemic cell line was dependent on external glutamine availability.

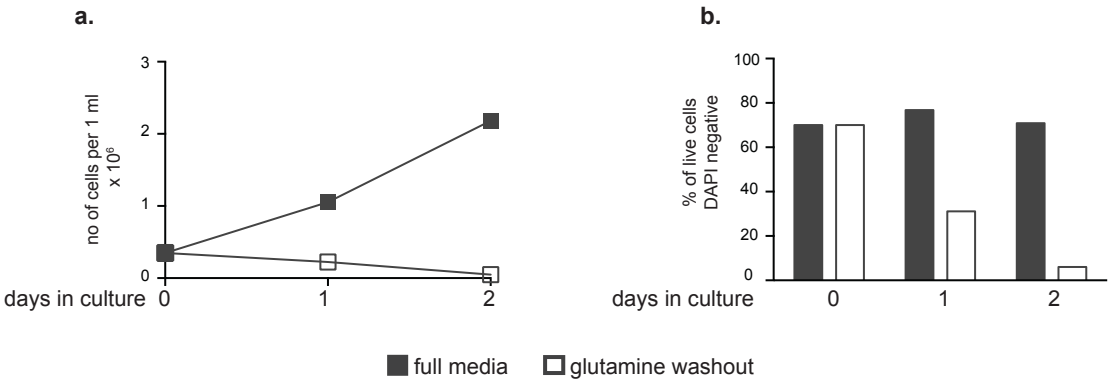

Figure 3-6 **The impact of glutamine withdrawal on PTEN$^{-/-}$ T cell lymphoma/leukaemia cells survival.**

PTEN$^{-/-}$ leukaemic cells were cultured either in full media or media deprived of glutamine for 48 hours. **a.** Proliferation curve and **b.** percentage of alive-DAPI negative cells. Data shown as representative of 2 biological replicates from 2 independent experiments.

3.2.4 PTEN$^{-/-}$ T cell lymphoma/leukaemia cells increase uptake of leucine compared to WT thymocytes

We next investigated if PTEN$^{-/-}$ T cell lymphoma/leukaemia cells show any changes in leucine uptake. This amino acid is crucial for the de novo protein synthesis but also for mTORc1 activity (BEUGNET et al. 2003; Schriever et al. 2013). System L amino acid transporters transport leucine (Verrey et al. 2004; Sinclair et al. 2013) and the proteomic data showed that the PTEN$^{-/-}$ T cell lymphoma/leukaemia cells had

increased expression of CD98, a subunit of the System L amino acid transporters (Fig. 3-7a). On average $PTEN^{-/-}$ T cell lymphoma/leukaemia cells upregulated expression of CD98 by 2-fold compared to WT thymocytes. Interestingly, one of the tumour sample showed that CD98 was upregulated more than 5-fold. System L amino acid transporters comprise a heterodimer of CD98 (Slc3a2) and either Slc7a5 (also known as LAT1), Slc7a8 (LAT2), Slc7a7 (y^+LAT1) or Slc7a6 (y^+LAT2) (Sinclair et al. 2013). We detected both Slc7a5 and Slc7a6 in the $PTEN^{-/-}$ T cell lymphoma/leukaemia cells, however there was huge variability between expression of these molecules in the different T cell Tumour samples and the WT thymocytes (data not shown).

CD98 expression can also be monitored by flow cytometry and the data (Fig. 3-7b) show increased surface expression of CD98 in *ex vivo* isolated $PTEN^{-/-}$ T cell lymphoma/leukaemia cells compared to WT thymocytes. Accordingly, we examined the System L amino acid transport capacity (^{3}[H]-Leucine uptake) of the primary *ex vivo* isolated $PTEN^{-/-}$ T cell lymphoma/leukaemia cells and compared to WT thymocytes and to IL-2 maintained CTLs. Figure 3-7c shows that e*x vivo* isolated WT thymocytes had low level of ^{3}[H]-Leucine uptake in contrast to CTLs that upregulated leucine uptake by more than 30-fold. Primary $PTEN^{-/-}$ T cell lymphoma/leukaemia cells increased the rates of leucine uptake compared to WT thymocytes and interestingly, they were as capable or even better than CTLs (Fig. 3-7c). The analysis of the ability of $PTEN^{-/-}$ T cell lymphoma/leukaemia cells to take up leucine expressed per mass of cellular protein showed that T cell lymphoma/leukaemia cells isolated from $PTEN^{fl/fl}$ x Lck^{Cre+} mice increased this process 11 to 18-fold compared to WT thymocytes (Fig. 3-7d). These data indicated

that PTEN$^{-/-}$ T cell lymphoma/leukaemia cells did increase their leucine uptake through System L amino acid transporters.

a.

Protein name	Gene name	WT copy numbers	KO1 copy numbers	KO1 fold change	KO2 copy numbers	KO2 fold change	KO3 copy numbers	KO3 fold change
CD98	Slc3a2	18,466	112,191	**5.22**	48,158	**2.24**	56,985	**2.65**

KO = PTEN$^{-/-}$ T cell lymphoma/leukaemia

b.

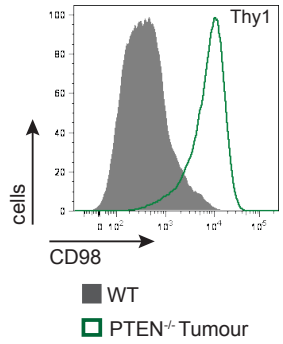

c.

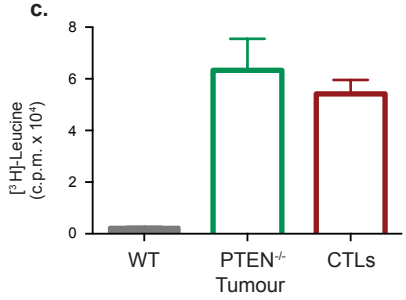

PTEN$^{-/-}$ Tumour = PTEN$^{-/-}$ T cell lymphoma/leukaemia

d.

	size (averaged)	**leucine uptake**
fold change (normalised to WT)	1.67	19.9 - 30.8
	protein content (averaged)	**leucine uptake**
fold change (normalised to WT)	1.73	11.5 - 17.9

Figure 3-7 **A comparison of CD98 expression and leucine uptake by PTEN$^{-/-}$ T cell lymphoma/leukaemia cells and WT thymocytes**.

a. Protein copy numbers estimated from IBAQ values identified in LFQ-MS experiment for WT thymocytes and PTEN$^{-/-}$ T cell lymphoma/leukaemia cells and their fold change. Data calculated for 3 biological replicates from 1 experiment. **b.** Flow cytometric analysis presented as histogram showing expression of CD98 surface marker for *ex vivo* WT thymocytes and PTEN$^{-/-}$ T cell lymphoma/leukaemia cells. Data are representative of at least 3 biological replicates. **c.** *Ex vivo* isolated WT thymocytes, PTEN$^{-/-}$ T cell lymphoma/leukaemia cells and IL-2 maintained CTLs were assayed for ^{3}[H]- leucine uptake. Units show counts per minute per 1x10^{6} cells. Error bars show SD of 1 biological replicate. Data are representative of 3 biological replicates from 3 independent experiments. **d.** Fold change of leucine uptake by WT thymocytes and PTEN$^{-/-}$ T cell lymphoma/leukaemia cells in units per mass of cellular protein (1mg/ml) normalised to WT thymocytes. The analysis was performed on 3 biological replicates from 3 independent experiments.

3.2.5 PTEN$^{-/-}$ T cell lymphoma/leukaemia cells upregulate transferrin uptake compared to WT thymocytes

Expression of transferrin and high levels of transferrin are a hallmark of rapidly proliferating cells (O'Donnell et al. 2006). The proteomic data showed that PTEN$^{-/-}$ T cell lymphoma/leukaemia cells had increased expression of CD71 (Fig. 3-8a). Two of the T cell lymphoma/leukaemia samples had the fold change of approximately 7 while the third T cell lymphoma/leukaemia sample showed upregulation of CD71 by 22-fold compared to WT thymocytes. We also measured CD71 expression by flow cytometry on surface of PTEN$^{-/-}$ T cell lymphoma/leukaemia cells and WT thymocytes. Figure 3-8b shows that while WT thymocytes maintained low level of CD71 expression, PTEN$^{-/-}$ T cell lymphoma/leukaemia cells had much higher expression of CD71. In the next experiment, we tested whether the CD71 receptor was functional by measuring the cellular uptake of transferrin by PTEN$^{-/-}$ T cell lymphoma/leukaemia cells, WT thymocytes and IL-2 maintained CTLs. We used a FACS based assay to monitor cellular uptake of APC conjugated transferrin. Cells were starved of transferrin for 2 hours after which the uptake of transferrin was performed at 37ºC for 10 minutes. The data in Fig. 3-8c show that WT thymocytes did not have the ability to take up transferrin compared to CTLs, which showed the highest uptake of transferrin (red line). However, primary PTEN$^{-/-}$ T cell lymphoma/leukaemia cells showed a marked increase in transferrin uptake that was comparable with the uptake observed in CTLs, implying that tumour cells have great capacity in transferrin uptake. The uptake of labeled transferrin by the PTEN$^{-/-}$ T cell lymphoma/leukaemia cells was specific as it was blocked by unlabeled holo-transferrin and by incubating the cells treated with labeled transferrin on ice (Fig. 3-8d). These data indicated that CD71 expressed on PTEN$^{-/-}$ T cell

lymphoma/leukaemia cells was thus functional and permitted the uptake of transferrin into the cells.

a.

Protein name	Gene name	WT copy numbers	KO1 copy numbers	KO1 fold change	KO2 copy numbers	KO2 fold change	KO3 copy numbers	KO3 fold change
CD71	Tfrc	5,683	126,710	**22.30**	37,943	**6.68**	43,135	**7.59**

KO = PTEN$^{-/-}$ T cell lymphoma/leukaemia

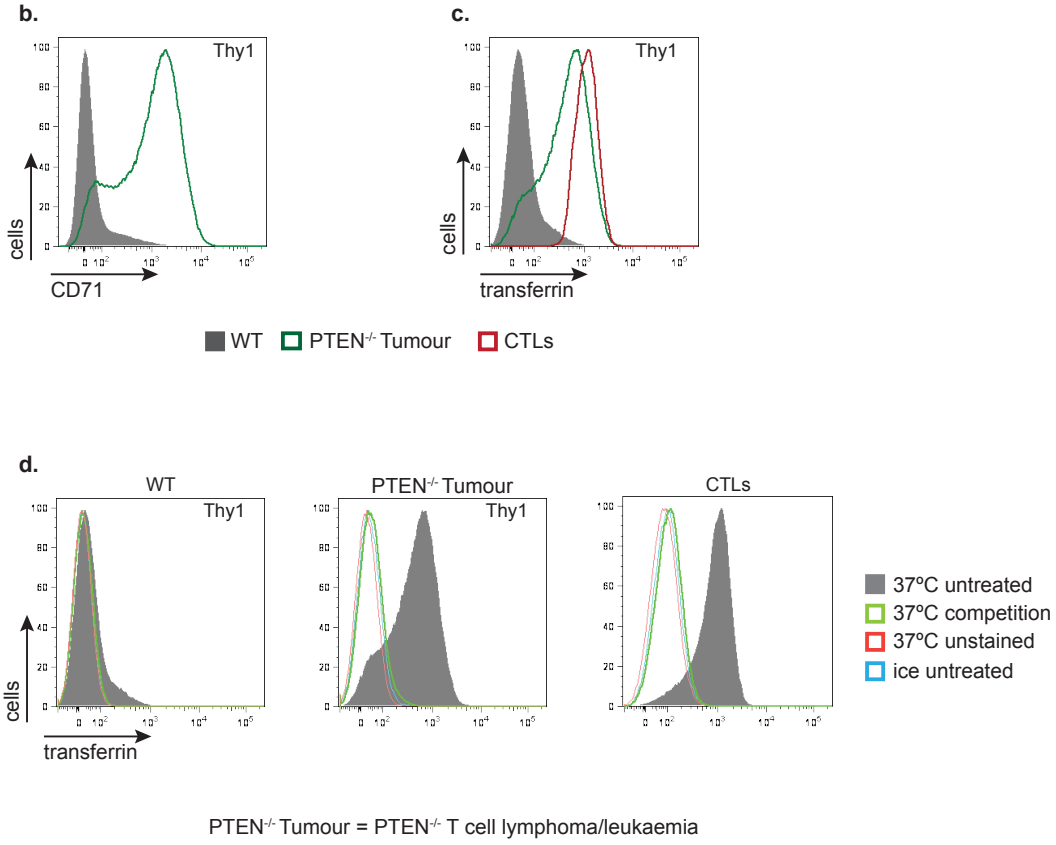

PTEN$^{-/-}$ Tumour = PTEN$^{-/-}$ T cell lymphoma/leukaemia

Figure 3-8 **A comparison of expression of CD71 and transferrin uptake by PTEN$^{-/-}$ T cell lymphoma/leukaemia cells and WT thymocytes.**

a. Protein copy numbers estimated from IBAQ values identified in LFQ-MS experiment for WT thymocytes and PTEN$^{-/-}$ T cell lymphoma/leukaemia cells and their fold change. Data calculated for 3 biological replicates from 1 experiment. **b. c. d.** Flow cytometric analysis presented as histograms showing **b.** expression CD71 and **c.** transferrin uptake by WT thymocytes, PTEN$^{-/-}$ T cell lymphoma/leukaemia cells and IL-2 maintained CTLs. Untreated cells were tested to take up transferrin at 37ºC. **d.** Histograms depicting transferrin uptake for untreted cells kept at 37ºC (solid grey) or cells kept at 37ºC incubated together with holo-transferrin to block transferrin uptake (green), or kept at 37ºC where no labeled transferrin was added (orange) or kept on ice to block the transport (blue). Expression of CD71 and transferrin uptake was measured on Thy1 positive cells. Data are representative of at least 3 biological replicates from 3 independent experiments.

3.3 Discussion

In this chapter we explored nutrient uptake in primary T cell lymphoma/leukaemia cells that develop in $PTEN^{fl/fl}$ x Lck^{Cre+} mice, a mouse model for T-ALL. The data showed that these primary T cell lymphoma/leukaemia cells had high rates of glucose uptake and they expressed high levels of glycolytic enzymes.

Cells that exhibit an increased need for energy and macromolecule synthesis switch from metabolising glucose by oxidative phosphorylation to utilizing aerobic glycolysis (Finlay 2012). Aerobic glycolysis has an important advantage over oxidative phosphorylation – the intermediates produced during glycolysis act as a source of carbon to generate biosynthetic precursors that are then used for production of DNA, proteins and phospholipids (Finlay 2012; Lunt & Vander Heiden 2011). One crucial requirement in aerobic glycolysis is to sustain high levels of glucose uptake by maintaining expression of the glucose transporters. Our MS-based analysis of the protein content of $PTEN^{-/-}$ T cell lymphoma/leukaemia cells revealed that Glut3 could be the putative glucose transporter in $PTEN^{-/-}$ T cell lymphoma/leukaemia cells. It is interesting that in activated CTLs the transporters Glut1 and Glut3 are expressed at comparable levels (personal communication with Dr Jens Heukelmann). However, Glut3 has a higher affinity for glucose and greater transport capacity for glucose (Simpson et al. 2008). It is thus possible that $PTEN^{-/-}$ T cell lymphoma/leukaemia cells selectively upregulated the more efficient glucose transporter to increase uptake of glucose. In this respect, microarray analysis of samples from pediatric precursor B-ALL cells revealed that the elevated expression of Glut3 corresponds with increased rates of glucose uptake (Hulleman et al. 2009) suggesting that Glut3 alone is sufficient for the increased glucose metabolism in ALL. However, the failure of the

$PTEN^{-/-}$ T cell lymphoma/leukaemia cells to expressed both Glut1 and Glut3 could explain why their glucose transport capacity was less than that of CTLs.

Another interesting observation from the MS data of the primary $PTEN^{-/-}$ T cell lymphoma/leukaemia cells isolated from $PTEN^{fl/fl}$ x Lck^{Cre+} mice was the high abundance of PKM2 versus PKM1 (33^{rd} vs. 3727^{th} rank according to protein abundance). In this context, it was shown that overexpression of PKM2, but not PKM1 is frequently observed in cancer and other rapidly proliferating cells (Mazurek et al. 2005). PKM2 thus, can exist in a dimeric form with low catalytic activity and this leads to accumulation of phosphoenolpyruvate and other glycolytic intermediates that serve as biosynthetic precursors for synthesis of amino acids and phospholipids. The PKM1/2 isoforms both use phosphoenolpyruvate as a substrate during glycolysis but PKM2 can also function as a protein kinase for STAT3 and MEK5 (Gao et al. 2012) and is co-activator for Hif-1α mediated transcription (Luo et al. 2011). The quantity of PKM2 in the $PTEN^{-/-}$ T cell lymphoma/leukaemia cells could permit this enzyme to have multiple roles as a transcriptional and metabolic regulator.

The present data did show evidence for an increase in lactate production in the $PTEN^{-/-}$ T cell lymphoma/leukaemia cells. Lactate is the end product of glycolysis produced from pyruvate by lactate dehydrogenase (Vander Heiden et al. 2009). Several groups have shown that leukaemic cell lines are highly glycolytic and that inhibiting glycolysis but not oxidative phosphorylation (Boag et al. 2006; Akers et al. 2011) leads to reduction in proliferation and cells viability. Proteomics data showed that $PTEN^{-/-}$ T cell lymphoma/leukaemia cells increased expression of rate-limiting glycolytic enzymes. The most changed was hexokinase 2, a crucial enzyme, as it

catalyses the first reaction of glycolytic pathway (Lunt & Vander Heiden 2011; Wilson 2003). However, we observed that although PTEN$^{-/-}$ T cell lymphoma/leukaemia cells produced lactate they did not have the high glycolytic rates seen in CTLs, a control population of normal proliferating T cells.

The cell cycle status of PTEN$^{-/-}$ T cell lymphoma/leukaemia cells indicated that they were a proliferating population of cells. An important nutrient for proliferating cells is transferrin (Ponka & Lok 1999; White et al. 1990; Kemp et al. 1995) as it transports iron inside the cell. Iron is a crucial cofactor for a number of cellular enzymes, including ribonucleotide reductase that enables for progression of cell cycle (Robbins & Pederson 1970). The present data showed that the PTEN$^{-/-}$ T cell lymphoma/leukaemia cells expressed high levels of CD71, the transferrin receptor, and had high rates of transferrin uptake. This is consistent with the fact that high levels of CD71 have been reported on some although not all primary human leukaemic samples (Q. Liu et al. 2014).

Glutamine, next to glucose, is an important nutrient for rapidly proliferating cells. Our MS experiment identified that glutamine transporters such as Slc38a1 and Slc1a5, were more abundant in PTEN$^{-/-}$ T cell lymphoma/leukaemia cells compared to WT thymocytes. Furthermore, we also showed that PTEN$^{-/-}$ T cell lymphoma/leukaemia cells could efficiently take up glutamine. Elevated levels of glutamine uptake and subsequent glutaminolysis are frequently observed in tumour cells that are described as being ‘glutamine addicted’ (Duran et al. 2012; Wise & Thompson 2010). One important function for glutamine in cells is to regulate the activity of mTORc1 (Duran et al. 2012). Simultaneous efflux of glutamine from the

cell with the uptake of large neutral amino acids such as leucine is rate-limiting step in activation of mTORc1 (Nicklin et al. 2009). Glutamine uptake and glutaminolysis can also control mTORc1 activity by facilitating the lysosomal localisation of this kinase. In this respect, it is important to mention that lysosome is thought to be a platform for optimal mTORc1 activation. Even though the process is not fully understood, the presence of leucine on the lysosomal lumen initiates a series of events, involving the vATPase that activates GEF activity of the Ragulator complex towards RagA. Active RagA then recruits mTORc1 to the lysosome that can be activated by RHEB (Bar-Peled et al. 2012; Sancak et al. 2010; Zoncu et al. 2011; Sancak et al. 2008).

In this chapter we showed that primary $PTEN^{-/-}$ T cell lymphoma/leukaemia cells increased expression of CD98, the heavy chain of the transporter that pairs up with Slc7a5, Slc7a6 or Scl7a7, compared to WT thymocytes. We also detected expression of Slc7a5 and Slc7a6 but their expression was very variable precluding from forming firm conclusions. It is possible, that with the approach that we took, we might have underrepresented membrane proteins due to technical problems. Because we used urea based lysis buffer that did not contain any detergents, we might have not fully solubilised hydrophobic membranes. Nonetheless, we showed that T cell lymphoma/leukaemia cells from $PTEN^{fl/fl}$ x Lck^{Cre+} mice had very high rates leucine uptake consistent with high expression of System L amino acid transporters. In this context, LNAA such as leucine are major positive regulator of mTORc1 activity (Sinclair et al. 2013; BEUGNET et al. 2003). We, therefore, speculate that glutamine together with leucine might contribute to elevated mTORc1 activity in $PTEN^{-/-}$ T cell lymphoma/leukaemia cells and we will discuss it further in Chapter 5.

Taken together, we have established that primary PTEN$^{-/-}$ T cell lymphoma/leukaemia cells express elevated levels of glucose, glutamine and leucine and transferrin receptors and as a result show an increase in the uptake of key nutrients. In the next chapter we will discuss whether PTEN deletion alone is sufficient to initiate these metabolic changes or whether they are a consequence of secondary mutations acquired during the malignant transformation.

4 Chapter: PTEN deletion is not sufficient to initiate glucose, glutamine or leucine uptake in T cell progenitors

4.1 Introduction

In the previous chapter we showed that $PTEN^{-/-}$ T cell lymphoma/leukaemia cells had high rates of transport of several key nutrients: glucose, glutamine, leucine and transferrin. In this chapter, we will examine if these high levels of nutrient uptake are immediate consequence of PTEN deletion or due to accumulation of secondary mutations in $PTEN^{-/-}$ T cell lymphoma/leukaemia cells.

The main function of PTEN is to act as a lipid phosphatase and its best understood function is in the antagonism of PI3K mediated signalling (Leslie & Downes 2004). Once PTEN is deleted or downregulated, $PI(3,4,5)P_3$ accumulates in the plasma membrane and permits binding of PH domains to the $PI(3,4,5)P_3$. $PI(3,4,5)P_3$ recruitment of the PH domain of AKT allows the kinase PDK1 to phosphorylate AKT on Thr308 site and hence allows for the catalytic activation of AKT. PDK1 also contains a PH domain that binds to $PI(3,4,5)P_3$ with high affinity and PDK1 binding in the plasma membrane is required for efficient induction of high levels of AKT activity, probably by ensuring co-localisation of AKT and PDK1 (L. R. Pearce et al. 2010).

In many cell systems, AKT plays a key role in maintaining glucose homeostasis and cell metabolism (Mahfouz et al. 2014; Hajduch et al. 2001; C. J. Green et al. 2008). Indeed, in normal thymocytes development, it is clear that loss of PDK1 and AKT

causes defects in glucose transport in T cell progenitors in the thymus precluding their development (Hinton et al. 2004; Juntilla et al. 2007). However, it has been described that PTEN null progenitors have normal expression of transferrin receptor and System L amino acid transporter (CD98) (Finlay et al. 2009). These data question whether the increased $PI(3,4,5)P_3$ signalling resulting from loss of PTEN activity is sufficient to cause changes in T cell metabolism seen in $PTEN^{-/-}$ T cell lymphoma/leukaemia cells.

4.2 Results

4.2.1 PTEN$^{-/-}$ non-transformed thymocytes do not actively proliferate

The molecular changes that are associated with malignancy appear in PTEN$^{fl/fl}$ x Lck^{Cre+} mice in a timed and synchronous manner (Xue et al. 2008). Thus to analyse the PTEN$^{-/-}$ non-transformed thymocytes, we have only used mice younger than 6 weeks old that did not present any signs of tumour development. These PTEN$^{-/-}$ non-transformed thymocytes are polyclonal, like WT thymocytes (Fig.4-1). PTEN$^{-/-}$ non-transformed thymocytes are devoid of secondary mutations, therefore any observed changes are due to PTEN loss.

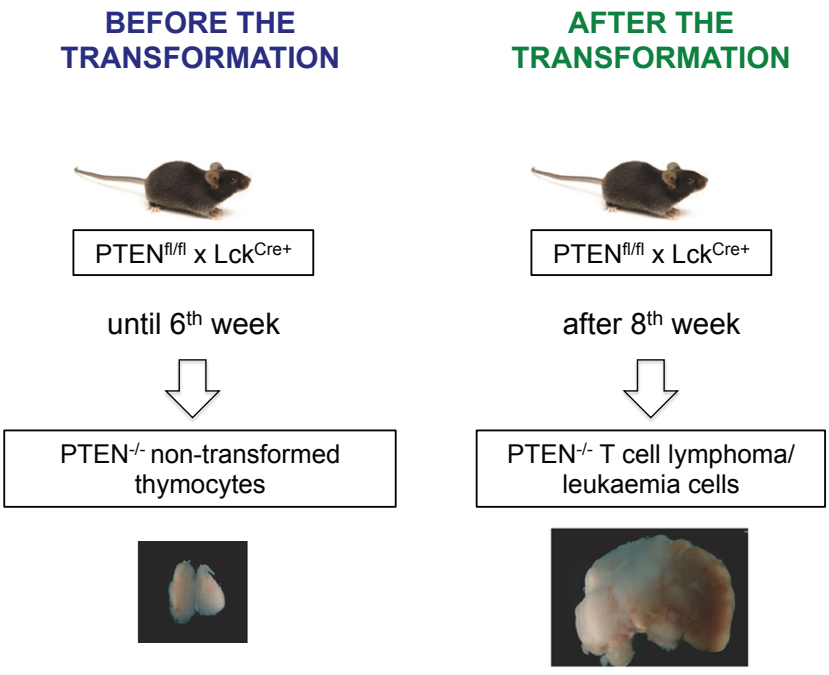

Figure 4-1 **Schematic illustration of how malignant transformation affects the thymus.**

Initially, PTEN$^{fl/fl}$ x Lck^{Cre+} mice remain tumour free and PTEN$^{-/-}$ non-transformed thymocytes are phenotypically like WT thymocytes. However, around 8-10 weeks of age, PTEN$^{fl/fl}$ x Lck^{Cre+} mice undergo malignant transformation and develop tumours. These PTEN$^{-/-}$ T cell lymphoma/leukaemia cells are mainly monoclonal and have additional secondary mutations.

PTEN deletion causes accumulation of $PI(3,4,5)P_3$ in the cell membrane and subsequent activation of AKT in $PTEN^{-/-}$ non-transformed thymocytes (Finlay et al. 2009). As AKT can drive proliferation in cells, we assessed the cell cycle status of $PTEN^{-/-}$ non-transformed thymocytes. Thus, we examined the percentage of cells in each cell cycle phase by staining with the intracellular DNA of viable WT thymocytes and $PTEN^{-/-}$ non-transformed thymocytes with Hoechst 33342 and then fitted to the Watson-pragmatic model (Watson et al. 1987). The cell cycle analysis in Fig. 4-2 showed that the majority of WT thymocytes (approximately 80%) were in G1 phase, around 8% were in S phase and 1% were in G2 phase. Similar results were achieved for $PTEN^{-/-}$ non-transformed thymocytes, as they had approximately 84% of cells in G1 phase, 8% in S phase and 1% in G2 phase. These data indicated that the $PTEN^{-/-}$ non-transformed thymocytes did not actively proliferate, which was similar to WT thymocytes and in contrast to $PTEN^{-/-}$ T cell lymphoma/leukaemia cells that were actively proliferating.

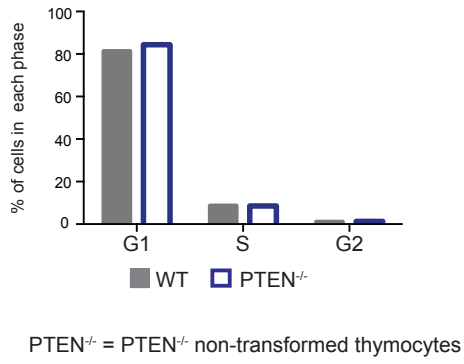

Figure 4-2 **Analysis of cell cycle of $PTEN^{-/-}$ non-transformed and WT thymocytes.**

Bar graph showing the percentage of viable cells in each stage of cell cycle in WT and $PTEN^{-/-}$ non-transformed thymocytes. DNA was stained with Hoechst 33342 and non-viable cells excluded with DAPI. Cell cycle populations were determined by fitting the data to the Watson-pragmatic model. Data are shown as means from 2 biological replicates from 2 independent experiments.

4.2.2 PTEN$^{-/-}$ non-transformed thymocytes remain small in size

The above data showed that PTEN$^{-/-}$ non-transformed thymocytes remained mostly quiescent, like WT thymocytes. The actively proliferating PTEN$^{-/-}$ T cell lymphoma/leukaemia cells were big, blast-like cells (Fig. 3-2a). To examine the size of PTEN$^{-/-}$ non-transformed thymocytes we analysed the forward scatter and side scatter profiles and found that PTEN$^{-/-}$ non-transformed thymocytes were small cells and their size was only marginally bigger that WT thymocytes (Fig. 4-3a), however they did not blast like PTEN$^{-/-}$ T cell lymphoma/leukaemia cells. Consistent with the cells not actively proliferating, the numbers of PTEN$^{-/-}$ non-transformed thymi were comparable to WT thymi (Fig. 4-3b).

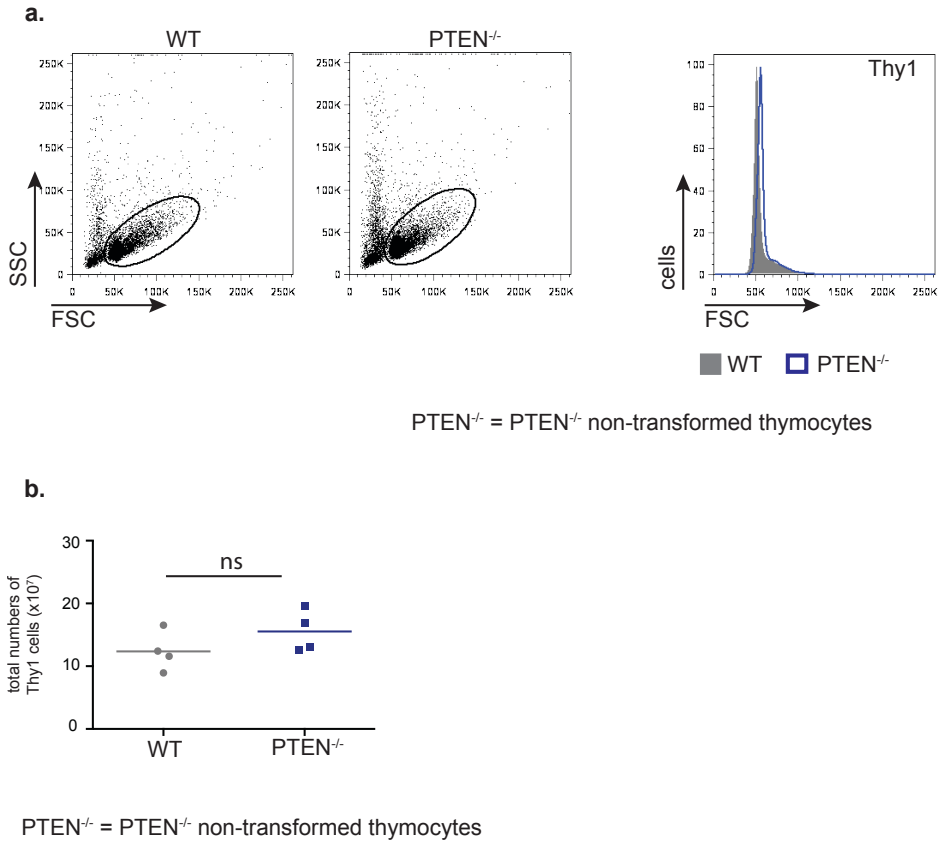

Figure 4-3 **A comparison of thymocytes size and cellularity of PTEN$^{-/-}$ non-transformed and WT thymi.**

a. Flow cytometric analysis of the size of WT thymocytes and PTEN$^{-/-}$ non-transformed thymocytes presented as dot plot graph (left) and histogram of Thy1 positive cells (right) showing their size. **b.** Total numbers of Thy1 positive cells in WT and PTEN$^{-/-}$ non-transformed thymi. Data are mean of 4 biological replicates from 4 independent experiments. P-value was calculated from t-test; ns – not significant.

4.2.3 AKT is phosphorylated in PTEN$^{-/-}$ non-transformed thymocytes

AKT activity can be monitored by assessing its phosphorylation on Thr308 and Ser473 by Western blot analysis. Fig. 4-4 shows that WT thymocytes had no detectable AKT phosphorylation on Thr308 and Ser473. In contrast, AKT phosphorylation was readily detected in PTEN$^{-/-}$ non-transformed thymocytes. As comparison, we show that high levels of AKT phosphorylation on Thr308 and Ser473 were also seen in PTEN$^{-/-}$ T cell lymphoma/leukaemia cells (Fig. 4-4). The total

levels of AKT were equal in WT and PTEN$^{-/-}$ non-transformed thymocytes and PTEN$^{-/-}$ T cell lymphoma/leukaemia cells. Furthermore, in these experiments we used pervanadate, a potent inhibitor of protein-tyrosine phosphatase (Mikalsen & Kaalhus 1998), that can stimulate PI3K signalling (Atrih et al. 2010) as pharmacological tool to achieve the maximal phosphorylation in the cell. The presented data show that phosphorylation levels of AKT at Thr308 and Ser473 in PTEN$^{-/-}$ non-transformed thymocytes and PTEN$^{-/-}$ T cell lymphoma/leukaemia cells were lower compared to the samples treated with pervanadate. The MS-based stoichiometric quantification of AKT phosphorylation in human effector CD8+ T cells by Atrih *at al*., has suggested that treatment with pervanadate leads to phosphorylation of 40% of AKT (Thr308) site and 11% of AKT (Ser473) site (Atrih et al. 2010). Our data thus showed that PTEN deletion did not activate the entire pool of AKT.

Importantly, we showed that phosphorylation of AKT on Thr308 and Ser473 sites was efficiently blocked in PTEN$^{-/-}$ non-transformed and PTEN$^{-/-}$ T cell lymphoma/leukaemia cells by the AKTi inhibitor which prevents PI(3,4,5)P_3 binding to the PH domain of AKT (C. J. Green et al. 2008). These data, thus, support the notion that the increased AKT activity caused by PTEN deletion required PI(3,4,5)P_3 binding to the PH domain of AKT.

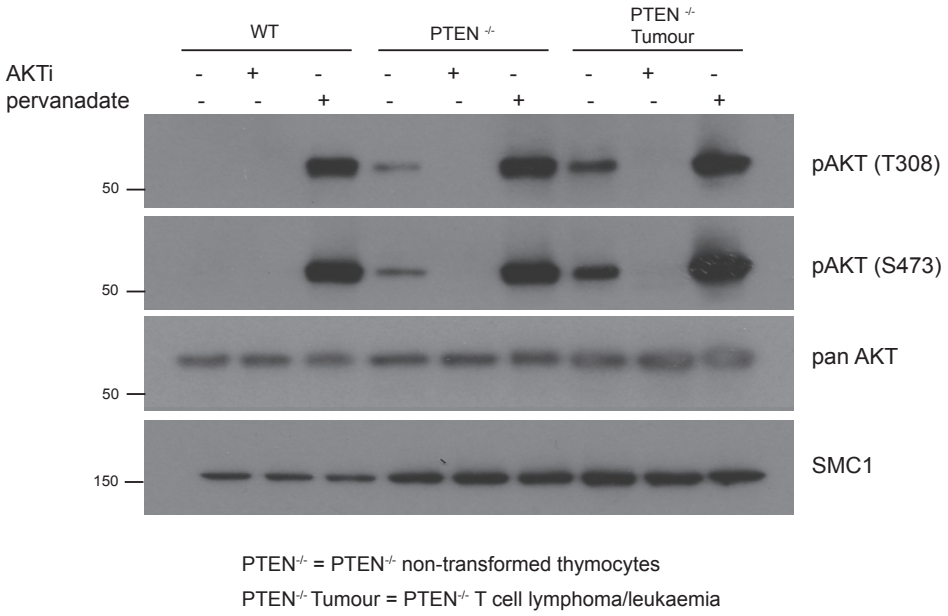

Figure 4-4 **The effect of PTEN deletion on AKT phosphorylation in PTEN$^{-/-}$ non-transformed and PTEN$^{-/-}$ T cell lymphoma/leukaemia cells.**

Total *ex vivo* isolated WT thymocytes, PTEN$^{-/-}$ non-transformed thymocytes and PTEN$^{-/-}$ T cell lymphoma/leukaemia cells were either left untreated or treated with 1μM of AKTi for 1 hour or pervanadate for 5 minutes. AKTi was used as negative control and pervanadate as positive control for AKT phosphorylation. Western blot analysis was performed with antibodies against phosphorylated forms of AKT: Thr308 and Ser473, and pan AKT, and SMC1 antibodies. SMC1 was used as a loading control. Equal numbers of cells were lysed. Numbers represent molecular weights markers and are given in kDa. Data are representative of 3 biological replicates from 3 independent experiments.

Finlay et al. showed that the activation of AKT results in the phosphorylation of Foxo1 and 3a in PTEN$^{-/-}$ non-transformed and PTEN$^{-/-}$ T cell lymphoma/leukaemia cells (Finlay et al. 2009). Phosphorylated Foxos are excluded from the nucleus and thus cannot induce the expression of target genes i.e. IL-7 receptor alpha (IL-7R) (Hedrick et al. 2012; Kerdiles et al. 2009; Brunet et al. 1999). We measured the expression of IL-7R to explore if the active AKT seen in PTEN$^{-/-}$ non-transformed thymocytes was sufficient to inactivate expression of Foxo regulated genes. Figure 4-5 shows that naïve T cells expressed high levels of the IL-7R whereas the expression of IL-7R was downregulated in TCRb+ cells isolated from PTEN$^{fl/fl}$ x Lck^{Cre+} mice.

There were also low levels of IL-7R in TCRb+ cells isolated from PTEN$^{fl/fl}$ x Lck^{Cre+} tumour bearing mice. These data confirmed the previous results that PTEN deletion was sufficient to inactivate Foxo transcription factors.

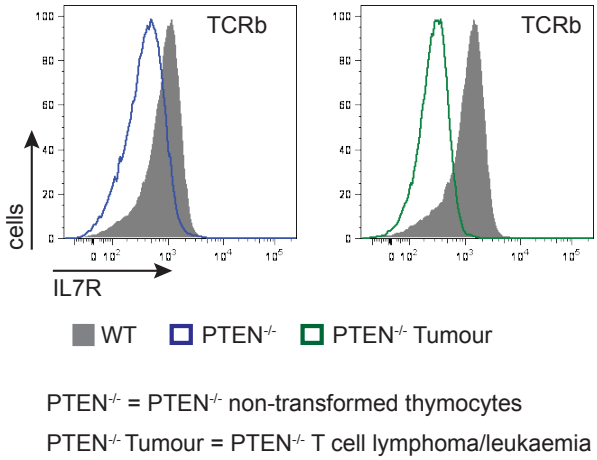

Figure 4-5 **The expression of IL-7R in TCRb+ cells from PTEN null mice.**

Flow cytometric analysis presented as histograms showing expression of IL-7R on *ex vivo* isolated TCRb+ cells from LN from WT mice, PTEN$^{fl/fl}$ x Lck^{Cre+} mice (green) and PTEN$^{fl/fl}$ x Lck^{Cre+} tumour bearing mice (blue). Data are representative of 3 biological replicates from 3 independent experiments.

Another target of AKT is the protein PRAS40 (Sancak et al. 2007; H. Wang et al. 2012). The presented data (Fig. 4-6) show that WT thymocytes did not show evidence of PRAS40 phosphorylation on AKT substrate sequence, Thr246. However, both PTEN$^{-/-}$ non-transformed and PTEN$^{-/-}$T cell lymphoma/leukaemia cells had high levels of Thr246 phosphorylated on PRAS40. The phosphorylation of PRAS40 on Thr246 was abolished when cells were treated with the AKT inhibitor, AKTi. The maximal level of PRAS40 phosphorylation set by pervanadate treatment in PTEN$^{-/-}$ non-transformed and PTEN$^{-/-}$ T cell lymphoma/leukaemia cells was similar to the one observed in untreated samples suggesting that maximal PRAS40 phosphorylation was achieved when PTEN was lost. We also noted that the total levels of PRAS40 were

higher in PTEN$^{-/-}$ T cell lymphoma/leukaemia cells compared to PTEN$^{-/-}$ non-transformed or WT thymocytes (Fig. 4-6).

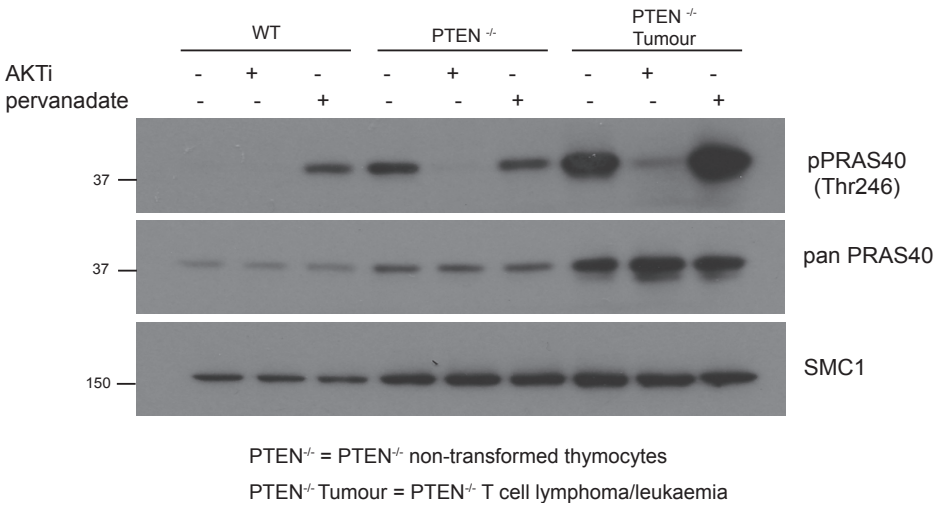

Figure 4-6 **Phosphorylation of PRAS40 in WT, PTEN$^{-/-}$ non-transformed thymocytes and PTEN$^{-/-}$ T cell lymphoma/leukaemia cells.**

Total e*x vivo* isolated WT thymocytes, PTEN$^{-/-}$ non-transformed thymocytes and PTEN$^{-/-}$ T cell lymphoma/leukaemia cells were either left untreated or treated with 1μM of AKTi for 1 hour or pervanadate for 5 minutes. AKTi was used as negative control and pervanadate as positive control for PRAS40 phosphorylation. Western blot analysis was with antibodies against phosphorylated form of PRAS40 (Thr246), pan PRAS40 and SMC1 antibodies. SMC1 was used as a loading control. Equal numbers of cells were lysed. Numbers represent molecular weights markers and are given in kDa. Data are representative of 3 biological replicates from 3 independent experiments.

Together, these data indicated that PTEN$^{-/-\ cells}$ isolated prior and after the malignant transformation had phosphorylated AKT as a result of PTEN loss. Furthermore, phosphorylated AKT induced activation of its downstream substrates.

4.2.4 PTEN$^{-/-}$ non-transformed thymocytes do not show increased rates of glucose, glutamine and leucine transport

We previously showed that PTEN$^{-/-}$ T cell lymphoma/leukaemia cells had increased rates of nutrient uptake. In this chapter we also showed that both PTEN$^{-/-}$ T cell lymphoma/leukaemia cells and PTEN$^{-/-}$ non-transformed thymocytes had phosphorylated AKT. As AKT is known to control growth and nutrient uptake in other cell systems (Hajduch et al. 2001; C. J. Green et al. 2008; Mahfouz et al. 2014), we determined if PTEN$^{-/-}$ non-transformed thymocytes upregulated nutrient uptake by testing the ability of *ex vivo* isolated WT and PTEN$^{-/-}$ non-transformed thymocytes to take up radioactively labelled glucose analogue, 2-DG. As a positive control we used IL-2 maintained CTLs. We found that WT thymocytes took lesser amounts of 2-DG compared to CTLs that showed 30-fold increase in glucose uptake (Fig. 4-7a). Similar to WT thymocytes, PTEN$^{-/-}$ non-transformed thymocytes also had very low rates of 2-DG uptake (Fig. 4-7a).

We therefore speculated that PTEN loss may promote the uptake of other nutrient that can be used to produce energy and macromolecules, such as glutamine (van der Windt & E. L. Pearce 2012). Thus, we measured ^{3}[H]-Glutamine transport in WT and PTEN$^{-/-}$ non-transformed thymocytes and compared with IL-2 maintained CTLs. The data presented here show that WT thymocytes took 40-fold less glutamine than CTLs indicating that they had low levels of glutamine uptake. PTEN$^{-/-}$ non-transformed thymocytes showed no increase in glutamine uptake compared to WT thymocytes (Fig. 4-7b). It is thus evident, that thymocytes prior to malignant transformation cannot upregulate either glucose or glutamine uptake.

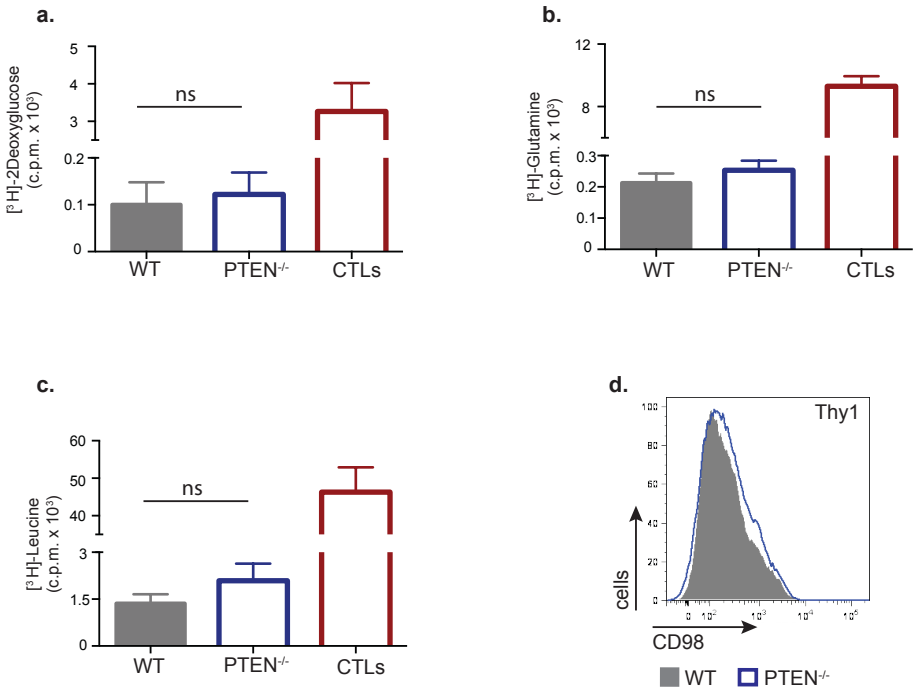

Figure 4-7 **A comparison of glucose, glutamine and leucine uptake by WT and PTEN$^{-/-}$ non-transformed thymocytes.**

Ex vivo isolated WT and PTEN$^{-/-}$ non-transformed thymocytes, and IL-2 maintained CTLs were assayed for uptake of **a.** ^{3}[H]-2-Deoxyglucose, **b.** ^{3}[H]-Glutamine and **c.** ^{3}[H]-Leucine. Units show counts per minute per 1x10^{6} cells. Data are shown as means +/- SD from 3 biological replicates from 3 independent experiments. P-values were calculated from t-test, ns – not significant. **d.** Flow cytometric analysis presented as histogram showing expression of CD98 on surface of Thy1 positive cells from WT and PTEN$^{-/-}$ non-transformed thymocytes. Data are representative of at least 3 biological replicates from at least 3 independent experiments.

In the previous chapter we showed that PTEN$^{-/-}$ T cell lymphoma/leukaemia cells had high levels of leucine uptake (Fig. 3-7c). The data presented in Fig. 4-7c show that WT thymocytes had low level of leucine uptake compared to CTLs that upregulated this process by 33-fold. PTEN$^{-/-}$ non-transformed thymocytes showed a 2-fold increase in leucine uptake compared to WT thymocytes but this was a very small response compared to CTLs. We also examined expression of the heavy subunit of LNAA transporter, CD98. The data indicated that the basal level of CD98 expression

observed in WT thymocytes was only marginally increased in PTEN$^{-/-}$ non-transformed thymocytes compared to the high expression of CD98 seen in the PTEN$^{-/-}$ T cell lymphoma/leukaemia cells (Fig. 3-7b).

4.2.5 PTEN$^{-/-}$ non-transformed thymocytes take up transferrin at similar rates to WT thymocytes

Lastly, we assessed the expression of the transferrin receptor (CD71) and the uptake of transferrin because these processes were upregulated in PTEN$^{-/-}$ T cell lymphoma/leukaemia cells. We found that WT thymocytes had low levels of CD71 expression (Fig. 4-8a) and PTEN$^{-/-}$ non-transformed thymocytes expressed CD71 at similar levels compared to WT thymocytes. Moreover, WT thymocytes and PTEN$^{-/-}$ non-transformed thymocytes showed minimal level of transferrin uptake compared to CTLs (Fig. 4-8b).

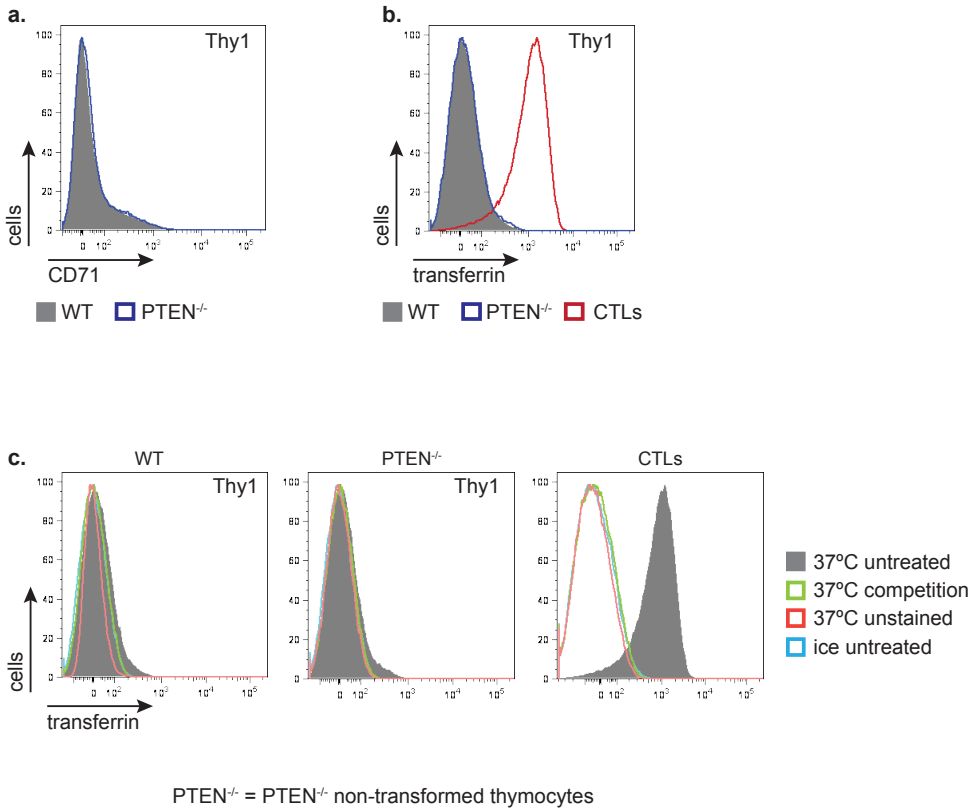

Figure 4-8 **A comparison of the transferrin uptake by WT and PTEN$^{-/-}$ non-transformed thymocytes.**

Flow cytometric analysis presented as histograms showing **a.** expression of CD71 and **b.** transferrin uptake on WT and PTEN$^{-/-}$ non-transformed thymocytes, and IL-2 maintained CTLs (red line). Untreated cells were tested to take up transferrin at 37ºC. **c.** Histograms depicting transferrin uptake for untreted cells kept at 37ºC (solid grey) or cells kept at 37ºC incubated together with holo-transferrin to block transferrin uptake (green), or kept at 37ºC where no labeled transferrin was added (orange) or kept on ice to block the transport (blue). Expression of CD71 and transferrin uptake was measured on Thy1 positive cells. Data are representative of at least 3 biological replicates from 3 independent experiments.

Taken together, all the above data indicated that PTEN$^{-/-}$ non-transformed thymocytes were small cells that were predominantly quiescent, not actively proliferating cells that did not upregulate nutrient uptake. It is, therefore, apparent that PTEN deletion, and hence activation of AKT, did not regulate nutrient uptake and proliferation of thymocytes.

4.2.6 PTEN$^{-/-}$ T cell lymphoma/leukaemia cells accumulate secondary mutations

As PTEN loss alone could not account for the increase in nutrient uptake and cell growth and proliferation that we observed in PTEN$^{-/-}$ T cell lymphoma/leukaemia cells, we concluded that other mutations must regulate these processes. *c-Myc* translocations are known secondary mutation in PTEN induced T-ALLs (Guo et al. 2008) and are not present in non-transformed stage (Bonnet et al. 2011). We therefore assessed PTEN$^{-/-}$ non-transformed and PTEN$^{-/-}$ T cell lymphoma/leukaemia cells for c-Myc expression. The data in Fig. 4-9 show that while WT and PTEN$^{-/-}$ non-transformed thymocytes did not express c-Myc, all primary PTEN$^{-/-}$ T cell lymphoma/leukaemia cells tested, did express c-Myc. c-Myc overexpression can occur as a result of overactivation of Notch1 (Weng et al. 2006). Hagenbeek *at al*., showed that all PTEN$^{-/-}$ T cell lymphoma/leukaemia cells express active Notch1 (Hagenbeek et al. 2014). In our study, using the same mouse model, we observed that active Notch1 was not expressed uniformly in all tested PTEN$^{-/-}$ T cell lymphoma/leukaemia cells samples (Fig. 4-9). Of note, the MS data revealed that only one tested PTEN$^{-/-}$ T cell lymphoma/leukaemia cells sample showed massive upregulation of Notch1 expression (1026 molecules per cell in PTEN$^{-/-}$ T cell lymphoma/leukaemia cells compared to approximately 50 molecules per cell in WT). These data thus, argue that PTEN$^{-/-}$ T cell lymphoma/leukaemia cells do carry secondary mutations i.e. c-Myc and Notch1 and that there is heterogeneity in the mutations that drive the same phenotype. However, we would like to further analyse PTEN$^{-/-}$ T cell lymphoma/leukaemia cells to establish what is the frequency of Notch1 activation.

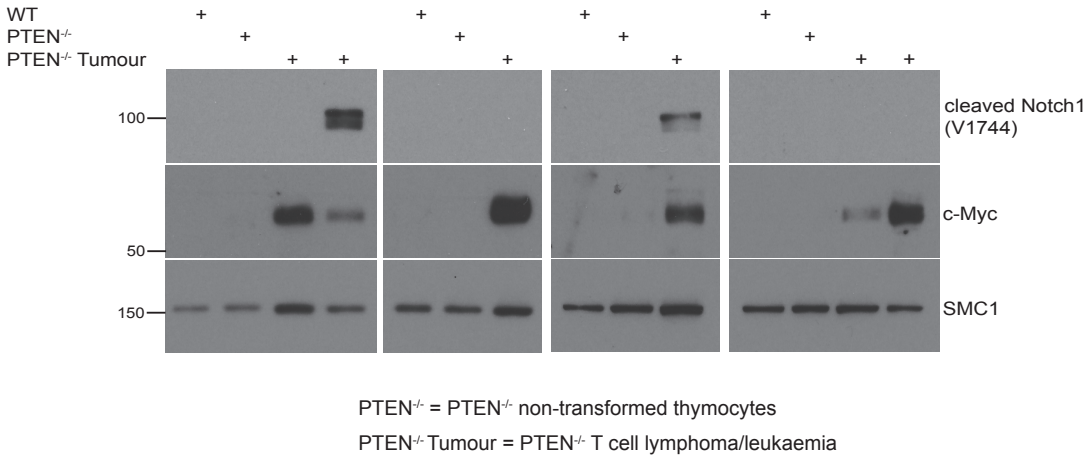

Figure 4-9 **Expression of active Notch1 and c-Myc in WT and PTEN$^{-/-}$ non-transformed thymocytes and PTEN$^{-/-}$ T cell lymphoma/leukaemia cells.**

Total e*x vivo* isolated WT and PTEN$^{-/-}$ non-transformed thymocytes, and PTEN$^{-/-}$ T cell lymphoma/leukaemia cells were subjected to Western blot analysis for cleaved Notch1 (Val1744) (NICD), c-Myc and SMC1. SMC1 was used as a loading control. Equal numbers of cells were lysed. Numbers represent molecular weights markers and are given in kDa. Data are from 6 PTEN$^{-/-}$ T cell lymphoma/leukaemia cells samples (Notch1) and representative of 10 PTEN$^{-/-}$ T cell lymphoma/leukaemia cells samples (c-Myc).

4.2.7 Notch1 induces leucine uptake and mTORc1 activity

Notch1 expression is strictly regulated during normal T cell development in the thymus. It is highly expressed in cells undergoing β selection, a process that requires T cells to become metabolically active and upregulate nutrient uptake (Kelly et al. 2007). Early work from our laboratory revealed that Notch1 signalling is crucial to upregulate CD98 expression (Fig. 4-10a) (Kelly et al. 2007). In this context, we observed that only PTEN$^{-/-}$ T cell lymphoma/leukaemia cells but not PTEN$^{-/-}$ non-transformed thymocytes, upregulated expression of CD98 (Fig. 3-7c and 4-7d, respectively). To examine if Notch1 can control leucine uptake in T cells, we cultured purified CD4/CD8 double negative T cell progenitors isolated from WT thymocytes on either OP9 cells or OP9 cells expressing the Notch ligand DL1 (OP9-DL1) and

tested their ability to take up radioactively labelled leucine. We found that T cell progenitor cells cultured on OP9-DL1, i.e. in the presence of Notch1 ligand, increased leucine transport compared to T cell progenitors exposed to OP9 cells lacking Noch1 ligands (Fig. 4-10b). Therefore, these data support a model where the expression of CD98 and subsequent leucine uptake is dependent on active Notch signalling.

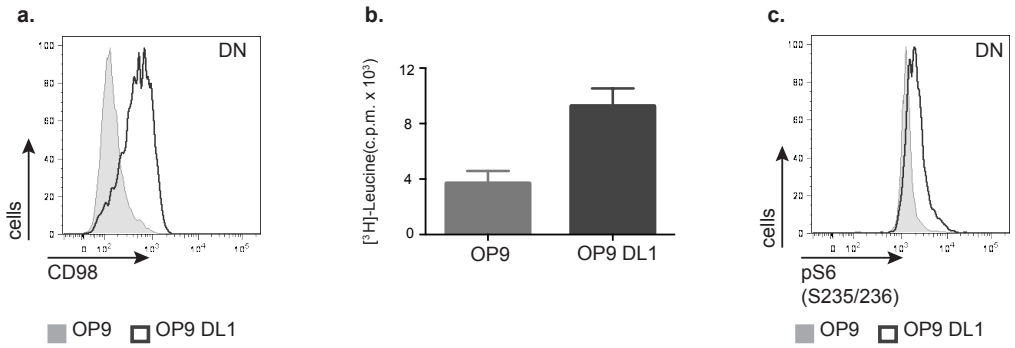

Figure 4-10 **The effects on Notch1 signalling on leucine uptake and mTORc1 activation.**

Purified WT CD4/CD8 DN thymocytes were cultured in the presence (OP9-DL1) or absence (OP9) of Notch ligand DL1 on stromal cell monolayers for 3 days. **a.** Flow cytometric analysis presented as histogram of CD98 expression on WT DN thymocytes. **b.** WT DN thymocytes were assayed for uptake of ^{3}[H]-Leucine. Units show counts per minute per $1x10^{6}$ cells. Error bars show SD of 1 biological replicate. **c.** Flow cytometric analysis of intracellular pS6 (Ser235/236) performed on WT DN thymocytes. All data are representative of 3 biological replicates from 1 experiment.

Leucine availability is necessary to induce activation of mTORc1 (BEUGNET et al. 2003). Because we noted that T cell progenitor cells grown on OP9-DL1 cells could increase the uptake of leucine, we speculated that these cells would have active mTORc1. Therefore, we analysed the activity of mTORc1 pathway by testing the phosphorylation of S6 ribosomal protein, a direct substrate of the mTORc1-regulated S6K. Figure 4-10c shows that T cell progenitors cultured in the presence of Notch1 ligand had a higher phosphorylation of S6 on Ser235/236 than T cell progenitors

cultured in the absence of the Notch1 ligand. These data thus imply that Notch activity was essential for activation of mTORc1.

4.3 Discussion

Deregulations of PTEN and PI3K/AKT pathway are frequently observed in T-cell acute lymphoblastic leukaemia (Gutierrez et al. 2009). PTEN is a potent suppressor of PI3K activity and PTEN deletion leads to accumulation of $PI(3,4,5)P_3$ and resultant activation of AKT (Fig. 4-1). While the increase in AKT activity was thought to drive tumourigenesis by controlling cell metabolism, we have found that nutrient uptake and cell growth was not increased in $PTEN^{-/-}$ non-transformed thymocytes. Therefore, we concluded that these changes were driven by secondary mutations that occur during the malignant transformation (Guo et al. 2008).

Asking whether PTEN-PI3K-AKT pathway is involved in regulation of nutrient uptake in $PTEN^{-/-}$ T cell lymphoma/leukaemia cells is an interesting question that stems from multiple observations, for example, AKT is the key kinase in regulating glucose metabolism in muscle (Mahfouz et al. 2014) or fat cells (C. J. Green et al. 2008; Hajduch et al. 2001) or in DN3 cells during thymus development (Hinton et al. 2004; Ciofani & Zúñiga-Pflücker 2005). However, there were also some opposing data arguing that in effector T cells active AKT is dispensable for glucose metabolism (Macintyre et al. 2011). Further evidence showed that increased expression of CD71 and CD98 nutrient receptors is a requirement for metabolically active and proliferating DN3 cells during normal thymus development (Kelly et al. 2007). In this context, PDK1 null T cell progenitors cannot sustain the expression of either CD71 or CD98 (Kelly et al. 2007). However, deletion of PDK1 in PTEN null T cell progenitors does not lead to a decreased expression of nutrient receptors, rather it restores its expression to the level observed in WT thymocytes (Finlay et al. 2009). Hence, PTEN deletion drives expression of CD71 and CD98 in T cell progenitors by

PDK1 – independent pathways. We observed that PTEN loss was sufficient to increase AKT phosphorylation and activity towards substrates including PRAS40 in $PTEN^{-/-}$ non-transformed thymocytes and $PTEN^{-/-}$ T cell lymphoma/leukaemia cells. However, only $PTEN^{-/-}$ T cell lymphoma/leukaemia cells showed an increase in nutrient uptake and $PTEN^{-/-}$ non-transformed thymocytes were phenotypically like WT cells in this respect. The data presented in this chapter also demonstrated that $PTEN^{-/-}$ non-transformed thymocytes remained small in size and the resulting increase in AKT phosphorylation was not able to initiate and/or sustain the increase of nutrient uptake that was observed in $PTEN^{-/-}$ T cell lymphoma/leukaemia cells.

Arguably, although PTEN loss was not directly promoting increased metabolism or proliferation, it might have been conferring a survival advantage to cells. We demonstrated that loss of PTEN resulted in a decrease in the expression of IL-7R as a result of AKT-mediated inhibition of Foxo transcription. During thymus development, cells undergo two waves of proliferation and one of them is mediated by IL-7 signalling. Therefore, early T cell progenitors need to upregulate IL-7R expression to respond to IL-7 signalling in order to maintain their survival (Ciofani & Zúñiga-Pflücker 2005). With low levels of IL-7R expression, it would therefore be expected that PTEN null thymocytes would have decreased survival. However, we showed that $PTEN^{-/-}$ non-transformed thymocytes survived normally and thymi of $PTEN^{fl/fl}$ x Lck^{Cre+} mice had similar numbers as their WT counterparts. Indeed, loss of PTEN has been shown to rescue T cell numbers in IL-7R knockout mice as PTENxIL-7 DKO mice develop normal levels of CD4/CD8 double negative and CD4/CD8 double positive thymocytes (Hagenbeek et al. 2004).

Increasing the output of the PI3K pathway via PTEN loss was clearly not sufficient to increase the nutrient uptake required to increase metabolism. One of the most common mutation found in PTEN null T leukaemic cells is the overexpression of c-Myc (Guo et al. 2008). In this chapter we also showed that c-Myc protein was overexpressed in $PTEN^{-/-}$ T cell lymphoma/leukaemia cells but not in $PTEN^{-/-}$ non-transformed or WT thymocytes. In transformed cells, c-Myc has been shown to control metabolism e.g. glycolysis, iron metabolism or cellular proliferation (C. V. Dang et al. 2009). What about nutrient uptake? In this respect, c-Myc has been shown to regulate glutamine uptake and glutaminolysis (Duran et al. 2012; R. Wang et al. 2011a), forcing transformed cells to glutamine addition (Wise et al. 2008). It has also been shown that c-Myc controls both glucose and glutamine metabolism in T cell antigen receptor activated effector CD8+ T cells (R. Wang et al. 2011a). Furthermore, PTEN deletion cannot induce the development of T cells lymphoma/leukaemias in the absence of c-Myc (J Zhang et al. 2011). Therefore, c-Myc is a potential candidate that might regulate metabolism in $PTEN^{-/-}$ T cell lymphoma/leukaemia cells.

One mechanism by which c-Myc can be upregulated is through Notch1 signalling (Palomero et al. 2006; Medyouf et al. 2010; Sulis et al. 2008; Weng et al. 2004; Herranz et al. 2014). Despite the fact that activating mutations in PEST or HD domain of Notch1 are not observed in PTEN induced T-ALL (Hagenbeek et al. 2014; Guo et al. 2008), several groups reported that proliferation and viability of PTEN null T cell lymphoma/leukaemia cells are sensitive to treatment with Notch1 inhibitors (Medyouf et al. 2010; Hagenbeek et al. 2014). In this context, Hagenbeek *at al*., reported that $PTEN^{-/-}$ T cell lymphoma/leukaemia cells express active Notch1 (Hagenbeek et al. 2014) and suggested that PTEN loss enables for

initiation/maintenance of sustained Notch1 signalling via interactions with DL4 ligand. The data presented in this chapter, however, showed that active Notch1 was not uniformly expressed in PTEN$^{-/-}$ T cell lymphoma/leukaemia cells. One possible explanation as to why there was this discrepancy was the fact that we used different antibody to the one used in the published work. The authors used an antibody that detected all forms of Notch1, i.e. full-length peptide and the short extracellular juxtamembrane peptide, and a transmembrane sequence, and the intracellular domain (NICD). Instead, we used antibody that detected only the active NICD cleaved after Val(1744).

Equally, it is possible then that PTEN$^{-/-}$ T cell lymphoma/leukaemia cells accumulate different mutations and active Notch1 is present only in a subset of PTEN induced T-ALLs and when present, can regulate metabolism in these cells. In this context, Notch1 regulates glucose and glutamine uptake (Ciofani & Zúñiga-Pflücker 2005), personal communication with Dr Mahima Swamy) and expression of nutrient receptors, i.e. CD98 (Kelly et al. 2007) in T cell progenitors. We confirmed that Notch1 signalling induced expression of CD98 and triggered leucine uptake in T cell progenitors. Leucine in turn is an important amino acid that can induce activation of mammalian target of rapamycin complex 1 (mTORc1) (Sinclair et al. 2013; BEUGNET et al. 2003), a kinase that regulates metabolism also in T cells (Finlay et al. 2012).

We, therefore, demonstrated that PTEN deletion and hence AKT activation does not regulate nutrient uptake in PTEN$^{-/-}$ T cell lymphoma/leukaemia cells. We propose that secondary mutations that occur during the malignant transformations are likely to

regulate these processes in PTEN$^{-/-}$ T cell lymphoma/leukaemia cells, such as active Notch1 and/or overexpressed c-Myc. Both Notch1 signalling and c-Myc upregulation would link to mTORc1 activation and nutrient uptake. Therefore, mTORc1 activation might be a critical step in tumour formation.

5 Chapter: mTORc1 activity and function in PTEN$^{-/-}$ T cell lymphoma/leukaemia cells

5.1 Introduction

In the previous chapter we demonstrated that PTEN alone was not sufficient to initiate/maintain nutrient uptake and proliferation. We proposed then that increased nutrient uptake in PTEN$^{-/-}$ T cell lymphoma/leukaemia cells was caused by secondary mutations, such as c-Myc and/or Notch1 overactivation. In this context, we showed that triggering of Notch1 signalling could induce CD98 expression and subsequently leucine uptake and that these events led to activation of mTORc1.

mTORc1 is proposed to regulate cell size, proliferation and tumour growth in PTEN null induced solid tumours (Neshat et al. 2001; Podsypanina et al. 2001) and leukaemia derived cell lines (Recher et al. 2005; Avellino et al. 2005; Evangelisti et al. 2011; Schwarzer et al. 2014). Additionally, the administration of the mTORc1 inhibitor, rapamycin, to mice with inducible PTEN deletion eliminates actively proliferating cells that have the potential to promote tumour formation, called leukaemia initiating cells (Yilmaz et al. 2006). Therefore, the first question we asked was whether the primary PTEN$^{-/-}$ T cell lymphoma/leukaemia cells have active mTORc1.

A common assumption is that mTORc1 activation is caused by PI3K signalling. In this respect it should be noted that a lot of published studies about the role of PI3K as an mTOR regulator in lymphocytes used inhibitors of PI3K that are now known to

have multiple off target effects. For example, it has been described that IL-7 regulation of metabolism and survival of T-ALL cell lines is mediated via PI3K but these data are based on experiments with Ly294002 that will inhibit PI3K, mTOR and PIM serine/threonine kinases (Gharbi et al. 2007; Bain et al. 2007). There is also evidence in effector CD8+ T cells that it is mTORc1 that regulates T cell metabolism (Finlay et al. 2012) and not PI3K/AKT (Macintyre et al. 2011). Loss of mTORc1 activity, induced by rapamycin treatment leads to the loss of expression of glucose transporters and rate-limiting enzymes and decreased glucose uptake and glycolysis. Additionally, it was proposed that mTORc1 regulates expression of glucose transporters and glycolytic enzymes by controlling expression of Hif1α. Hence, functional deletion of Hif1 complexes in CTLs has similar impact on glucose uptake and glycolysis as treatment with rapamycin (Finlay et al. 2012). We, thus, tested whether mTORc1 can regulate nutrient uptake in $PTEN^{-/-}$ T cell lymphoma/leukaemia cells and if $PTEN^{-/-}$ T cell lymphoma/leukaemia cells express Hif1α, and if Hif1α expression is regulated by mTORc1.

Finally, we investigated how mTORc1 is activated in PTEN null T cells isolated prior and after the malignant transformation. There are thus two main inputs that control mTORc1 activation. One comes from the active AKT-TSC2 pathway (Yecies & Manning 2011; Menon et al. 2014; Dibble & Cantley 2015). Since we showed that AKT is phosphorylated in T cells isolated from $PTEN^{fl/fl}$ x Lck^{Cre+} mice prior and after malignant transformation, we tested if the observed phosphorylation is sufficient to phosphorylate TSC2. Second mechanism depends on amino acids availability, in particular leucine (Sinclair et al. 2013; Sancak et al. 2010; Sancak et al. 2008; Bar-

Peled et al. 2012; Zoncu et al. 2011). Therefore, we assessed if leucine is critical in maintenance of mTORc1 in $PTEN^{-/-}$ T cell lymphoma/leukaemia cells.

5.2 Results

5.2.1 mTORc1 is active in PTEN$^{-/-}$ T cell lymphoma/leukaemia cells

We first sought to establish if PTEN$^{-/-}$ T cell lymphoma/leukaemia cells have active mTORc1. In our study we assessed the activity of mTORc1 by measuring the phosphorylation of S6K (Thr389) and its substrate S6 (Ser235/236). Figure 5-1a shows that there were no detectable levels of phosphorylated S6K in untreated WT thymocytes. In contrast, untreated PTEN$^{-/-}$ T cell lymphoma/leukaemia cells showed a marked increase in S6K phosphorylation. Treatment with rapamycin leads to rapid dephosphorylation of S6K and Fig.5-1a shows that PTEN$^{-/-}$ T cell lymphoma/leukaemia cells treated with rapamycin had no detectable phosphorylation of S6K (Thr389). In contrast, treatment with phorbol ester, which induces maximal levels of S6K phosphorylation in the cell via stimulation of Protein Kinase C (Hinton et al. 2006), showed that S6K phosphorylation in PTEN$^{-/-}$ T cell lymphoma/leukaemia cells was not maximal and could be further phosphorylated. In addition to primary thymocytes isolated from PTEN$^{fl/fl}$ x Lck^{Cre-} mice (WT) and primary T leukaemic cells isolated from PTEN$^{fl/fl}$ x Lck^{Cre+} mice, we also examined the levels of mTORc1 activity in a murine cell line, F15, derived from PTEN$^{-/-}$ T cell lymphoma/leukaemia cells developed in PTEN$^{fl/fl}$ x Lck^{Cre+} mice. Accordingly, F15 cells had high levels of phosphorylated S6K (Thr389). This phosphorylation of S6K (Thr389) was lost when cells were treated with the mTORc1 inhibitor, rapamycin. Therefore, PTEN$^{-/-}$ T cell leukaemic cultured cells presented similar behaviour to *ex vivo* isolated primary PTEN$^{-/-}$ T cell lymphoma/leukaemia cells and they both had S6K phosphorylated on Thr389. This indicates that mTORc1 was active in both cell types.

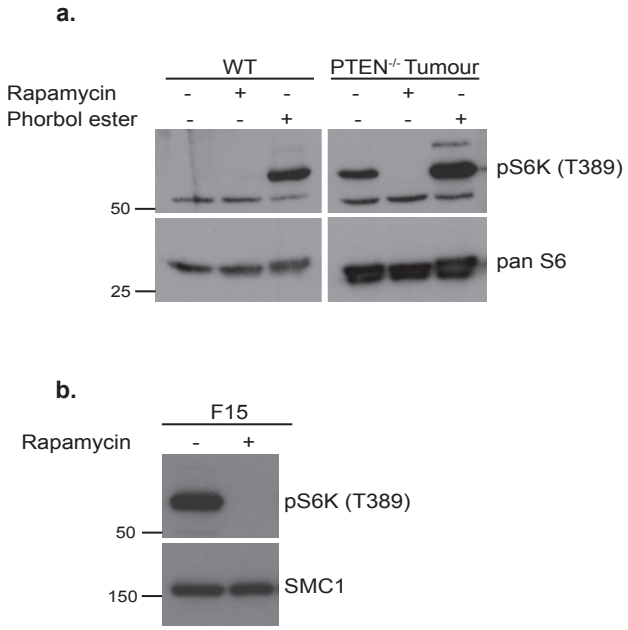

Figure 5-1 **Phosphorylation of S6K (Thr389) in WT thymocytes and PTEN$^{-/-}$ T cell lymphoma/leukaemia cells.**

a. WT CD4/CD8 DP thymocytes and PTEN$^{-/-}$ T cell lymphoma/leukaemia cells were either left untreated or treated with 20 nM rapamycin as negative control or 25 ng/ml phorbol ester as positive control for 30 minutes. Western blot analysis with phosphorylated form of S6K (Thr389) and panS6 antibodies. Pan S6 was used as a loading control. Equal numbers of cells were lysed. Numbers represent molecular weights markers and are given in kDa. Data are representative of 3 biological replicates from 3 independent experiments. **b.** PTEN$^{-/-}$ leukaemic cultured cells (F15) were either left untreated or treated with 20 nM rapamycin as negative control for 30 minutes. Western blot analysis with phosphorylated form of S6K (Thr389) and SMC1 antibodies. SMC1 was used as loading control. Equal numbers of cells were lysed. Numbers represent molecular weights markers and are given in kDa. Data are representative of 3 independent experiments.

To quantify how many cells in a population of PTEN$^{-/-}$ T cell lymphoma/leukaemia cells have active mTORc1 we used flow cytometric based assay where measured S6 phosphorylation on Ser235/236 in *ex vivo* isolated WT thymocytes and PTEN$^{-/-}$ T cell lymphoma/leukaemia cells. WT thymocytes were heterogeneous for pS6, the majority of cells were pS6^{low} and only a small percentage of cells, approximately 10%, were pS6^{high} (Fig. 5-2b). In contrast, approximately 40-55% of leukaemic cells isolated from PTEN$^{fl/fl}$ x Lck^{Cre+} mice were pS6^{high} (Fig. 5-2a-b). The data in Figure 5-2b

show that pS6 staining in WT thymocytes and PTEN$^{-/-}$ T cell lymphoma/leukaemia cells was lost when cells were treated with rapamycin. S6 phosphorylation in PTEN$^{-/-}$ T cell lymphoma/leukaemia cells was not maximal and could be further phosphorylated by treatment with phorbol ester (Fig. 5-2b).

We also evaluated mTORc1 activity in F15 PTEN$^{-/-}$ leukaemic cell line and noted that the majority of untreated F15 cells were pS6^{high} and that rapamycin treatment led to dephosphorylation of pS6 (Ser235/236) (Fig. 5.2c). These data, thus, imply that PTEN$^{-/-}$ T cell lymphoma/leukaemia cells had active mTORc1, where approximately half of the population showed high levels of S6 phosphorylation.

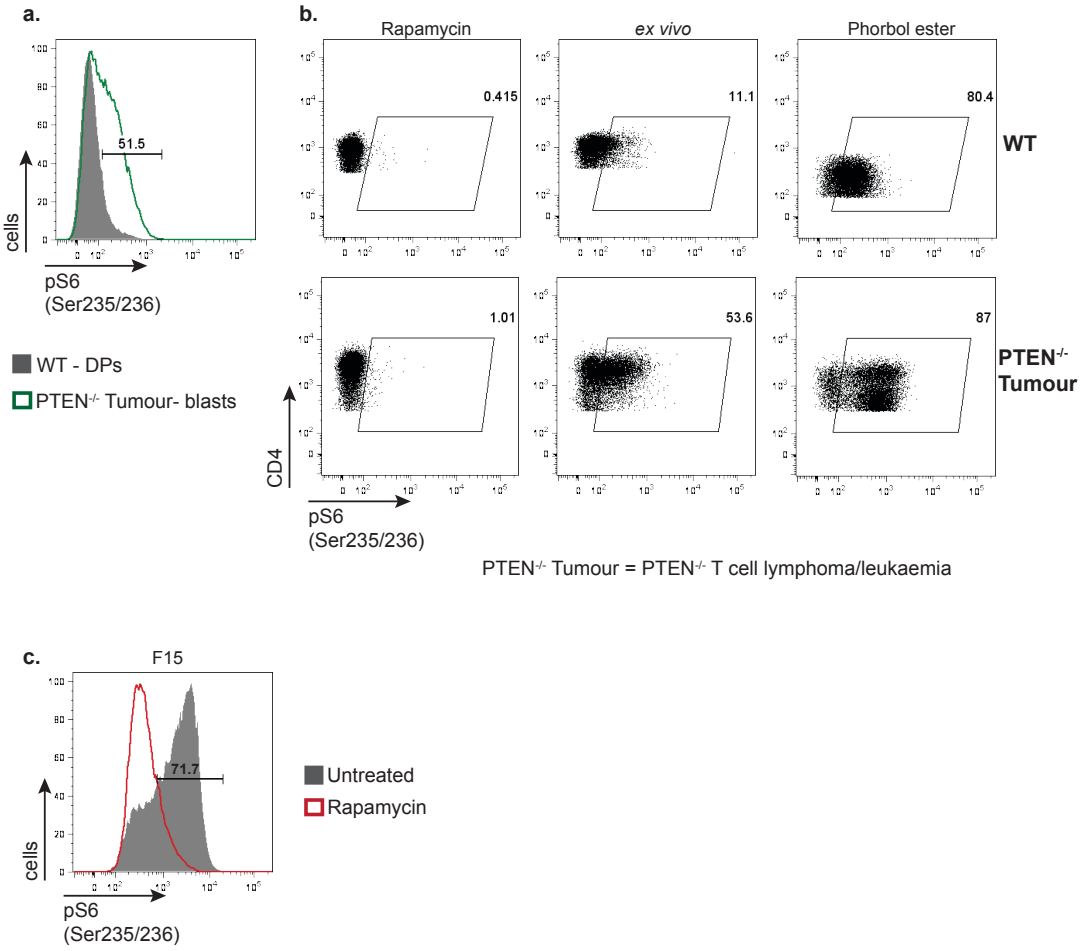

Figure 5-2 **Phosphorylation of S6 (Ser235/236) in WT thymocytes and PTEN$^{-/-}$ T cell lymphoma/leukaemia cells.**

Ex vivo isolated WT and PTEN$^{-/-}$ T cell lymphoma/leukaemia cells were either left untreated or treated with 20 nM rapamycin as negative control or treated with 25 ng/ml phorbol ester as positive control, both for 30 minutes. Then, cells were intracellularly stained for pS6 (Ser235/236) and surface stained for co-markers CD4 and CD8. Flow cytometric analysis of intracellular pS6 (Ser235/236) from WT CD4/CD8 DP thymocytes and PTEN$^{-/-}$ T cell lymphoma/leukaemia cells shown as **a.** hisogram and **b.** dot plots, the numbers denote frequencies of pS6 positive cells. Gates were set up based on rapamycin treated cells and transferred into untreated *ex vivo* cells and phorbol ester treated cells. Data are representative of 3 biological replicates from 3 independent experiments. **c.** Flow cytometric analysis of intracellular pS6 (Ser235/236) from PTEN$^{-/-}$ leukaemic cultured cells (F15) presented as histogram. Data are representative of 3 independent experiments.

5.2.2 mTORc1 inhibition downregulates nutrient uptake in PTEN$^{-/-}$ T cell lymphoma/leukaemia cells

The presented data indicated that mTORc1 was indeed active in PTEN$^{-/-}$ T cell lymphoma/leukaemia cells and in PTEN$^{-/-}$ leukaemic murine cell line, F15. In this context, it was shown that active mTORc1 can regulate glucose metabolism in activated T cells (Finlay et al. 2012). *Ex vivo* isolated PTEN$^{-/-}$ T cell lymphoma/leukaemia cells are not easily maintained in culture. Studies in normal effector T cells have shown that long-term (24-48 hours) treatment with rapamycin is required to repress glucose transport. Hence, to study the impact of long-term inhibition of rapamycin (48 hours), we decided to perform these experiments on the PTEN$^{-/-}$ leukaemic cell line - F15. We first examined if glucose uptake is regulated by mTORc1. Figure 5-3a shows that untreated F15 cells readily took up the radiolabelled glucose analogue, 2-DG. In contrast, rapamycin-treated cells showed a marked decrease of glucose uptake (approximately 70%). These data argue that mTORc1 was controlling glucose uptake also in PTEN$^{-/-}$ T cell lymphoma/leukaemia cells.

PTEN$^{-/-}$ T cell lymphoma/leukaemia cells increased uptake rates of other nutrients such as glutamine, leucine and transferrin. We, therefore, tested if mTORc1 regulates the uptake of these nutrients. First, we measured the capacity of glutamine uptake by untreated and rapamycin treated F15 cells. We found that untreated F15 cells had high rates of glutamine uptake. In contrast, mTORc1 inhibition led to a decrease in glutamine uptake by approximately 50-55% (Fig. 5-3b). We then measured ^{3}[H]-Leucine uptake by unstimulated and rapamycin treated cells. We found that while untreated PTEN$^{-/-}$ leukaemic cells had high levels of leucine uptake, treatment with rapamycin resulted in approximately 60% reduction of leucine uptake (Fig. 5-3c).

Finally, we examined the expression of transferrin receptor, CD71 and transferrin uptake in control and rapamycin treated F15 cells. The data presented in Fig. 5-3d show that rapamycin treatment decreased the expression of CD71 compared to untreated cells, however the reduction was only partial. Untreated and rapamycin treated cells were starved from transferrin for 2 hours after which the uptake of fluorescently labelled transferrin was measured. We found that untreated F15 cells readily took up transferrin and rapamycin treatment resulted in a decreased transferrin uptake. However, rapamycin did not have such a prominent effect as the complete block of transferrin uptake either by competition with holo-transferrin or by incubation on ice (Fig. 5-3e). These data then, argue that CD71 expression and transferrin uptake were controlled by a combination of mTORc1 dependent and independent pathways.

To determine if the block in nutrient uptake mediated by rapamycin impacted on the ability of the cells to grow and divide, we measured the proliferation rate of untreated and rapamycin treated F15 cells. Untreated cells expanded in culture approximately 5-fold, whereas rapamycin treated F15 cells increased their numbers approximately by 2.5 fold over 48 hours (Fig.5-3f). Therefore, treatment with rapamycin led to 2 times slower proliferation (Fig.5-3g). Additionally, the analysis of the forward and side scatter of control and rapamycin treated F15 cells showed that rapamycin treated cells were smaller compared to untreated cells (Fig. 5-3h).

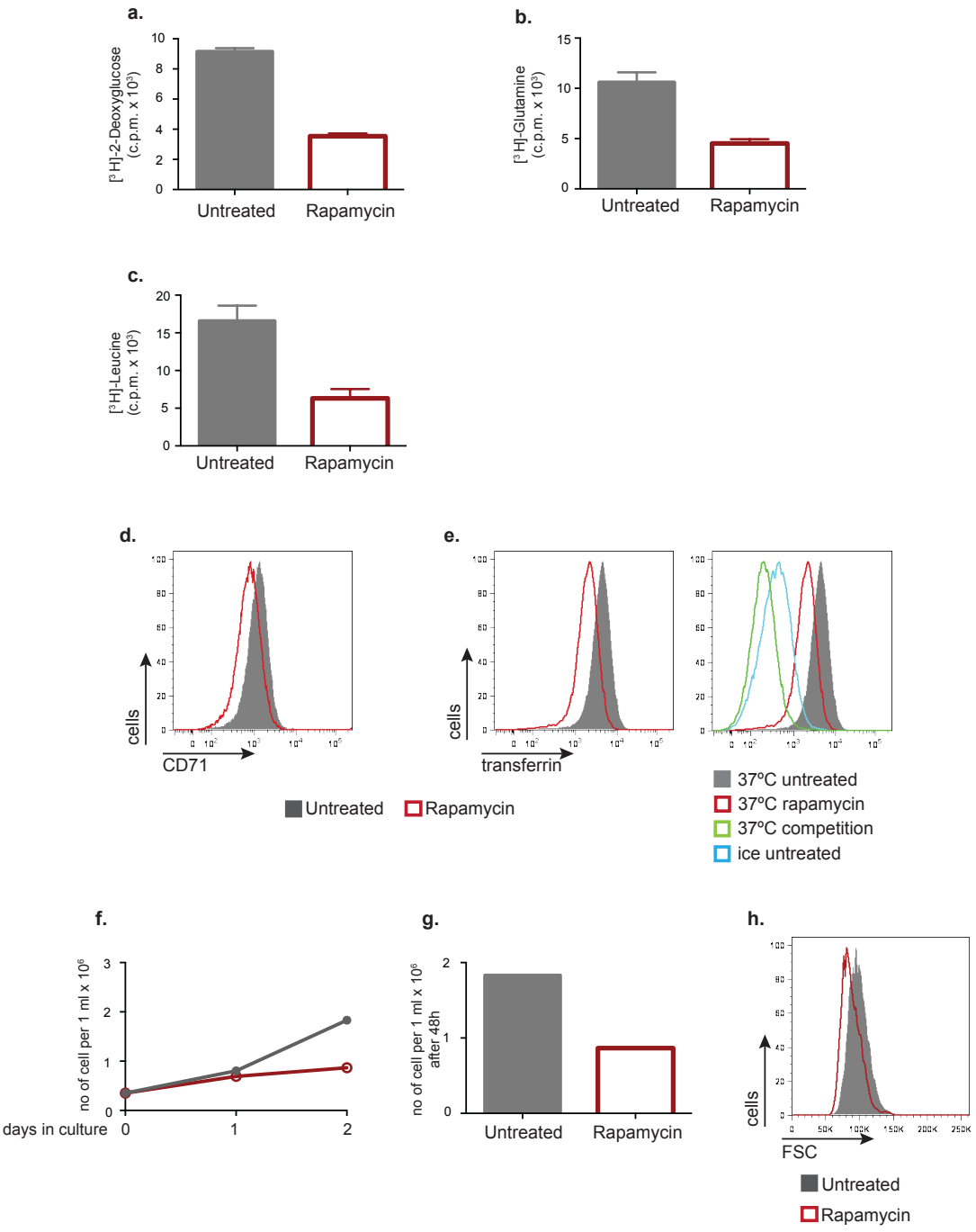

Figure 5-3 **The effects of mTORc1 inhibition on nutrient uptake in PTEN$^{-/-}$ T leukaemic cell line**.

PTEN$^{-/-}$ leukaemic cultured cells (F15) were either left untreated or treated with rapamycin for 48 hours. The ability of F15 cells to take up **a.** ^{3}[H]-2Deoxyglucose or **b.** ^{3}[H]-Glutamine or **c.** ^{3}[H]-Leucine was measured. Units show counts per minute per 1x10^{6} cells. Error bars show SD from 1 experiment and are representative of 2 independent experiments. **d.** Flow cytometric analysis presented as histograms showing expression of CD71 and **e.** transferrin uptake. The ability of cells to take up fluorescently labeled transferrin at 37ºC was measured. **e.** (right graph) Histogram depicting transferrin uptake for untreted cells kept at 37ºC (solid grey) or treated with rapmycin kept in 37ºC (red) or kept at 37ºC incubated together with transferrin competitor (green) or kept on ice (blue) to block transferrin uptake. Data are

representative of 2 independent experiments. **f.** Proliferation curve of cells cultured for two days and **g.** final number of cells per 1 ml after 2 days in the culture. Data shows the mean of 2 independent experiments. **f.** Flow cytometric analysis presented as histogram showing the size of cells grown for 2 days in rapamycin. Data are representative for 2 independent experiments.

5.2.3 PTEN$^{-/-}$ T cell Tumours express c-Myc and Hif1α

So far, we showed that PTEN$^{-/-}$ T cell lymphoma/leukaemia cells could readily take up nutrients and that these processes were downregulated when mTORc1 activity was inhibited. In activated T cells, c-Myc and Hif1α are important for initiation and maintenance of glucose metabolism and glycolysis. In chapter 4 we showed that PTEN$^{-/-}$ T cell lymphoma/leukaemia cells expressed c-Myc, whereas WT and PTEN$^{-/-}$ non-transformed thymocytes did not (Fig. 4-9). Fig. 5-4b shows that all PTEN$^{-/-}$ leukaemic murine cell lines expressed c-Myc.

It is not known if Hif1α is expressed in primary PTEN$^{-/-}$ T cell lymphoma/leukaemia cells. Immune activated effector T cells express only the Hif1α isoform, with Hif1α message and protein being only present after activation, irrespective of the oxygen tension that cells are exposed to (Finlay et al. 2012; Lukashev et al. 2001; Makino et al. 2003). Under normoxic conditions, Hif1α is targeted by PHDs and rapidly degraded whereas its expression is stabilised under hypoxia (1% O_2) (Jianhe Huang et al. 2002). We aimed to determine if Hif1α is present in PTEN$^{-/-}$ non-transformed thymocytes and in PTEN$^{-/-}$ T cell lymphoma/leukaemia cells under normoxic (we have used 21% O_2) or hypoxic (we have used 1% O_2) conditions or in cells directly analysed *ex vivo*. Figure 5-4a shows that *ex vivo* isolated WT and PTEN$^{-/-}$ non-transformed thymocytes did not express Hif1α. Similarly, Hif1α was not expressed in

WT and PTEN$^{-/-}$ non-transformed thymocytes cultured in either normoxic or hypoxic conditions. In contrast, PTEN$^{-/-}$ T cell lymphoma/leukaemia cells showed expression of Hif1α even in *ex vivo* isolated samples and this expression was further upregulated when cells were cultured in hypoxic (1% O_2) environment. We also found, that PTEN$^{-/-}$ leukaemic murine cell lines expressed Hif1α under hypoxia and in two of the cell lines (F04 and F15), Hif1α protein was stabilised and expressed even under normoxic conditions (Fig. 5-4b). The proper function of Hif1α requires its binding with Hif1β and Hif1β is constitutively expressed in cells (Semenza 2001). We examined expression of Hif1β and found that WT and PTEN$^{-/-}$ non-transformed thymocytes, and PTEN$^{-/-}$ T cell lymphoma/leukaemia cells expressed Hif1β (Fig. 5-4c). To summarise we showed that PTEN$^{-/-}$ T cell lymphoma/leukaemia cells expressed Hif1α and c-Myc whereas PTEN$^{-/-}$ non-transformed and WT thymocytes did not.

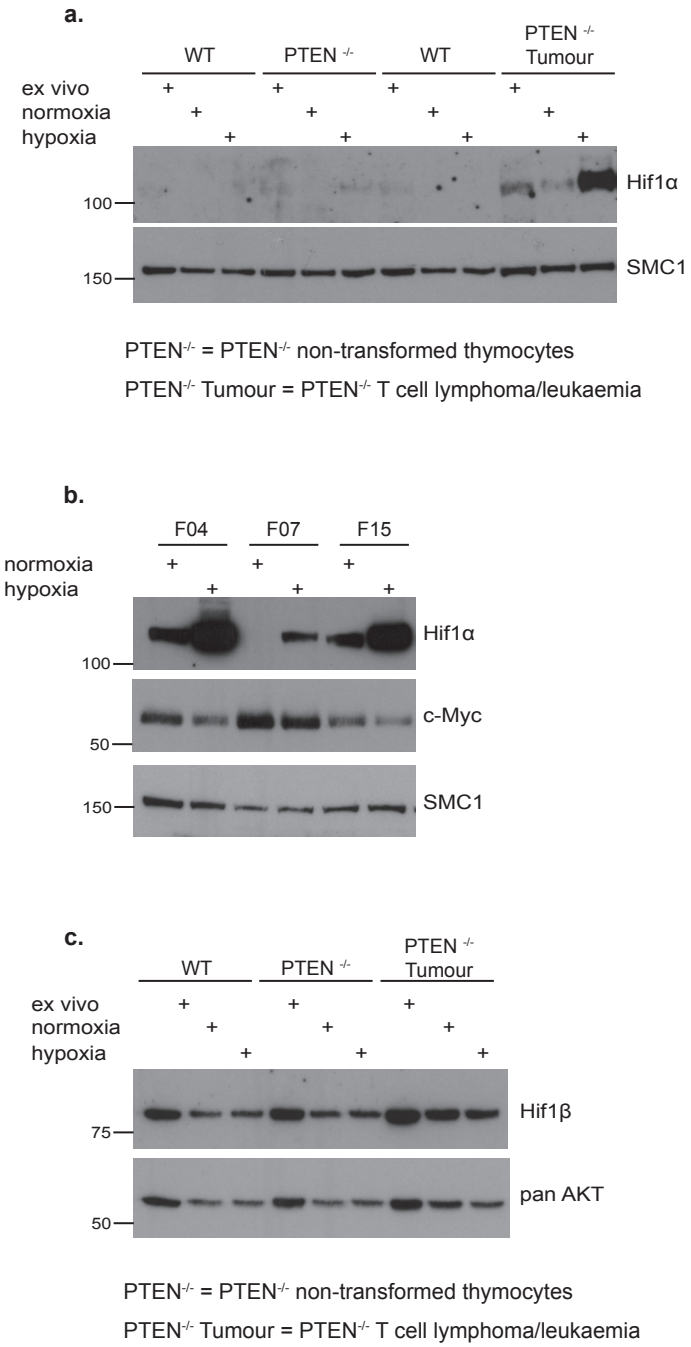

Figure 5-4 **Expression of Hif1α and c-Myc by WT thymocytes and primary PTEN$^{-/-}$ T cells and PTEN$^{-/-}$ leukaemic cell lines.**

Ex vivo isolated total WT thymocytes, PTEN$^{-/-}$ non-transformed thymocytes and PTEN$^{-/-}$ T cell lymphoma/leukaemia cells were either lysed immediately after isolation (*ex* vivo) or cultured under normoxia (21% O_2) or hypoxia (1% O_2) for 4 hours. **a.** and **c.** Western blot analysis with Hif1α, Hif1β, SMC1 and pan AKT antibodies. SMC1 and pan AKT were used as loading controls. Equal numbers of cells were lysed. Numbers represent molecular weights markers and are given in kDa. Data are representative of 3 biological replicates from 3 independent experiments. **b.** PTEN$^{-/-}$ leukaemic cultured cells (F15) were either cultured under normoxia (21% O_2) or hypoxia 1% O_2) for 4 hours. Western blot analysis with Hif1α, c-Myc and SMC1 antibodies. SMC1 was used as a loading control. Equal numbers of cells

were lysed. Numbers represent molecular weights markers and are given in kDa. Data are representative of 3 independent experiments.

5.2.4 mTORc1 inhibition leads to a loss of Hif1α expression in PTEN$^{-/-}$ T cell lymphoma/leukaemia cells

In activated T cells mTORc1 controls expression of Hif1α (Finlay et al. 2012). Hif1α known target genes include glucose transporters and rate-limiting enzymes. Earlier in this chapter, we showed that chronic inhibition of mTORc1 with rapamycin led to decrease in glucose, glutamine and leucine uptake (experiments were performed in 21% O_2 environment). Thus we asked if mTORc1 could regulate expression of Hif1α in PTEN$^{-/-}$ T cell lymphoma/leukaemia cells. Because Hif1α expression in F04 and F15 cells was readily detected under normoxic conditions, we performed the following experiments in this condition. We treated PTEN$^{-/-}$ leukaemic F04 and F15 cells with rapamycin for 24 or 48 hours to understand if/when Hif1α expression was blocked when mTORc1 is inhibited. The presented data show that rapamycin treatment was effective at blocking mTORc1 activity in F04 and F15 cells, because it resulted in dephosphorylation of S6K on Thr389 (Fig. 5-5). Furthermore, Hif1α expression was strongly decreased in rapamycin treated cells (Fig. 5-5). Therefore, these data indicate that mTORc1 regulated Hif1α expression in PTEN$^{-/-}$ T cell lymphoma/leukaemia cells. We also assessed expression of Hif1β, a binding partner of Hif1α that is required for Hif1α transcriptional activity, and showed that its expression was intact in untreated cells, however rapamycin treatment led to a reduction in its expression (Fig. 5-5). In activated T cells, mTORc1 does not regulate AKT phosphorylation/activity (Finlay et al. 2012) and we also observed that

rapamycin treated F15 cells retained AKT phosphorylation on Thr308, similar to untreated cells (Fig. 5-5). The evidence that mTORc1 controlled expression of Hif1α meant that there was the potential for Hif1α to be involved in the regulation of metabolism in PTEN$^{-/-}$ T cell lymphoma/leukaemia cells.

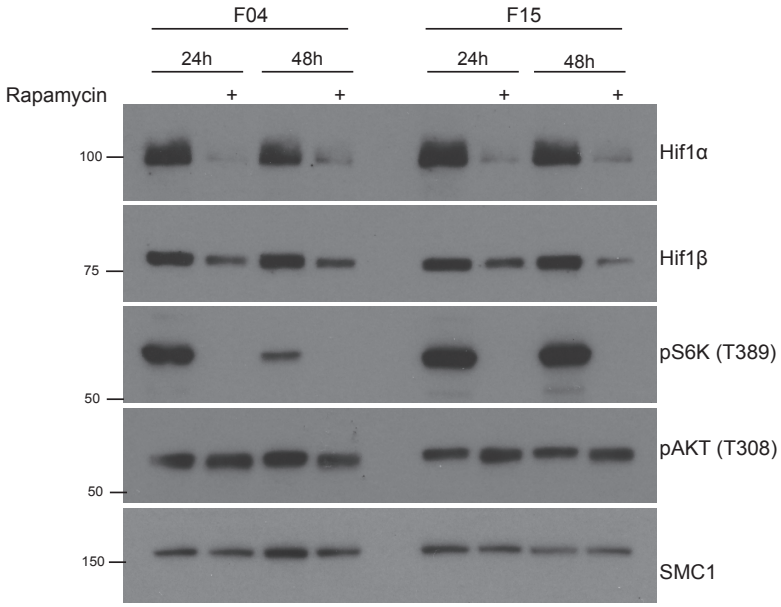

Figure 5-5 **The effect of mTORc1 inhibition of Hif1α expression in PTEN$^{-/-}$ leukaemic cell lines.**

PTEN$^{-/-}$ leukaemic cells, F04 and F15 cells were either left untreated or treated with 20 nM rapamycin for 24 hours or 48 hours under normoxia condition. Western blot analysis was for antibodies against Hif1α, Hif1β, pS6K (Thr389), pAKT (Thr308) and SMC1. SMC1 was used as a loading control. Equal numbers of cells were lysed. Numbers represent molecular weights markers and are given in kDa. Data are representative of 2 independent experiments.

5.2.5 PTEN$^{-/-}$ non-transformed thymocytes have very low mTORC1 activity

We showed that PTEN$^{-/-}$ T cell lymphoma/leukaemia cells had active mTORc1 and expressed Hif1α. Do PTEN$^{-/-}$ non-transformed thymocytes have active mTORc1? To test this, we first probed PTEN$^{-/-}$ non-transformed thymocytes for the phosphorylated form of S6K on Thr389 site. Figure 5-6a shows that there was only a small increase

in phosphorylation of S6K (Thr389) compared to $PTEN^{-/-}$ T cell lymphoma/leukaemia cells (the same Western blot analysis as in Fig. 5-1a). Treatment with rapamycin of $PTEN^{-/-}$ non-transformed thymocytes resulted in loss of S6K phosphorylation, whereas the treatment with phorbol ester showed that S6K phosphorylation in $PTEN^{-/-}$ non-transformed thymocytes was not maximal and could be further phosphorylated.

The data presented above caused us to question whether the lower mTORc1 activity in $PTEN^{-/-}$ non-transformed thymocytes compared to $PTEN^{-/-}$ T cell lymphoma/leukaemia cells reflected that in the non-transformed thymocytes mTORc1 is only active in a small subset of cells. Thus, we used the flow cytometric based assay to quantify S6 phosphorylation on Ser235/236 in *ex vivo* isolated WT and $PTEN^{-/-}$ non-transformed thymocytes. WT thymocytes were heterogeneous for pS6, the majority of cells were $pS6^{low}$ and only a small percentage of cells (5% to 7%) were $pS6^{high}$ (Fig. 5-6b-c), whereas approximately 11% of $PTEN^{-/-}$ non-transformed thymocytes were $pS6^{high}$ (Fig. 5-6b-c). The data in Figure 5-6c show that pS6 staining in WT thymocytes and $PTEN^{-/-}$ non-transformed thymocytes was lost when cells were treated with rapamycin. In contrast, stimulation with phorbol ester induced S6 phosphorylation in the $pS6^{low}$ population (Fig. 5-6c). These data show that only in a very small subset of $PTEN^{-/-}$ non-transformed thymocytes mTORc1-S6K signalling was active to mediate phosphorylation of S6. In most thymocytes, PTEN deletion was not sufficient to activate mTORc1.

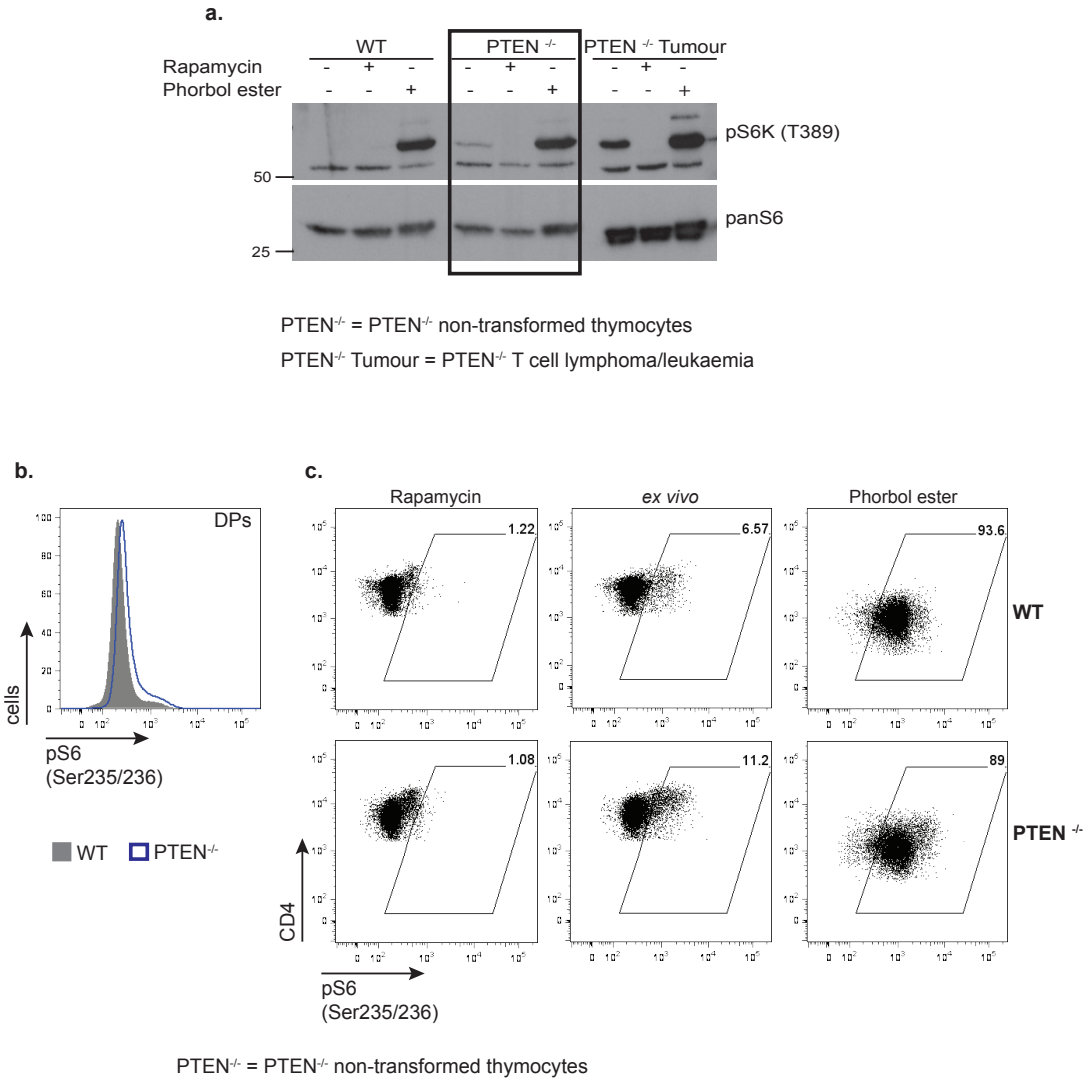

Figure 5-6 **mTORc1 activity in PTEN$^{-/-}$ non-transformed thymocytes.**

a. WT CD4/CD8 DP thymocytes, PTEN$^{-/-}$ non-transformed thymocytes and PTEN$^{-/-}$ T cell lymphoma/leukaemia cells were either left untreated or treated with 20 nM rapamycin as negative control or 25 ng/ml phorbol ester as positive control for 30 minutes. Western blot analysis with phosphorylated form of S6K (Thr389) and pan S6 antibodies. Pan S6 was used as a loading control. The same Western blot analysis as in Fig. 5-1a. Equal numbers of cells were lysed. Numbers represent molecular weights markers and are given in kDa. Data are representative of 3 biological replicates from 3 independent experiments. **b.** *Ex vivo* isolated WT thymocytes and PTEN$^{-/-}$ non-transformed thymocytes were either left untreated or treated with 20 nM rapamycin as negative control or treated with 25 ng/ml phorbol ester as positive control, both for 30 minutes and the stained intracellularly for pS6 (Ser235/236) and surface stained for co-receptors CD4 and CD8. Flow cytometric analysis presented as histograms showing pS6 (Ser235/236) expression in WT CD4/CD8 DP thymocytes and PTEN$^{-/-}$ non-transformed DP thymocytes. **c.** Flow cytometric analysis presented as dot plots of pS6 (Ser235/236) expression, the numbers denotes frequencies of pS6 positive cells. Gates were set up based on rapamycin treated cells and transferred into untreated *ex vivo* cells and phorbol ester treated cells. Data are representative of 3 biological replicates from 3 independent experiments.

5.2.6 TSC2 is phosphorylated in PTEN$^{-/-}$ non-transformed thymocytes and in PTEN$^{-/-}$ T cell lymphoma/leukaemia cells.

If mTORc1 activity may be the driving force in controlling nutrient uptake of PTEN$^{-/-}$ T cell lymphoma/leukaemia cells, we wanted to understand how mTORc1 activity is controlled in the tumours isolated from PTEN$^{fl/fl}$ x Lck^{Cre+} mice. mTORc1 activity is controlled via different ways and the best described are growth factors and amino acids availability.

AKT can phosphorylate TSC2 on several sites, among them there is Thr1462 (Manning et al. 2002; Inoki et al. 2002). This phosphorylation is important for mTORc1 activation as it inhibits TSC2 complex activity and enables RHEB to induce mTORc1 activity (Menon et al. 2014). We, therefore, assessed the phosphorylation status of TSC2 (Thr1462) in PTEN$^{-/-}$ non-transformed thymocytes and in PTEN$^{-/-}$ T cell lymphoma/leukaemia cells via two independent methods. In the first, we used immobilised 14-3-3 proteins to pull down the Thr1462 phosphorylated TSC2 from cells, and measured the extend of isolation using a pan TSC2 antibody. The rationale for this experiment is that AKT phosphorylation sites on TSC2 create 14-3-3 binding sites (Y. Li et al. 2002). We found that a low level of TSC2 was present in the 14-3-3 'pull downs' from untreated WT thymocytes. However, Figure 5-7a shows that more TSC2 was isolated by 14-3-3 proteins from untreated PTEN$^{-/-}$ non-transformed thymocytes and PTEN$^{-/-}$ T cell lymphoma/leukaemia cells. These data, thus, suggested that TSC2 was highly phosphorylated in these samples. In canonical signalling, treatment with AKTi should block TSC2 (Thr1462) phosphorylation and hence block sequestration by 14-3-3. Interestingly however, we did not notice

effective reduction of TSC2 expression in samples treated with AKTi in either PTEN$^{-/-}$ non-transformed thymocytes or PTEN$^{-/-}$ Tumour cells.

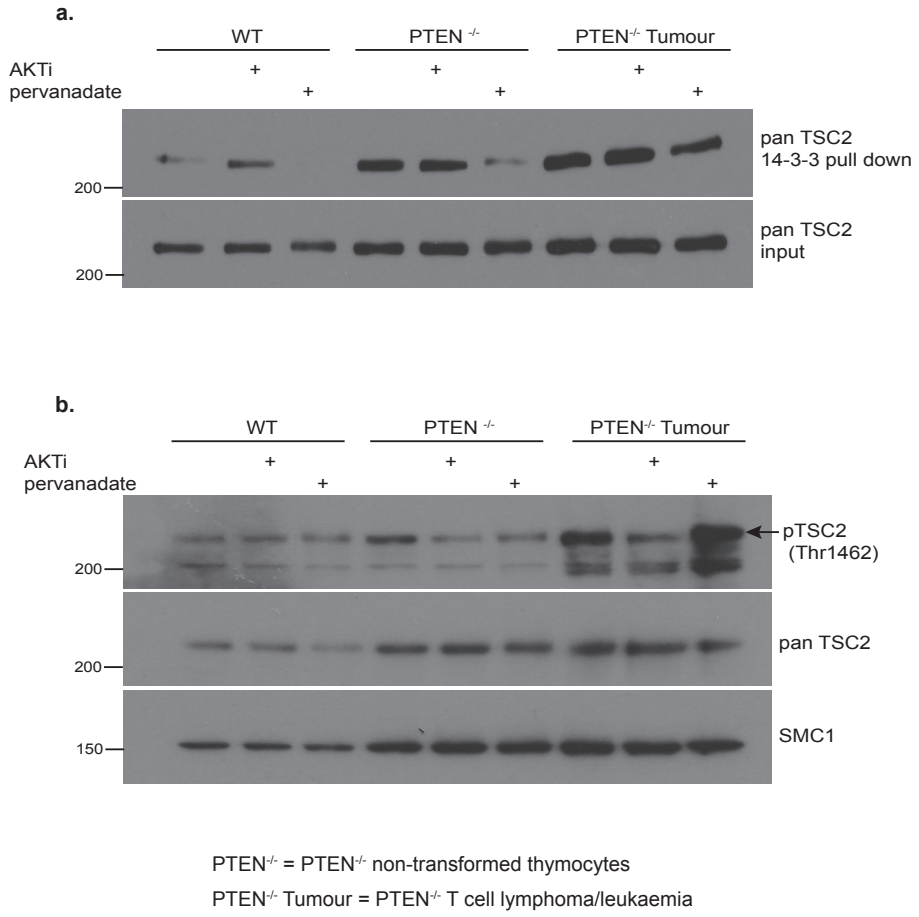

Figure 5-7 **Phosphorylation of TSC2 (Thr1462) in WT thymocytes, PTEN$^{-/-}$ non-transformed and PTEN$^{-/-}$ T cell lymphoma/leukaemia cells.**

Total e*x vivo* isolated WT thymocytes, PTEN$^{-/-}$ non-transformed thymocytes and PTEN$^{-/-}$ T cell lymphoma/leukaemia cells were either left untreated or treated with 1μM of AKTi for 1 hour or with pervanadate for 5 minutes. AKTi was used as negative control and pervanadate as positive control for TSC2 phosphorylation. **a.** Western blot analysis with pan TSC2 antibody from proteins pulled with 14-3-3 coated beads (upper panel) and from total lysates (lower panel). Pan TSC2 (input) was used as a loading control. **b.** Western blot analysis with phosphorylated form of TSC2 (Thr1462), pan TSC2 and SMC1 antibodies. SMC1 was used as a loading control. Equal numbers of cells were lysed. Numbers represent molecular weights markers and are given in kDa. Data are representative of 2 biological replicates from 2 independent experiments.

In the second approach we probed the lysates with antibodies against phosphorylated TSC2 (Thr1462) or pan TSC2. The data presented in Fig. 5-7b shows that WT thymocytes had basal level of phosphorylated TSC2 (Thr1462) whereas, the phosphorylation was slightly higher in $PTEN^{-/-}$ non-transformed thymocytes and $PTEN^{-/-}$ T cell lymphoma/leukaemia cells. However, the $PTEN^{-/-}$ non-transformed thymocytes and $PTEN^{-/-}$ T cell lymphoma/leukaemia cells appeared to have higher levels of total TSC2 protein. Additionally, the TSC2 phosphorylation in the PTEN null cells was partially reduced by AKTi treatment. These data are not clear-cut and it is possible, then, that in thymocytes, TSC2 is phosphorylated by kinases other than AKT.

5.2.7 Leucine is crucial for maintenance of mTORc1 activity in $PTEN^{-/-}$ T cell lymphoma/leukaemia cells.

The signalling pathways that feed in to the TSC2-RHEB-mTORc1 pathway include those derived from the cellular content of amino acids. Leucine, in particular, is the major activator of mTORc1 (Schriever et al. 2013; BEUGNET et al. 2003). To test if leucine is important for maintenance of mTORc1 activity in $PTEN^{-/-}$ T cell lymphoma/leukaemia cells we cultured $PTEN^{-/-}$ leukaemic cell lines – F15 in full media or in media deprived of leucine or all amino acids (HBSS, negative control) and then tested the phosphorylation of S6 (Ser235/236). The time-course analysis showed that as soon as 5 minutes after leucine withdrawal, there was a substantial loss of S6 phosphorylation in F15 cells compared to untreated cells (Fig. 5-8). After 15 minutes of leucine washout almost all mTORc1 activity was gone as judged by the S6 dephosphorylation (Ser235/236) (Fig. 5-8). Importantly, dephosphorylation of S6 (Ser235/236) after leucine withdrawal had similar kinetics to the rate of

dephosphorylation in cells switched to media lacking all amino acids (Fig. 5-8). Therefore, leucine was essential for switching on mTORc1 activity in PTEN$^{-/-}$ T cell lymphoma/leukaemia cells.

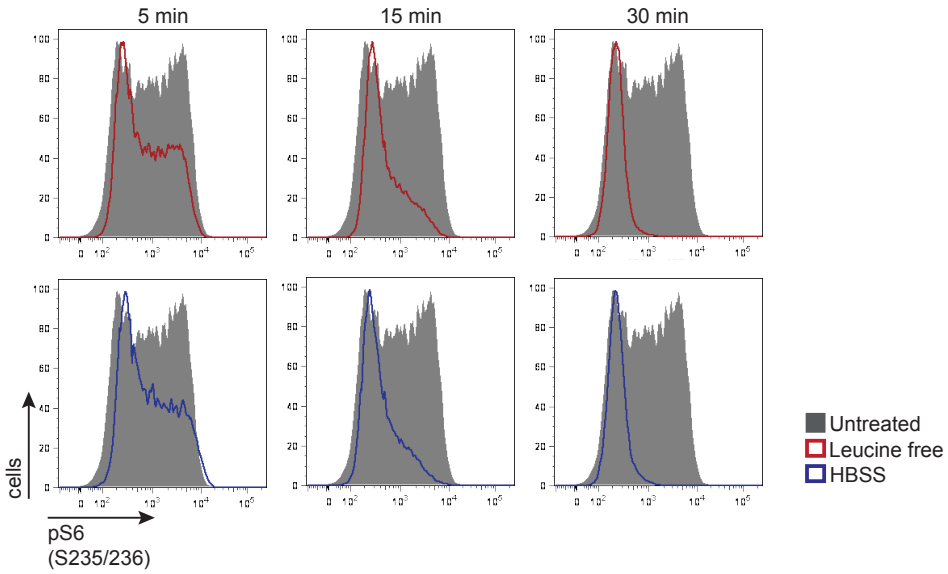

Figure 5-8 **The effects of leucine withdrawal on S6 phosphorylation (Ser235/236) in PTEN$^{-/-}$ leukaemic cell line - F15.**

PTEN$^{-/-}$ leukaemic cultured cells (F15) were either cultured for increased times in full media or media lacking leucine (red) or all amino acids (blue, the negative control). Flow cytometric analysis presented as histograms for expression of phosphorylated form of S6 on Ser235/236 as indicator of mTORc1 activity. Data are representative of 3 independent experiments.

5.2.8 PTEN$^{-/-}$ CTLs cannot sustain the nutrient uptake when deprived of IL-2

To further investigate whether PTEN deletion is sufficient to drive mTORc1 activity and signalling pathways in T cells, we switched to a different cell model, IL-2 maintained cytotoxic T cells (CTLs). These are very metabolically active and have a high level of nutrient uptake (Cornish 2006). IL-2 is a key cytokine that regulates peripheral T lymphocytes proliferation and differentiation. IL-2-maintained CTLs express high levels of Glut1 and upregulate glucose and amino acid uptake (Sinclair

et al. 2013; Cornish 2006). They also express high levels of c-Myc and Hif1α and have high levels of mTORc1 activity (Finlay et al. 2012). Therefore understanding how PTEN$^{-/-}$ CTLs will respond to IL-2 deprivation could give us insight into whether PTEN deletion can keep these cells metabolically active. Importantly, IL-2 deprivation significantly reduces nutrient uptakes and mTORc1 activity, and expression of c-Myc and Hif1α in CTLs (Cornish 2006; Macintyre et al. 2011; Finlay et al. 2012).

To generate cultures of WT and PTEN$^{-/-}$ CTLs, purified CD8+ cells were stimulated with CD3 antibody that trigger the T cell antigen receptor complex for 2 days, then cultured in IL-2 for a further 4 days. Then, for the final 24 hours in culture, CTLs were either maintained in IL-2 or deprived of IL-2. Initially, we tested if IL-2 deprivation affects AKT phosphorylation. Figure 5-8 shows that WT CTLs maintained in IL-2 had AKT phosphorylated on Thr308 and Ser473 and this phosphorylation was further increased in PTEN$^{-/-}$ CTLs. Deprivation of IL-2 resulted in slight increase of AKT phosphorylation in both WT and PTEN$^{-/-}$ CTLs. Therefore, IL-2 loss did not adversely affect AKT phosphorylation (Fig. 5-9).

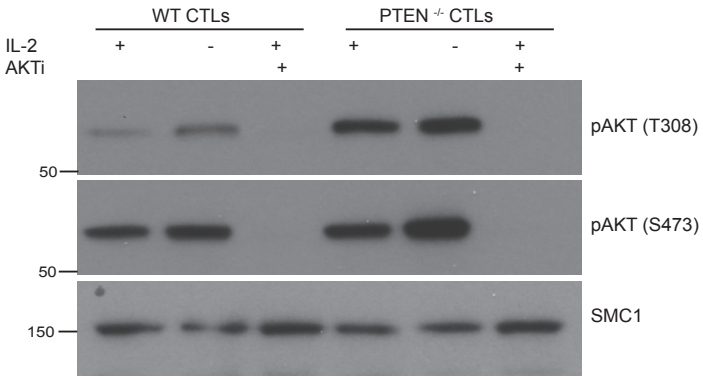

Figure 5-9 **WT and PTEN$^{-/-}$ CTLs deprived of IL-2 maintain phosphorylation of AKT**.

IL-2 maintained WT and PTEN$^{-/-}$ CTLs were either left untreated or treated with 1μM of AKTi, or deprived of IL-2 for the last 24 hours of culture. AKTi was used as negative control for AKT phosphorylation. Western blot analysis with phosphorylated forms of AKT: Thr308 and Ser473, and SMC1 antibodies. SMC1 was used as a loading control. Equal numbers of cells were lysed. Numbers represent molecular weights markers and are given in kDa. Data are representative of 3 biological replicates from 3 independent experiments.

We then tested the ability of IL-2 maintained and IL-2 deprived CTLs to take up nutrients. First, we measured if PTEN$^{-/-}$ CTLs deprived of IL-2 could take up radiolabeled 2-DG. Both WT and PTEN$^{-/-}$ CTLs maintained in IL-2 had high rates of glucose uptake (Fig. 5-10a). However, deprivation of IL-2 resulted in virtually no uptake in WT CTLs and PTEN$^{-/-}$ CTLs (Fig. 5-10a). Similarly, WT and PTEN$^{-/-}$ CTLs maintained in IL-2 had high rates of glutamine uptake but both WT and PTEN$^{-/-}$ CTLs starved of IL-2 failed to uptake ^{3}[H]-Glutamine (Fig. 5-10b). Next, we tested CD71 expression and subsequent uptake of transferrin and observed that IL-2 maintained WT and PTEN$^{-/-}$ CTLs had high expression of CD71 as well as high rates of transferrin uptake (Fig. 5-10c-d). In contrast, WT and PTEN$^{-/-}$ null CTLs deprived of IL-2 showed downregulated expression of CD71 and could not take up transferrin (Fig. 5-10c-d). Furthermore, expression of CD98 was measured and Figure 5-10e shows that both WT and PTEN$^{-/-}$ CTLs maintained in IL-2 had high expression of

CD98. Interestingly, and in contrast to previous observations, we noticed that PTEN$^{-/-}$ CTLs deprived of IL-2 expressed similar levels of CD98 compared to WT CTLs maintained in IL-2 (Fig. 5-10e), whereas IL-2 deprived WT CTLs downregulated CD98 expression. Moreover, IL-2 maintained WT and PTEN$^{-/-}$ CTLs had high rates of leucine uptake (Fig. 5-10f). Moreover, deprivation of IL-2 resulted in decrease of leucine uptake by WT CTLs. However, IL-2 deprivation did not cause a major decrease in ^{3}[H]-Leucine uptake in PTEN$^{-/-}$ CTLs. These cells, thus, had comparable ability to take up leucine as WT IL-2 maintained CTLs (Fig. 5-10f). Together, these data implied that PTEN deletion was not sufficient to maintain glucose and glutamine uptakes in CTLs but it could sustain leucine uptake.

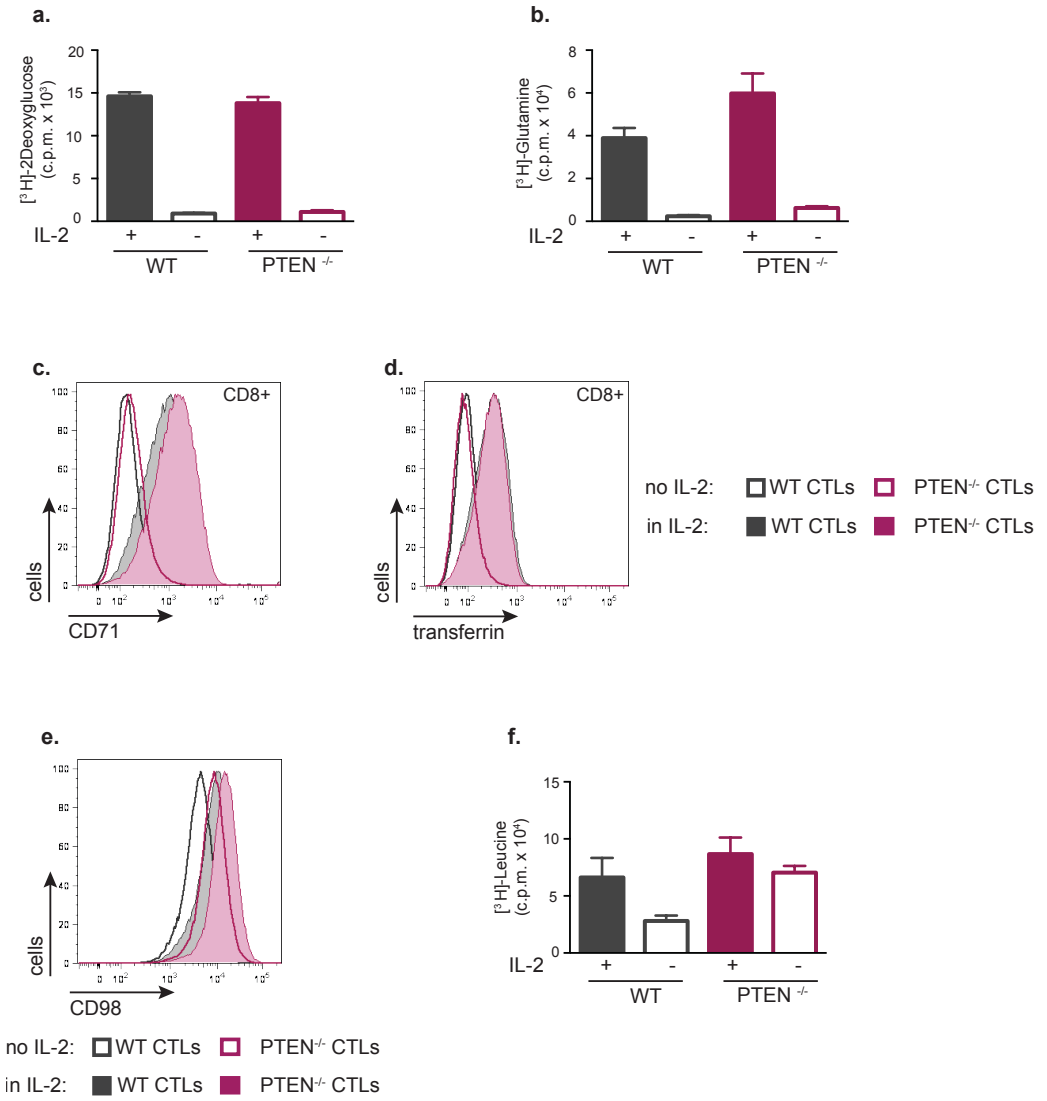

Figure 5-10 **The effects of IL-2 deprivation on nutrient uptake by WT and PTEN$^{-/-}$ CTLs.**

IL-2 maintained WT and PTEN$^{-/-}$ CTLs were either left untreated or deprived of IL-2 for the last 24 hours of culture and their ability to take up **a.** 3[H] –Glucose, **b.** ^{3}[H]-Glutamine and **f.** ^{3}[H]-Leucine was measured. Units show counts per minute per 1x10^{6} cells. Error bars show mean SD for 1 biological replicate and the data are representative for 3 independent experiments. **c.** Flow cytometric analysis presented as histograms showing expression of CD71 and **d.** transferrin uptake. Data are representative of 3 biological replicates from 3 independent experiments.

To test if leucine taken up by the PTEN$^{-/-}$ CTLs deprived of IL-2 was sufficient to sustain mTORc1 activity, we tested WT and PTEN$^{-/-}$ IL-2 maintained and IL-2 deprived CTLs for expression of phosphorylated S6K (Thr389) and its substrate S6

(Ser235/236). Figure 5-11a-b shows that while there were high levels of mTORc1 activity in WT and PTEN$^{-/-}$ CTLs maintained in IL-2, there was no detectable activity of mTORc1 in WT and PTEN$^{-/-}$ CTLs deprived of IL-2. mTORc1 regulates expression of Hif1α; therefore we tested for its expression. WT and PTEN$^{-/-}$ CTLs maintained in IL-2 had high levels of Hif1α expression (Fig. 5-11c). The loss of mTORc1 activity observed in CTLs deprived of IL-2 led to a loss of Hif1α expression in these cells (Fig. 5-11c). We also tested expression of c-Myc and found that IL-2 maintained WT and PTEN$^{-/-}$ CTLs expressed c-Myc, whereas IL-2 deprived WT and PTEN$^{-/-}$ CTLs lost c-Myc expression (Fig. 5-11c).

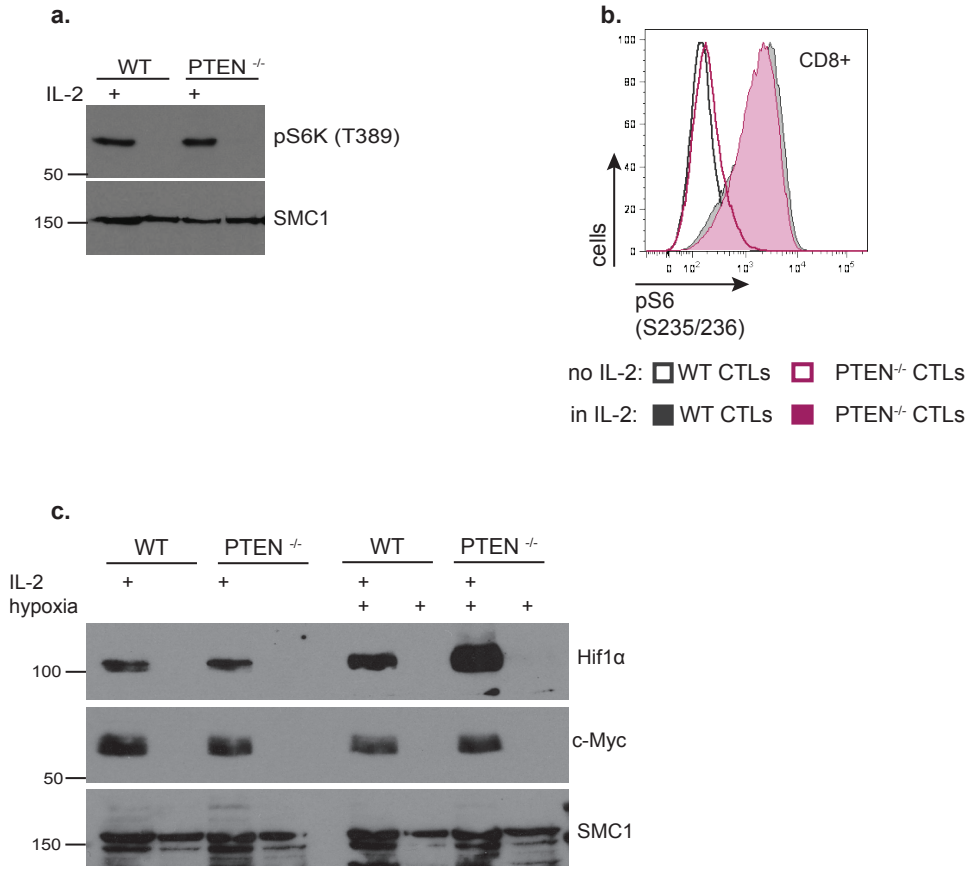

Figure 5-11 **The effects of IL-2 deprivation on mTORc1 activity and expression of Hif1α and c-Myc in WT and PTEN$^{-/-}$ CTLs.**

a. IL-2 maintained WT and PTEN$^{-/-}$ CTLs were either left untreated or deprived of IL-2 for the last 24 hours of culture. Western blot analysis with phosphorylated form of S6K (Thr389) and SMC1 antibodies. SMC1 was used as a loading control. **b.** Flow cytometric analysis presented as histogram showing pS6 (Ser235/236) expression. Data are representative of 3 biological replicates from 3 independent experiments. **c.** IL-2 maintained WT and PTEN$^{-/-}$ CTLs were either left untreated or deprived of IL-2 for the last 24 hours of culture. Additionally, for the last 4 hours they were cultured either under normoxia (21% O_2) or hypoxia (1% O_2). Western blot analysis with Hif1α, c-Myc and SMC1 antibodies. Equal numbers of cells were lysed. Numbers represent molecular weights markers and are given in kDa. Data are representative of 3 biological replicates from 3 independent experiments.

Overall, we showed that when challenged PTEN null cytotoxic T cells could not maintain the nutrient uptake and molecules that are important for mTORc1 activity. This confirmed our previous data showing that PTEN deletion was not sufficient for mTORc1 activation in T cells.

5.3 Discussion

In the previous chapters we established that PTEN did not induce the metabolic switch in $PTEN^{-/-}$ T cell lymphoma/leukaemia cells. Therefore, we proposed mTORc1 as a potential candidate in controlling nutrient uptake in $PTEN^{-/-}$ T cell lymphoma/leukaemia cells. We, thus, found that mTORc1 was active in tumour samples isolated from primary $PTEN^{fl/fl}$ x Lck^{Cre+} mice. Moreover, we demonstrated that mTORc1 activity was required to sustain nutrient uptake in $PTEN^{-/-}$ T cell lymphoma/leukaemia cells and hence required to maintain metabolism in these cells.

Upregulation and maintaining of glucose uptake and glycolysis are important for activated T cells and mTORc1, via Hif1α, plays a crucial role in regulation of these processes (Finlay et al. 2012). Earlier studies reported expression of Hif1α in cancer stem cells from mouse splenic-derived lymphoma and in leukaemic cell lines (Y. Wang et al. 2011b; Evangelisti et al. 2011). However, it was not known whether PTEN induced T cell lymphomas express Hif1α. We found that primary tumours isolated from $PTEN^{fl/fl}$ x Lck^{Cre+} mice did express Hif1α and that its expression was detected even in *ex vivo* isolated samples. In this respect, studies using the drug pimonidazole, which acts as a marker for hypoxic tissues, identified the thymus as a hypoxic organ with the mean of partial pressure of oxygen (PO_2) less than 10 mmHg (Hale et al. 2002). As expression of Hif proteins is known to mediate the adaptation to cellular hypoxia, we would expect that Hif1α would be present in all our tested tissues, i.e. WT and $PTEN^{-/-}$ non-transformed thymocytes and $PTEN^{-/-}$ T cell lymphoma/leukaemia cells. The fact that we found Hif1α only in tumour samples suggested that probably Hif1α expression was induced by secondary mutations that occur around the malignant transformation.

We, therefore, proposed that expression of Hif1α is regulated by mTORc1, as we found its activity in tumour samples isolated from primary $PTEN^{fl/fl}$ x Lck^{Cre+} mice. In this respect, effector CD8+ T cells and effector CD4+ Th17 producing cells treated with rapamycin loose expression of Hif1α and as a result decrease their metabolism (Finlay et al. 2012; Shi et al. 2011). We demonstrated that $PTEN^{-/-}$ T cell lymphoma/leukaemia cells could regulate these processes in a similar way because rapamycin treated $PTEN^{-/-}$ T cell lymphoma/leukaemia cells decreased glucose uptake. Preliminary experiments (data not shown) indicated that $PTEN^{-/-}$ T cell lymphoma/leukaemia cells also had decreased rate of lactate production. It might be beneficial to also determine the expression of rate limiting enzymes in $PTEN^{-/-}$ T cell lymphoma/leukaemia cells treated with rapamycin to gain better understanding of mTORc1-Hif1α regulation of glucose metabolism.

Interestingly, we also found that mTORc1 could control uptake of other nutrients in $PTEN^{-/-}$ T cell lymphoma/leukaemia cells such as glutamine and leucine, as rapamycin treatment led to decrease in uptake of these amino acids. Nicklin *at al.*, proposed that there is a continuous requirement for glutamine efflux with simultaneous import of leucine to fuel mTORc1 activation (Nicklin et al. 2009), but it was not clear if mTORc1 can regulate the expression of transporters for glutamine and leucine. Our data suggested that at least in $PTEN^{-/-}$ T cell lymphoma/leukaemia cells it is possible. Interestingly, rapamycin treatment of $PTEN^{-/-}$ T cell lymphoma/leukaemia cells did not result in cell death. Instead, the cells retained their ability to proliferate, albeit at lower rate than the untreated controls. Then, how could $PTEN^{-/-}$ T cell lymphoma/leukaemia cells proliferate given that they had reduced levels of nutrient uptake? One key point here would be that rapamycin treatment

decreased glucose uptake by approximately 70% but it did not reduce it to zero. In this context, rapidly proliferating cells, like CTLs, will use glucose to produce pyruvate that then is used for production of biosynthetic precursors. It is therefore possible that the reduced glucose uptake was sufficient to maintain proliferation of rapamycin treated PTEN$^{-/-}$ T cell lymphoma/leukaemia cells. Additionally, low mTORc1 activity has been linked to the increased formation of autophagosomes (Korolchuk et al. 2011). Autophagy is a catabolic process by which the degradation of dysfunctional or unwanted proteins and cellular components occurs and takes place in lysosomes (Yang & Klionsky 2010). Importantly, metabolites of autophagy can be reused to fuel biosynthesis of new macromolecules and hence promote cell survival and maintenance of cellular energy levels (Boya et al. 2013). Therefore, low amino acids availability observed in rapamycin treated PTEN$^{-/-}$ T cell lymphoma/leukaemia cells could further inhibit mTORc1 activity and thus force cells to perform autophagy that provided nutrients to support cell division.

What controls mTORc1 activity in PTEN$^{-/-}$ T cell lymphoma/leukaemia cells? In this respect our data showed that PTEN deletion and AKT activation was not sufficient to activate mTORc1 in most PTEN$^{-/-}$ non-transformed thymocytes or in CTLs. In the thymus, the most probable reason for the minimal mTORc1 activity was that PTEN deletion was not sufficient to induce glucose, glutamine and leucine uptake, and the supply of these nutrients is essential for mTORc1 activity (Finlay et al. 2012; Nicklin et al. 2009; Sinclair et al. 2013; Rolf et al. 2013). As a result, PTEN$^{-/-}$ non-transformed thymocytes that were not able to upregulate uptake of these nutrients, also could not induce/sustain mTORc1 activity.

To summarise, we showed that leucine availability is critical for continuous mTORc1 activity in $PTEN^{-/-}$ T cell lymphoma/leukaemia cells. Active mTORc1 in turn regulates glucose uptake and glycolysis, and Hif1α expression (Finlay et al. 2012). In the next chapter, we will investigate the role of Hif1α after PTEN deletion in an *in vivo* mouse model of T lymphomagenesis and also whether Hif1α can contribute to the control of nutrient uptake and hence metabolism in $PTEN^{fl/fl}$ x Lck^{Cre+} mice.

6 Chapter: The role of Hif1α in tumour development of PTEN$^{fl/fl}$ x Lck^{Cre+} mice

6.1 Introduction

The importance of Hif1α activity in promoting lymphomagenesis was previously addressed. In particular, it was noticed that active Hif1α is needed for the survival of leukaemia initiating cells (LIC) and hence tumour initiation and its progression (Y. Wang et al. 2011b; Giambra et al. 2015). LIC are haematopoietic cells that are capable of promoting the development of lymphoma/leukaemias once transplanted to immunodeficient or syngeneic mice (Guo et al. 2008). Genetic ablation of Hif1α in leukaemic cells that are transplanted into secondary recipients leads to reduction of LIC frequency (Giambra et al. 2015). Similarly, pharmacological inhibition of Hif1α in cultured lymphoma cells results in reduction of LIC numbers when they are transplanted into secondary recipients (Y. Wang et al. 2011b).

Hif1α has been described to be important in non-transformed cells. Hence early studies done in embryonic stem (ES) cells revealed that ablation of Hif1α leads to reduction of enzymes involved in glucose metabolism (Ryan et al. 2000; Iyer et al. 1998). Additionally, studies done in T cells showed that deletion of Hif1α in either CD4+ Th17 producing cells or CD8+ CTLs also leads to downregulation of glucose transporter and glycolytic enzymes, arguing for the importance of Hif1 complexes in maintaining the metabolic switch in these cells (E. V. Dang et al. 2011; Shi et al. 2011; Finlay et al. 2012). Moreover, Tandon *at al.,* showed that knockdown of Hif1α in a PTEN deficient haematopoietic progenitor cell line results in decreased rates of

glycolysis and this phenotype can be rescued when these cells are forced to express a normoxia-stable Hif1α mutant (Tandon et al. 2011).

Given the fact that $PTEN^{-/-}$ T cell lymphoma/leukaemia cells expressed Hif1α and that mTORc1 controlled Hif1α expression and also controlled glucose uptake, we hypothesised that Hif1α deletion would prevent sustained expression of genes and proteins involved in glucose metabolism and hence prevent tumourigenesis in $PTEN^{-/-}$ T cell lymphoma/leukaemia cells. Therefore, to understand whether Hif1α plays a role in glucose metabolism and whether the loss of Hif1α can prevent formation of tumours in $PTEN^{fl/fl}$ x Lck^{Cre+} mice, we decided to simultaneously delete *Hif1α* and *Pten* genes in T cell progenitors in $PTEN^{fl/fl}$ x $Hif1\alpha^{fl/fl}$ x Lck^{Cre+} (DKO) mice.

6.2 Results

6.2.1 Hif1α loss does not impair T cell development

In order to study the impact of Hif1α loss on tumourigenesis in $PTEN^{fl/fl}$ x Lck^{Cre+} mice, we first examined if deletion of Hif1α in T cell progenitors has any effect on T cell development. Therefore, Hif1α-floxed mice (Ryan et al. 2000) were purchased from The Jackson Laboratory® and backcrossed with mice expressing Cre recombinase under the control of the Lck promoter. Thymi of WT and $Hif1\alpha^{fl/fl}$ x Lck^{Cre+} mice were similar in size and the total numbers of cells were comparable between the two, and were within the normal range. Average numbers of total thymocytes were 20.5 x 10^7 for WT and 17.9 x 10^7 in $Hif1\alpha^{-/-}$ thymi (Fig. 6-1a). Figure 6-1b shows that WT and $Hif1\alpha^{-/-}$ thymi had similar distribution of cells in each developmental stage. WT thymocytes typically contained around 85% of CD4/CD8 DPs and approximately 5% of single positive (SP) CD4+ and 1.5% of SP CD8+ cells. Accordingly, $Hif1\alpha^{-/-}$ thymi contained approximately 83% of CD4/CD8 DPs, 7% of SP CD4+ cells and 2% of SP CD8+ cells. The frequencies of thymic populations were reflected by their total numbers (Fig.6-1f). Staining with CD25 and CD44 markers that can differentiate between the double negative populations, also showed similar percentages of cells in DN1 to DN4 in WT and $Hif1\alpha^{-/-}$ thymocytes (Fig.6-1c). In addition, the surface expression of TCRb and the percentage of $TCRb^{high}$ cells were similar in WT and $Hif1\alpha^{-/-}$ thymocytes and on average they were 7.5% and 10%, respectively (Fig. 6-1d). Moreover, the total numbers for $TCRb^{high}$ cells were also comparable between WT and $Hif1\alpha^{-/-}$ thymocytes (Fig.6-1g). The similar ratios and numbers of $TCRb^{high}$ cells were also reflected in the production of mature SP cells in the thymus as indicated by comparable percentages of $TCRb^{high}$ $CD24^{low}$ cells in WT

and Hif1α$^{fl/fl}$ x Lck^{Cre+} mice with 5.5% and 8%, respectively (Fig. 6-1e). These data thus indicated that loss of Hif1α did not affect T cell development in the thymus.

Neither thymocytes nor naïve cells express Hif1α protein. However, immune activated CD8+ T cells induce expression of Hif1α protein and therefore, we used them to show that Hif1α is deleted in T cells. Thus, we stimulated cells isolated from spleen with CD3 antibody that trigger the T cell antigen receptor complex for 2 days and then cultured in IL-2 for the next 4 days. We left cells either untreated (normoxia) or treated with 1% O_2 (hypoxia) as the positive control, because hypoxia allows for the stabilization of Hif1α protein. Western blot analysis in Fig. 6-1h shows that while WT CTLs expressed Hif1α under normoxic and hypoxic conditions, Hif1α$^{-/-}$ CTLs lost Hif1α expression also under hypoxic condition. These data confirmed that T cell could develop in the absence of Hif1α.

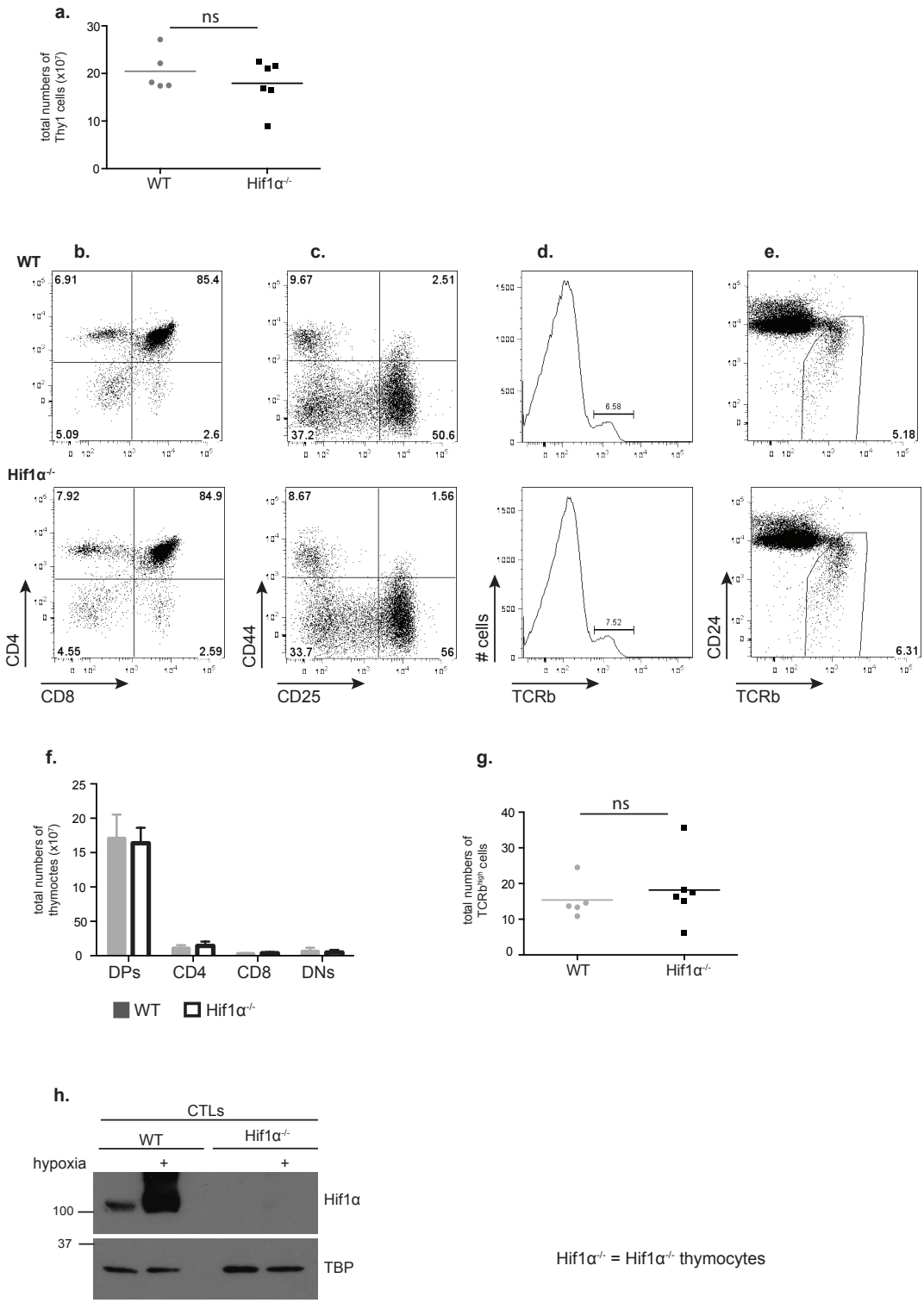

Figure 6-1 **Flow cytometric analysis of T cell development in WT and Hif1α$^{fl/fl}$ x Lck^{Cre+} mice.**

Ex vivo isolated thymi from WT and Hif1α$^{-/-}$ mice were stained with either Thy1, CD4, CD8, CD25 or CD44 or Thy1, CD4, CD8, TCRb and CD24 surface markers and subjected to flow cytometry analysis presented as: **a.** Total thymi numbers calculated for Thy1 positive cells. **b.** Dot blot showing expression of CD4 and CD8 markers on Thy1 positive cells. **c.** Dot plot analysis showing expression of CD44 and CD25 markers on double negative cells. **d.** Histogram showing expression of surface TCRb and the percentage of TCRb^{high} cells gated

on Thy1 positive cells. **e.** Dot plot showing expression of CD24 and TCRb surface markers, gated on Thy1 population. **f.** Total numbers of CD4/CD8 DP, SP CD4+, SP CD8+ and CD4/CD8 DN cells. **g.** Total numbers of $TCRb^{high}$ cells. All data are representative of 5 biological replicates from 2 independent experiments; p-values were calculated by t-test, ns – not significant. **h.** Western blot analysis of WT and $Hif1\alpha^{-/-}$ CTLs was with antibodies against Hif1α and TBP. TBP was used as a loading control. Equal numbers of cells were lysed. Numbers represent molecular weights markers and are given in kDa. Data are representative of 3 biological replicates from 3 independent experiments.

Peripheral lymphocyte populations in spleen (Fig. 6.2a) and lymph nodes (data not shown) of WT and $Hif1\alpha^{fl/fl}$ x Lck^{Cre+} mice were also isolated and analysed by flow cytometry. Figure 6-2a shows that percentages and ratios of T (TCRb+) cells and B (B220+) cells were normal. WT spleens typically contained approximately 20% of TCRb+ cells and 70% of B220+ cells and the same were found in $Hif1\alpha^{-/-}$ splenocytes. Additionally, both spleen (Fig.6-2b) and lymph nodes (data not shown) showed normal ratios of CD4+ and CD8+ cells within the TCRb population. WT spleen contained approximately 75% of CD4+ cells and 25% of CD8+ cells and we also observed similar distribution of splenocytes in $Hif1\alpha^{fl/fl}$ x Lck^{Cre+} mice (Fig. 6-2b). These data then suggested that in the absence of Hif1α, the ability of T cells to survive in secondary lymphoid organs was not impaired.

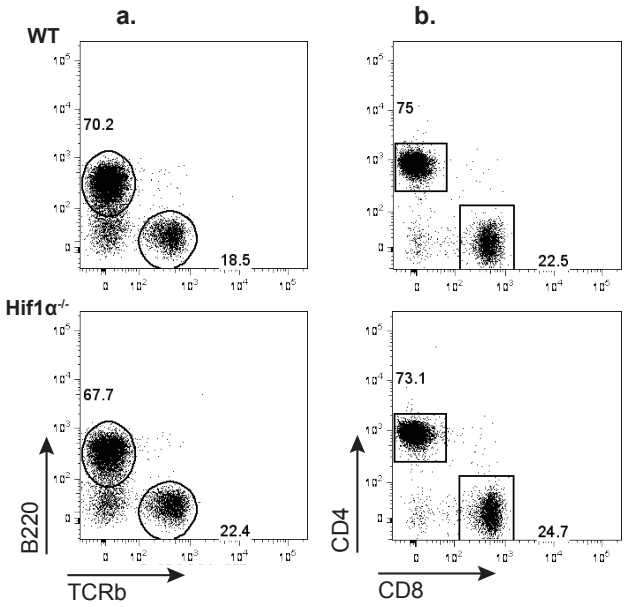

Figure 6-2 **Flow cytometric analysis of splenocytes in WT and Hif1α$^{fl/fl}$ x Lck^{Cre+} mice.**

Ex vivo isolated splenocytes from WT and Hif1α$^{-/-}$ mice were stained with TCRb, B220, CD4 and CD8 surface markers and subjected to flow cytometry analysis presented as: **a.** Dot blot showing expression of TCRb and B220 markers on total splenocytes. **b.** Dot plot analysis showing expression of CD4 and CD8 markers on TCRb+ cells. All data are representative of 5 biological replicates from 2 independent experiments.

6.2.1 Loss of Hif1α leads to prolonged lifespan of PTEN$^{fl/fl}$ x Hif1α$^{fl/fl}$ x Lck^{Cre+} mice compared to PTEN$^{fl/fl}$ x Lck^{Cre+} mice

Having established that Hif1α loss did not impair T cell development in the thymus, we sought to understand if Hif1α was involved in the development of T cell lymphoma/leukaemia that occurs following deletion of PTEN in T cell progenitors in the thymus. Therefore, we analysed mice with double deletion of PTEN and Hif1α, PTEN$^{fl/fl}$ x Hif1α$^{fl/fl}$ x Lck^{Cre+} (DKO) mice. We then allowed a cohort of PTEN$^{fl/fl}$ x Lck^{Cre+} and PTEN$^{fl/fl}$ x Hif1α$^{fl/fl}$ x Lck^{Cre+} mice to age. During this time we closely monitored the welfare of these animals, and when any signs of tumours appeared, such as hunched posture, rough coat, lack of mobility and/or swollen abdomen/neck, mice were culled. PTEN$^{fl/fl}$ x Lck^{Cre+} had a median survival of 68 days and only a

small percentage of these mice (14%) survived beyond 100 days. In contrast, the majority of DKO mice (76%) at 100 days appeared healthy, without any symptoms of tumour development (Fig. 6-3a). Figure 6-3b compares the survival kinetics of $PTEN^{fl/fl}$ x Lck^{Cre+} mice and $PTEN^{fl/fl}$ x $Hif1\alpha^{fl/fl}$ x Lck^{Cre+} mice. Control WT mice remained healthy during the course of the study and typically had a life span of more than 12 months (data not shown). As already mentioned, $PTEN^{fl/fl}$ x Lck^{Cre+} mice developed massive T lymphomas and 90% of these mice died by 13^{th} week of age and the remaining 10% by 20^{th} week of age. When PTEN and Hif1α were both deleted in T cell progenitors, 39 out of 40 mice developed tumours. However, unlike $PTEN^{fl/fl}$ x Lck^{Cre+} mice, DKO mice died between 10^{th} and 50^{th} week of age with the median life span of 128 days. These data, thus, implied that simultaneous loss of Hif1α and PTEN led to prolonged survival, because DKO mice lived almost twice as long as $PTEN^{fl/fl}$ x Lck^{Cre+} mice. These data would argue that Hif1α was important in tumour development and its presence in $PTEN^{fl/fl}$ x Lck^{Cre+} mice accelerated this process.

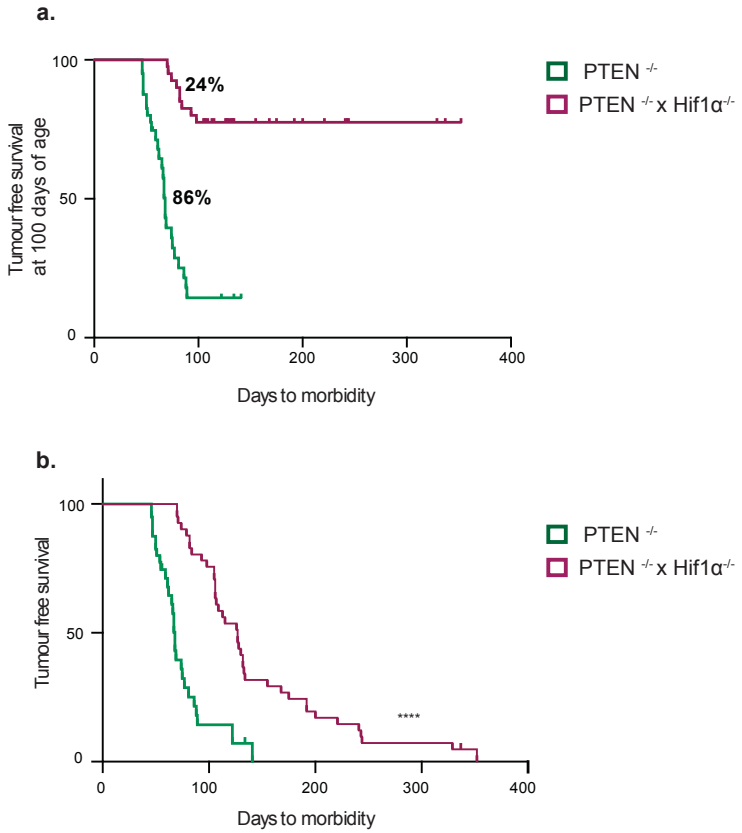

Figure 6-3 **The analysis of survival of PTEN$^{fl/fl}$ x Lck^{Cre+} and PTEN$^{fl/fl}$ x Hif1α$^{fl/fl}$ x Lck^{Cre+} mice.**

Graphs showing the Kaplan-Meier curves for PTEN$^{fl/fl}$ x Lck^{Cre+} (green) and PTEN$^{fl/fl}$ x Hif1α$^{fl/fl}$ x Lck^{Cre+} (purple) mice. **a.** Survival analysis at 100 days, the numbers indicate percentages of animals that were tumour free at that time. **b.** Survival analysis until 350 days. *** $p<0.0001$ was calculated by Log-rank (Mantel-Cox) test and by Gehan-Breslow-Wilcoxon test. Data are for 40 mice in each genotype.

To assess that the tumours from the DKO mice did not express Hif1α and PTEN proteins, we tested all PTEN$^{-/-}$ x Hif1α$^{-/-}$ T cell lymphoma for genomic deletion of *Hif1α* and *Pten* genes. To do this we performed genotyping of the tumours using a PCR protocol that utilised three primers (Fig. 6-4a-b). The protocol was designed by Elizabeth Emslie. Two primers (LoxP F and LoxP R) amplified the region surrounding the proximal *loxP* site, generating a product of approximately 290bp for Hif1α or 230bp for PTEN when the *loxP* site was absent (WT) or approximately 350bp and 280bp (Hif1α and PTEN, respectively) when the site was present (FL).

When the site recognised by LoxP R primer was removed following *loxP* excision (Del), primers LoxP F and R amplified the region in between them generating a product of approximately 450bp and 380bp for Hif1α and PTEN, respectively. If the *loxP* sites were intact, primers LoxP F and R could not amplify the region in between them, therefore, generated no product, as they were more than 1kbp apart from each other.

The analysis of genomic DNA in Fig. 6-4c showed that in the 'ear control' we detected two products of PCR amplification: *loxP* flanked (FL) and WT *Pten* or *Hif1α* alleles. The analysis of genomic DNA isolated from thymocytes from $PTEN^{fl/fl}$ x $Hif1\alpha^{fl/fl}$ x Lck^{Cre-} (WT) mice detected one product of PCR amplification of *loxP* flanked (FL) *Pten* or *Hif1α* alleles. In contrast, we found that in the DNA from T cell lymphoma cells isolated from $PTEN^{fl/fl}$ x $Hif1\alpha^{fl/fl}$ x Lck^{Cre+} mice there were no *Pten* and *Hif1α* alleles, as we detected only deleted (Del) product of PCR amplification for these alleles.

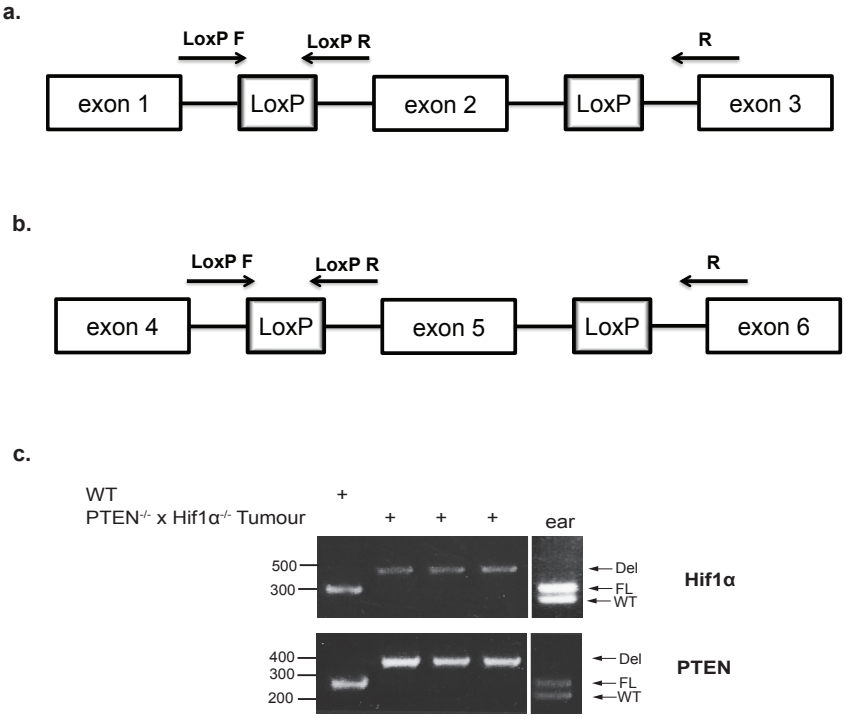

Figure 6-4 **Analysis of genomic deletion of *Hif1α* and *Pten* genes in WT thymocytes and PTEN$^{-/-}$ x Hif1α$^{-/-}$ T cell lymphoma.**

DNA from *ex vivo* isolated WT thymocytes and PTEN$^{-/-}$ x Hif1α$^{-/-}$ T cell lymphoma was tested for the presence of *Hif1α* and *Pten* genes. **a.** Hif1α^{fl} and **b.** PTEN^{fl} exon structure showing exons plus PCR primer binding sites. **c.** PCR analysis of Hif1α^{WT}, Hif1α^{FL}, Hif1α^{Del} (upper gel) and PTEN^{WT}, PTEN^{FL}, PTEN^{Del} (lower panel) genomic DNA. The analysis was performed for all tumour samples that developed in PTEN$^{fl/fl}$ x Hif1α$^{fl/fl}$ x Lck^{Cre+} mice and at least 3 tumour samples isolated from PTEN$^{fl/fl}$ x Lck^{Cre+} mice.

6.2.2 PTEN$^{fl/fl}$ x Hif1α$^{fl/fl}$ x Lck^{Cre+} mice develop lymphoma

Flow cytometric analysis of forward and side scatter of *ex vivo* isolated PTEN$^{-/-}$ x Hif1α$^{-/-}$ T cell lymphomas showed that tumours comprised cells that were large and blast-like in contrast to WT thymocytes (Fig. 6-5a). Additionally, we found that thymi isolated from PTEN$^{fl/fl}$ x Lck^{Cre+} mice were massively enlarged and accordingly, the number of cells from PTEN$^{-/-}$ x Hif1α$^{-/-}$ thymi was increased on average 2-fold compared to the numbers of WT thymi (Fig. 3-2b). Next, we tested the

expression of the surface markers CD4 and CD8 Thy1 positive cells. In this respect, $PTEN^{fl/fl}$ x Lck^{Cre+} tumour bearing mice has been shown to have altered thymic populations and typically contain either CD4/CD8 DPs only or a mix of CD4/CD8 DPs and SP CD4, or a mix of CD4/CD8 DN, CD4/CD8 DPs and SP CD4 cells (Hagenbeek & Spits 2007). Flow cytometric analysis of surface markers CD4 and CD8 on Thy1 positive cells in $PTEN^{-/-}$ x $Hif1\alpha^{-/-}$ T cell lymphoma showed that these were abnormally expressed compared to WT thymi (Fig. 6-5c). While WT thymocytes were mostly CD4/CD8 DPs, with SP CD4 cells and SP CD8 cells being the next biggest populations, 10 out of 16 tumour samples expressed either only CD4/CD8 DPs or CD4/CD8 DPs and SP CD4 cells. Another characteristic of $PTEN^{-/-}$ T cell lymphoma/leukaemia cells is that they disseminate into peripheral lymphoid organs i.e. spleen and lymph nodes (Hagenbeek & Spits 2007). We found that tumour-bearing mice with double deletion of PTEN and Hif1α had enlarged spleen (Fig. 6-5d) and LN (data not shown) and increased their spleen numbers by more than 3-fold comparing to WT spleen (Fig. 6-5d). Flow cytometric analysis of surface markers of T cells (TCRb) and B cells (B220) showed that WT spleen typically contained approximately 24% of TCRb+ cells and 64% of B220+ cells, in contrast to tumours isolated from $PTEN^{fl/fl}$ x $Hif1\alpha^{fl/fl}$ x Lck^{Cre-} mice that had 75% of TCRb+ cells and only 6% of B220 cells (Fig. 6-5e). These altered ratios of T and B cells in $PTEN^{-/-}$ x $Hif1\alpha^{-/-}$ spleens were reflected in a massive 16-fold increase in numbers of TCRb+ cells with concomitant 5-fold decrease of B220+ cells (Fig. 6-5f). Collectively, these data showed that tumours that developed in $PTEN^{fl/fl}$ x $Hif1\alpha^{fl/fl}$ x Lck^{Cre+} mice had similar characteristics to $PTEN^{-/-}$ T cell leukaemia/lymphomas.

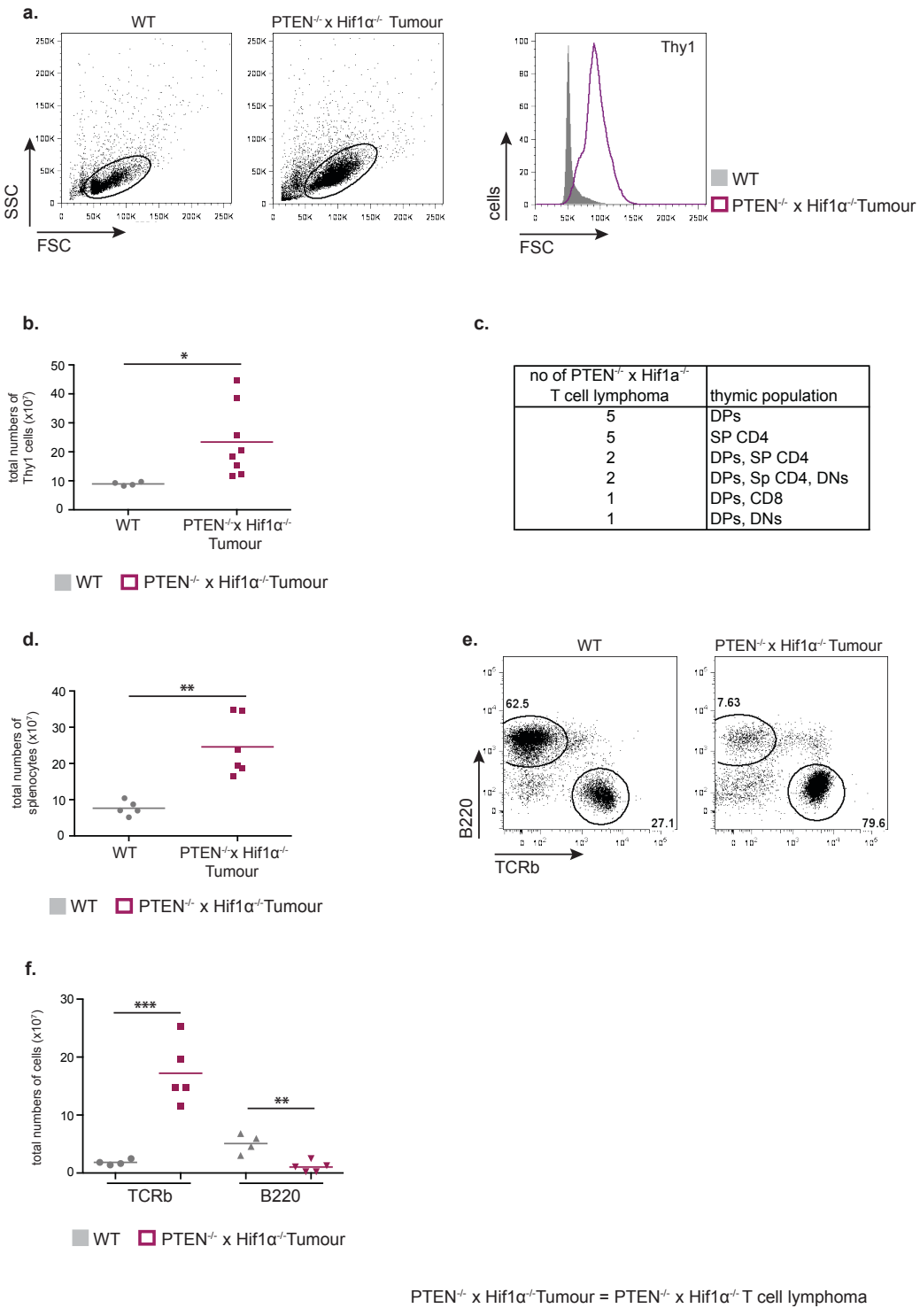

no of PTEN$^{-/-}$ x Hif1a$^{-/-}$ T cell lymphoma	thymic population
5	DPs
5	SP CD4
2	DPs, SP CD4
2	DPs, Sp CD4, DNs
1	DPs, CD8
1	DPs, DNs

PTEN$^{-/-}$ x Hif1α$^{-/-}$Tumour = PTEN$^{-/-}$ x Hif1α$^{-/-}$ T cell lymphoma

Figure 6-5 **The analysis of T cell lymphoma from PTEN$^{fl/fl}$ x Hif1α$^{fl/fl}$ x Lck^{Cre+} mice**.

Ex vivo isolated cells from WT and tumour-bearing PTEN$^{fl/fl}$ x Hif1α$^{fl/fl}$ x Lck^{Cre+} mice were stained with surface markers: thymus-Thy1, CD4 and CD8; spleen-TCRb, B220, CD4 and CD8 and subjected to flow cytometry analysis. **a.** Dot plots graphs and histogram showing the size (FSC) of cells isolated from thymus. **b.** Total number of Thy1 positive cells isolated from thymus; * $p<0.05$ calculated by t-test, each dot represent independent biological replicate. **c.** The table showing the flow cytometric analysis of CD4 and CD8 expression on DKO Tumours. **d.** Total number of cells isolated from spleen; ** $p=0.0015$ calculated by t-test, each dot represent independent biological replicate. **e.** Dot plots showing expression of

TCRb (T cells) and B220 (B cells) in spleen. **f.** Total number of TCRb+ and B220+ cells isolated from spleen; *** p=0.0008 (TCRB+) and ** p=0.0023 (B220+) calculated by t-test, each dot represent independent biological replicate. Dot plots and histograms are shown as representative of at least 4 biological replicates from at least 4 independent experiments. **b. d.** and **f.** graphs are shown as mean from 4 WT and 5 DKO biological replicates from 4 independent experiments.

6.2.3 PTEN$^{-/-}$ x Hif1α$^{-/-}$ T cell leukaemia/lymphoma increased glucose and glutamine uptake compared to WT thymocytes

The increase in cell size of PTEN$^{-/-}$ x Hif1α$^{-/-}$ T cell lymphoma/leukaemia cells could indicate that these cells were more metabolically active than quiescent thymocytes and, in this sense, were similar to PTEN$^{-/-}$ T cell lymphoma/leukaemia cells that expressed Hif1α. We therefore first monitored the cellular uptake of ^{3}[H]- 2-DG to assess glucose transport in primary *ex vivo* isolated tumour cells from the PTEN$^{fl/fl}$ x Hif1α$^{fl/fl}$ x Lck^{Cre+} mice. As controls we monitored the glucose transport capacity of quiescent WT thymocytes and metabolically active IL-2 maintained CTLs. The data in Fig.6-6a shows that *ex vivo* WT thymocytes had very low, approximately 20-fold decreased rates of glucose uptake compared to CTLs. In contrast, T leukemic cells from the PTEN$^{fl/fl}$ x Hif1α$^{fl/fl}$ x Lck^{Cre+} mice had 10-fold higher rates of glucose uptake compared to WT thymocytes (Fig. 6-6a). The rates of glucose uptake by the PTEN$^{-/-}$ x Hif1α$^{-/-}$ T cell lymphoma were thus 2-fold lower than in CTLs. We were not able to directly compare the ability of tumours isolated from PTEN$^{fl/fl}$ x Lck^{Cre+} and PTEN$^{fl/fl}$ x Hif1α$^{fl/fl}$ x Lck^{Cre+} mice to take up radiolabeled glucose, as the tumour development in these mice could not be predicted and synchronised. Therefore, we used the uptake of glucose by CTLs as a way to standardise and compare the glucose uptake capacity of each tumour indirectly. In this respect, we showed that both PTEN$^{-/-}$ T cell lymphoma/leukaemia cells and PTEN$^{-/-}$ x Hif1α$^{-/-}$ T cell

lymphoma/leukaemia cells were 2 times less efficient than CTLs in glucose uptake. We concluded, therefore, that PTEN$^{-/-}$ x Hif1α$^{-/-}$ T cell lymphoma/leukaemia cells had similar capacity to take up exogenous glucose compared to PTEN$^{-/-}$ T cell lymphoma/leukaemia cells.

An important amino acid for fuelling cell growth is glutamine. We thus examined the capacity of WT and PTEN$^{-/-}$ x Hif1α$^{-/-}$ T cell lymphoma/leukaemia cells to transport ^{3}[H]-Glutamine. We also monitored the ability to take up glutamine by CTLs. Figure 6-6b shows that WT thymocytes had low rate of glutamine uptake and on average it was reduced by 20-fold. However, tumours isolated from PTEN$^{fl/fl}$ x Hif1α$^{fl/fl}$ x Lck^{Cre+} had increased rates of glutamine uptake and were comparable to CTLs. We showed that PTEN$^{-/-}$ T cell lymphoma/leukaemia cells were approximately two times less efficient in uptake of glutamine than CTLs. Therefore, it is likely that the cells derived from tumours developed in PTEN$^{fl/fl}$ x Hif1α$^{fl/fl}$ x Lck^{Cre+} mice were more efficient at taking up glutamine than those derived from PTEN$^{fl/fl}$ x Lck^{Cre+} mice.

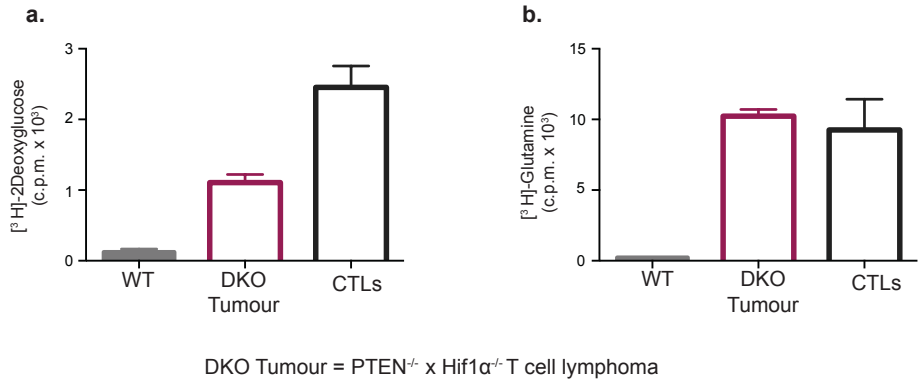

Figure 6-6 **Comparison of glucose and glutamine uptake by WT thymocytes and PTEN$^{-/-}$ x Hif1α$^{-/-}$ T cell lymphoma/leukaemia cells.**

Ex vivo isolated WT thymocytes and PTEN$^{-/-}$ x Hif1α$^{-/-}$ T cell lymphoma/leukaemia cells were assayed for uptake of **a.** ^{3}[H]-2-Deoxyglucose and **b.** ^{3}[H]-Glutamine. Units show counts per minute per 1x10^{6} cells. Error bars show mean SD of 1 biological replicate. All data are representative of 3 biological replicates from 3 independent experiments.

6.2.4 PTEN$^{-/-}$ x Hif1α$^{-/-}$ T cell lymphoma/leukaemia cells increased leucine uptake compared to WT thymocytes

Analysis of PTEN$^{-/-}$ T cell lymphoma/leukaemia cells showed that they had increased expression of subunit of System L amino acid transporter, CD98 and elevated uptake of leucine compared to WT thymocytes. Therefore, we first measured if tumours isolated from PTEN$^{fl/fl}$ x Hif1α$^{fl/fl}$ x Lck^{Cre+} mice expressed CD98 on their surface. Flow cytometric analysis showed that WT thymocytes had basal level of CD98 expression and this level was elevated in PTEN$^{-/-}$ x Hif1α$^{-/-}$ T cell lymphoma/leukaemia cells (Fig. 6-7a). These data implied that expression of System L amino acids transporters were increased in PTEN$^{-/-}$ x Hif1α$^{-/-}$ T cell lymphoma/leukaemia cells. System L amino acid transporters transport leucine inside the cell, therefore, we compared ^{3}[H]-Leucine uptake in PTEN$^{-/-}$ x Hif1α$^{-/-}$ T cell lymphoma, WT thymocytes and CTLs. Figure 6-7b shows that WT thymocytes were 6-fold less efficient in uptake of leucine compared to CTLs. In contrast, tumours

isolated from PTEN$^{fl/fl}$ x Hif1α$^{fl/fl}$ x Lck^{Cre+} mice increased leucine uptake by approximately 10-fold comparing to WT thymocytes. Therefore, these data indicated that primary PTEN$^{-/-}$ x Hif1α$^{-/-}$ T cell lymphoma/leukaemia cells had a higher capacity to take up exogenous leucine than CTLs. As we observed that PTEN$^{-/-}$ T cell lymphoma/leukaemia cells took up leucine at similar rates to CTLs, we propose that tumour samples from PTEN$^{fl/fl}$ x Lck^{Cre+} and PTEN$^{fl/fl}$ x Hif1α$^{fl/fl}$ x Lck^{Cre+} mice might have comparable abilities for transport of exogenous leucine.

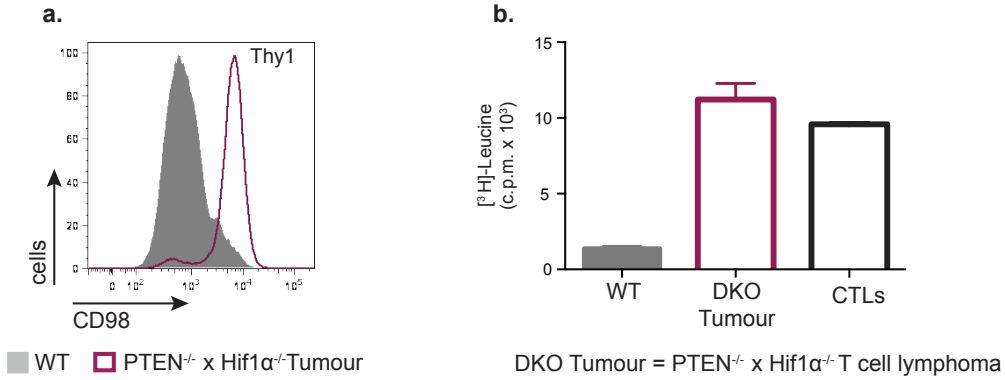

Figure 6-7 **Comparison of CD98 expression and leucine uptake by WT thymocytes and PTEN$^{-/-}$ x Hif1α$^{-/-}$ T cell lymphoma/leukaemia cells.**

a. Flow cytometric analysis presented as histogram showing expression of CD98 marker on surface of Thy1 positive cells from WT mice and PTEN$^{-/-}$ x Hif1α$^{-/-}$ T cell lymphoma. Data are representative of at least 3 biological replicates from at least 3 independent experiments. **b.** The ability of *ex vivo* isolated WT thymocytes and PTEN$^{-/-}$ x Hif1α$^{-/-}$ T cell lymphoma to take up ^{3}[H]-Leucine was tested. Numbers indicate counts per minute per 1x10^{6} cells. The error bars indicate mean SD of 1 biological replicate. The data are representative of 3 biological replicates from 3 independent experiments.

6.2.5 PTEN$^{-/-}$ x Hif1α$^{-/-}$ T cell lymphoma increased transferrin uptake compared to WT thymocytes

We found that PTEN$^{-/-}$ T cell lymphoma/leukaemia cells had increased expression of CD71, and, as a consequence, had increased ability to transport transferrin. Therefore,

using flow cytometry we measured the expression of CD71 on the cell surface of PTEN$^{-/-}$ x Hif1α$^{-/-}$ T cell lymphoma/leukaemia cells. We found that, WT thymocytes had very low expression of CD71, however tumours isolated from PTEN$^{fl/fl}$ x Hif1α$^{fl/fl}$ x Lck^{Cre+} mice had much higher expression of CD71 (Fig.6-8a). We then tested whether the receptor was functional by measuring the cellular uptake of transferrin by PTEN$^{-/-}$ x Hif1α$^{-/-}$ T cell lymphoma/leukaemia cells, WT thymocytes and IL-2 maintained CTLs. We used a FACS based assay to monitor cellular uptake of APC conjugated transferrin. Cells were starved of transferrin for 2 hours after which the uptake of transferrin was performed at 37ºC for 10 minutes. The data in Fig. 6-8b show that CTLs showed the highest uptake of transferrin (black line, **b.**) in contrast to WT thymocytes that did not have the ability to take up any transferrin. However, primary PTEN$^{-/-}$ x Hif1α$^{-/-}$ T cell lymphoma/leukaemia cells showed a marked increase in transferrin uptake that was comparable with the uptake observed in CTLs, implying that tumour cells had great capacity for iron uptake. The uptake of labeled transferrin by the PTEN$^{-/-}$ x Hif1α$^{-/-}$ T cell lymphoma/leukaemia cells was specific as it was blocked by unlabeled transferrin competitor and by incubating the cells treated with labeled transferrin on ice (Fig. 6-8c). These data demonstrated that CD71 expressed on PTEN$^{-/-}$ x Hif1α$^{-/-}$ leukaemia/lymphoma cells was functional and permitted the uptake of transferrin into the cells. Therefore, this data argue that PTEN$^{-/-}$ x Hif1α$^{-/-}$ T cell lymphoma/leukaemia cells had a similar ability to take up transferrin as PTEN$^{-/-}$ T cell lymphoma/leukaemia cells.

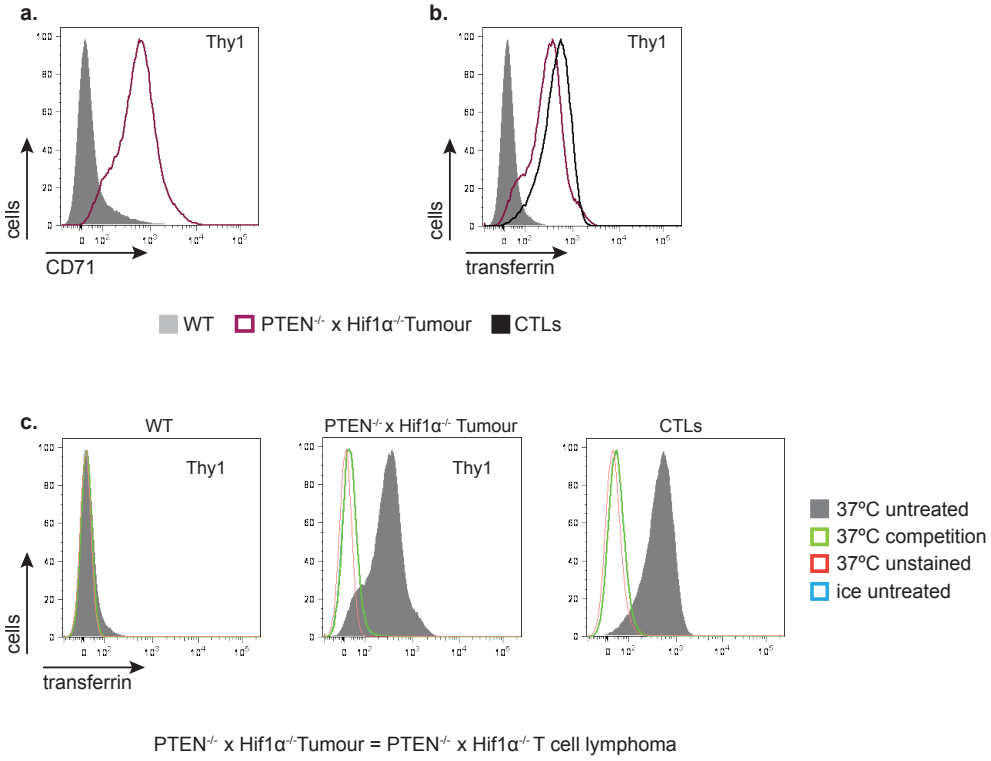

Figure 6-8 **Comparison of CD71 expression and transferrin uptake by WT thymocytes and PTEN$^{-/-}$ x Hif1α$^{-/-}$ T cell lymphoma.**

Flow cytometric analysis presented as histograms showing **a.** expression of CD71 and **b.** transferrin uptake of WT thymocytes, PTEN$^{-/-}$ x Hif1α$^{-/-}$ T cell lymphoma and CTLs (black line in **b**). **c.** Untreated cells were assayed for the uptake of transferrin at 37ºC. Flow cytometric analysis presented as histograms showing transferrin uptake for untreated cells kept in 37ºC (solid grey) or cells kept in 37ºC incubated together with holo-transferrin to block transferrin uptake (green), or kept in 37ºC where no labeled transferrin was added (orange) or kept on ice to block the transport (blue). Expression of CD71 and transferrin uptake was measured on Thy1 positive cells and CTLs. Data are representative of 3 biological replicates from 3 independent experiments.

The comparative analysis of primary tumours isolated from either PTEN$^{fl/fl}$ x Hif1α$^{fl/fl}$ x Lck^{Cre+} or PTEN$^{fl/fl}$ x Lck^{Cre+} mice to take up nutrients normalized to CTLs included in the previous paragraphs implied that PTEN$^{-/-}$ x Hif1α$^{-/-}$ leukaemia/lymphoma cells had similar abilities to take up glucose, leucine and transferrin but were better at taking up glutamine than PTEN$^{-/-}$ leukaemia/lymphoma cells. To further compare the metabolism of these cells, the uptake of nutrients was

normalized to WT thymocytes (Fig. 6-9). We observed that while PTEN$^{-/-}$ x Hif1α$^{-/-}$ leukaemia/lymphoma cells performed similar at taking up glucose, glutamine and transferrin, they were better at taking up leucine compared to PTEN$^{-/-}$ leukaemia/lymphoma cells. However, we also observed that there were big variabilities within the tested genotype for the uptakes (Fig.6-9). Due to this spread it is therefore difficult to judge whether tumours isolated from PTEN$^{fl/fl}$ x Hif1α$^{fl/fl}$ x Lck^{Cre+} mice could perform differently that tumours isolated from PTEN$^{fl/fl}$ x Lck^{Cre+} mice.

DKO	**size (averaged)**	**glucose uptake**	**glutamine uptake**	**leucine uptake**	**transferrin uptake**
fold change (normalised to WT)	1.62	6.7 - 16.8	8.4 - 44.6	19.9 - 30.8	2.9 - 23.9
KO	**size (averaged)**	**glucose uptake**	**glutamine uptake**	**leucine uptake**	**transferrin uptake**
fold change (normalised to WT)	1.67	7.2 - 15.1	6.6 - 70.6	8.1 - 10.5	4.2 - 9.3

DKO = PTEN$^{-/-}$ x Hif1α T cell lymphoma/leukaemia

KO = PTEN$^{-/-}$ T cell lymphoma/leukaemia

Figure 6-9 **The comparative analysis of the nutrient uptake by PTEN$^{-/-}$ x Hif1α$^{-/-}$ leukaemia/lymphoma cells and PTEN$^{-/-}$ leukaemia/lymphoma cells.**

The fold change of the nutrient uptake for PTEN$^{-/-}$ x Hif1α$^{-/-}$ leukaemia/lymphoma and PTEN$^{-/-}$ leukaemia/lymphoma cells normalised to WT thymocytes. The analysis was performed for 3 biological replicates from 3 independent experiments.

6.3 Discussion

In the previous chapter we established that mTORc1 controlled glucose uptake and expression of Hif1α in $PTEN^{-/-}$ T cell lymphoma/leukaemia cells. Therefore it was possible that mTORc1 via Hif1α expression regulated glucose uptake in $PTEN^{-/-}$ T cell lymphoma/leukaemia cells. Because glucose uptake and glycolysis are crucial for cells to initiate/sustain their metabolism, we hypothesised that the loss of Hif1α might be sufficient to inhibit the development of T cell lymphoma in $PTEN^{fl/fl}$ x $Hif1\alpha^{fl/fl}$ x Lck^{Cre+} mice.

Initially, we wanted to understand if Hif1α loss could adversely impact on T cell development in the thymus and T cell maintenance in secondary lymphoid organs. In chapter 5 we suggested that Hif1α expression was induced by secondary mutations. Hale *at al*., showed that expression of Hif1α regulated target genes is maintained at baseline level in thymus as a result of physiological adaptation to hypoxia in the thymus (Hale et al. 2002). Therefore, we could not exclude the possibility that Hif1α expression would be important for survival of thymic progenitors. However, analysis of $Hif1^{-/-}$ x Lck^{Cre+} mice revealed that ablation of Hif1α had no impact on survival of T cells in the thymus or their maintenance in the peripheral organs. The result that Hif1α was not needed for thymus development is reinforced by another study that investigated the role of Hif1α in the development of CD4+ Th17 producing cells and used $Hif1\alpha^{fl/fl}$ x $CD4^{Cre+/-}$ mice (E. V. Dang et al. 2011). The authors showed that thymi and peripheral organs had normal ratios of cells following the CD4 Cre mediated Hif1α deletion. Hif1α has to partner with Hif1β to induce transcription of Hif1α target genes. The loss of Hif1β also had no impact on T cell development in the thymus (Finlay et al. 2012).

However, Hif1α is undoubtedly important for the tumour development in $PTEN^{fl/fl}$ x $Hif1\alpha^{fl/fl}$ mice. Given the link that expression of Hif1α in immune activated T cells is regulated by mTORc1 (Finlay et al. 2012), it is relevant that a study has been published where the regulatory subunit of mTORc1, Raptor, was genetically deleted together with PTEN in mouse haematopoietic cells (HSC) (Kalaitzidis et al. 2012). As a result, the authors found that this double deletion (DKO^{HSC}) led to prolonged survival compared to mice where only PTEN was deleted. Therefore, we speculated that our $PTEN^{fl/fl}$ x $Hif1\alpha^{fl/fl}$ x Lck^{Cre+} mice would either behave exactly like the DKO^{HSC} mice or they would become sick faster, like $PTEN^{fl/fl}$ x Lck^{Cre+} mice or they would not develop tumours. The later two options would suggest that there is no direct regulation between mTORc1 activation and Hif1α expression in $PTEN^{fl/fl}$ x Lck^{Cre+} mice. Interestingly, the survival analysis of mice with double deletion of Raptor and PTEN in HSC showed that these mice had similar survival kinetics to our, $PTEN^{fl/fl}$ x $Hif1\alpha^{fl/fl}$ x Lck^{Cre+} mice. These data argue thus, that deletion of either Hif1α or Raptor in PTEN null T cell progenitors/haematopoietic cells leads to similar result in the overall survival of the mice. These data are consistent with a model that Hif1α mediates the effects of mTORc1 in $PTEN^{-/-}$ T cell lymphoma/leukaemia cells.

How would mTORc1 regulate expression of Hif1α? In peripheral T cells mTORc1 controls expression of Hif1α protein but not mRNA (Finlay et al. 2012) arguing that mTORc1 control translation of Hif1α mRNA (Finlay et al. 2012). In this respect, Tandon *at al*., proposed that S6K is the potential link. In their study, they genetically deleted S6K, the downstream target of mTORc1, in mouse haematopoietic cells (Tandon et al. 2011). Interestingly, their mice with double deletion of PTEN and S6K in HSC had similar survival kinetics as $PTEN^{fl/fl}$ x Lck^{Cre+} mice (our model) and

PTEN$^{fl/fl}$ x Raptor$^{fl/fl}$ x Mx1^{Cre+} mice (Kalaitzidis et al. 2012). Therefore, we propose that there is a strong correlation between all three studies and the pathway mTORc1-S6K-Hif1α is important in lymphomagenesis caused by PTEN deletion.

PTEN$^{fl/fl}$ x Hif1α$^{fl/fl}$ x Lck^{Cre+} mice still developed T cell lymphoma and these cells still had high rates of glucose uptake revealing that there are other transcription factors that can control expression of nutrient receptors. One potential option would be that PTEN$^{-/-}$ x Hif1α$^{-/-}$ T cell lymphoma/leukaemia cells substituted the loss of Hif1α with expression of Hif2α, despite the fact that normal T cells do not express this isoform (Patel & Simon 2008). We did attempt to test for the presence of Hif2α protein in PTEN$^{-/-}$ x Hif1α$^{-/-}$ T cell lymphoma/leukaemia cells. Unfortunately, the Western blot analysis did not give us the unequivocal answer. Therefore, we are planning to perform quantitative PCR to establish if PTEN$^{-/-}$ x Hif1α$^{-/-}$ T cell lymphoma/leukaemia cells have increased *Hif2α* mRNA.

Are there any other potential drivers that can control glucose uptake in PTEN$^{-/-}$ x Hif1α$^{-/-}$ T cell lymphoma/leukaemia cells? In this context, the comparison of the capacity to take up glucose by PTEN$^{-/-}$ x Hif1α$^{-/-}$ T cell lymphoma/leukaemia cells and PTEN$^{-/-}$ T cell lymphoma/leukaemia cells showed that these tumours had similar levels of glucose uptake. In this context, antigen activation of naïve T cells induces expression of c-Myc (Preston et al. 2015) that controls induction of glucose and glutamine metabolism (R. Wang et al. 2011a). It is possible therefore, that c-Myc expression in DKO mice (data not shown) directly contributed to elevated glucose uptake but we have no information about how glycolytic these tumours are. Equally, we also found that PTEN$^{-/-}$ x Hif1α$^{-/-}$ T cell lymphoma/leukaemia cells had higher

capacity to take up glutamine. Exogenous glutamine and its metabolites are also an alternative way of generating energy and supplying substrates for anabolic pathways and glutaminolysis was shown to be a potent stimulator of mTORc1 in activated T cells (Duran et al. 2012). Thus, mTORc1 activity in $PTEN^{-/-}$ x $Hif1\alpha^{-/-}$ T cell lymphoma (preliminary data not shown) can directly regulate their nutrient uptake but independently of Hif1α.

To summarise, we found that Hif1α plays an important role in tumourigenesis, as Hif1α loss enables for the significant delay in tumourigenesis in $PTEN^{fl/fl}$ x $Hif1\alpha^{fl/fl}$ x Lck^{Cre+} mice. We also proposed that Hif1α expression is regulated by mTORc1 in $PTEN^{-/-}$ T cell lymphoma/leukaemia. Despite the role in driving the malignancy, we found that Hif1α is not crucial for normal T cell development.

7 Final discussion

In the present thesis we questioned whether PTEN deletion-induced accumulation of $PI(3,4,5)P_3$ and activation of AKT could initiate the uptake of nutrients in T cells and thus maintain T cell metabolism. An important observation was that $PTEN^{-/-}$ T cell lymphoma/leukaemia cells had high levels of glucose, glutamine, leucine and transferrin uptake, nutrients that are important for rapidly proliferating cells. These cells also had high levels of the activity of the nutrient sensing serine/threonine kinase mTORc1. However, $PTEN^{-/-}$ non-transformed thymocytes did not have constitutively high levels of nutrients uptake nor did they have high mTORc1 activity. Therefore, the increase in nutrient uptake and mTORc1 activity was associated only with transformed phenotype and not with PTEN loss. Moreover, it is known that $PTEN^{-/-}$ T cell lymphoma/leukaemia cells carry secondary mutations that accumulate during the malignant transformation (Guo et al. 2008). Therefore, we propose that secondary mutations are responsible for the increase in nutrient uptake and mTORc1 activity to fuel metabolism in $PTEN^{-/-}$ T cell lymphoma/leukaemia cells.

Signals that may sustain nutrient signalling/mTORc1 activity in $PTEN^{-/-}$ T cell lymphoma/leukaemias

Two possible mechanisms by which an increase in nutrient uptake and mTORc1 activity can be brought about in $PTEN^{-/-}$ T cell lymphoma/leukaemia cells include the activation of Notch1 or the expression of c-Myc. Notch1 is a major driver in T-ALL (Weng et al. 2004; Sulis et al. 2008) and it is an important regulator of nutrient receptors expression in T cell progenitors, e.g. CD98 (Kelly et al. 2007). CD98 is a constant subunit of System L amino acid transporters that mediate the uptake of LNAA, e.g. leucine into cells (Sinclair et al. 2013). Our data showed that only $PTEN^{-}$

$^{-/-}$ T cell lymphoma/leukaemia cells, but not PTEN$^{-/-}$ non-transformed thymocytes, upregulated expression of CD98 and the uptake of leucine. Amino acids, in particular leucine, can act as direct activators of mTORc1 kinase complex (BEUGNET et al. 2003). We also found that PTEN$^{-/-}$ T cell lymphoma/leukaemia cells, but not PTEN$^{-/-}$ non-transformed thymocytes had active mTORc1 and its activity was fully dependent on constant leucine supply. Active Notch1 signalling can induce c-Myc expression in T-ALL (Weng et al. 2006). We confirmed that c-Myc was overexpressed in all tested PTEN$^{-/-}$ T cell lymphoma/leukaemia cells, but not in PTEN$^{-/-}$ non-transformed thymocytes, thus Notch1 could be a potential regulator of c-Myc expression in PTEN$^{-/-}$ T cell lymphoma/leukaemia cells. c-Myc can also regulate glutamine uptake and its metabolism in immune activated T cells (R. Wang et al. 2011a). mTORc1 activity is also dependent on glutamine availability (Nicklin et al. 2009; Duran et al. 2012), thus, c-Myc-induced glutamine uptake could further support mTORc1 activity. Additionally, expression of transferrin receptor in B cell lymphoma remains under the control of c-Myc (O'Donnell et al. 2006). We observed that only PTEN$^{-/-}$ T cell lymphoma/leukaemia cells upregulated transferrin uptake and hence these cells were able to actively proliferate. Therefore, we propose a model where PTEN$^{-/-}$ T cell lymphoma/leukaemia cells that carry active Notch1 mutations can induce expression of CD98, thus, allowing for the transport of leucine inside the cells. Notch1-induced c-Myc expression, promotes transferrin uptake as well as glutamine uptake, and together with leucine induces and sustains mTORc1 activity.

Is Notch1 signalling sufficient to explain nutrient regulation in our T-ALL model? In human T-ALL the common Notch1 mutations are found in PEST/HD domains (Weng et al. 2004). However, genetic screening of PTEN-induced murine T-ALL samples

found no Notch1 mutations in these domains (Hagenbeek et al. 2014; Guo et al. 2008). Our data showed that active Notch1 was expressed in 3 out of 9 of the tested T cell lymphoma/leukaemia cells produced in $PTEN^{fl/fl}$ x Lck^{Cre+} mice. This type of heterogeneity in terms of the involvement of Notch1 has been described previously where PTEN-induced T-ALLs were not uniformly sensitive to Notch inhibition (Palomero et al. 2006; Palomero & Ferrando 2008; Hagenbeek et al. 2014; Medyouf et al. 2010). However, all the T cell lymphoma/leukaemia cells isolated from the $PTEN^{fl/fl}$ x Lck^{Cre+} mice expressed c-Myc. If active Notch1 signalling was only found in a subset of the $PTEN^{-/-}$ T cell lymphoma/leukaemia cells, there must be a second Notch1 independent mechanism by which *c-Myc* message can be induced, e.g. chromosomal translocations and c-Myc protein stabilised, e.g. mutations in FBW7 domain that is responsible for degradation of c-Myc (O'Neil et al. 2007; Welcker, Orian, Grim, et al. 2004a). Furthermore, in the apparent absence of Notch1 signalling, in half of the T-ALL we studied, the increase in leucine transport that we observed must be stimulated through Notch1 independent mechanisms. In this respect, in normal immune activated T cells the key leucine transporter is the System L amino acid transporter subunit Slc7a5, which pairs with CD98 (Sinclair et al. 2013). One possibility is that Slc7a5 also plays an important role in $PTEN^{-/-}$ T cell lymphoma/leukaemia cells. The analysis of the proteome of $PTEN^{-/-}$ T cell lymphoma/leukaemia cells showed they expressed Slc7a5. In this respect, activation of calcineurin, a calcium-regulated phosphatase, positively regulates the expression of Slc7a5 in activated T cells (Sinclair et al. 2013). The proteomic analysis of $PTEN^{-/-}$ T cell lymphoma/leukaemia cells indicated that the expression of a regulatory subunit of calcineurin was increased almost 4-fold in one of the tested $PTEN^{-/-}$ T cell lymphoma/leukaemia cells sample compared to WT. Interestingly, this increase in the

calcineurin regulatory subunit was found in the sample that did not show overexpressed Notch1. Therefore, one speculation is that calcineurin activation might constitute a Notch1 independent way to control leucine uptake in $PTEN^{-/-}$ T cell lymphoma/leukaemia cells. A key follow-up experiment to test this model would be to use the calcineurin inhibitor Cyclosporin A or FK506, to determine if blocking the calcium-calcineurin signalling can block leucine transport in the $PTEN^{-/-}$ T cell lymphoma/leukaemia cells.

One other signal that controls Slc7a5 expression in T cell antigen receptor activated T cells is the activation of the JAK kinases by cytokines such as IL-15 and IL-2 (Preston et al. 2015). T-ALL can express constitutively active IL-7 receptor that signal to activate JAK kinases in a ligand independent fashion (Ribeiro et al. 2013). We have no information if the T-ALLs that develop in $PTEN^{fl/fl}$ x Lck^{Cre+} mice accumulate IL-7 receptor mutations. However, we could use JAK inhibitors to test the involvement of JAK signalling in the control of leucine uptake in the T-ALL.

In the context of PTEN induced T-ALL, inhibitors of Slc7a5 have been shown to efficiently reduce the viability and proliferation of T leukaemic cells (Rosilio et al. 2014). However, our analysis suggested that $PTEN^{-/-}$ T cell lymphoma/leukaemia cells expressed Slc7a5 and Slc7a6 subunits of System L amino acid transporters. As the expression of Slc7a6 may cause resistance to therapies that target Slc7a5, it is important to understand which subunits of System L amino acid transporters are expressed in the malignant cells. Our global analysis of proteins from $PTEN^{-/-}$ T cell lymphoma/leukaemia cells by MS did not give an unequivocal answer as to which System L amino acid transporter, Slc7a5 or Slc7a6, is preferentially expressed, as we

observed substantial variability in their expression within tested samples. Thus, rather than performing analysis of total cellular proteins, future studies may be required to focus the analysis on membrane extracts. One strategy would be to perform CD98 'pull down' experiments, and then subject the samples for MS analysis to look for binding partners of CD98. Once it is established which subunits of System L amino acid transporters are expressed in PTEN$^{-/-}$ T cell lymphoma/leukaemia cells, we can conditionally delete them together with PTEN in early thymic progenitors. This way, we can probe if the expression of Slc7a5 can compensate for the absence of the Slc7a6, and vice-versa and how each subunit can contribute to the progression of the T-ALL.

mTORc1 – a central player in PTEN$^{-/-}$ T cell lymphoma/leukaemia cells metabolism

Studies performed in T-ALL cells suggested that mTOR inhibitors are cytotoxic for these cells (Evangelisti et al. 2011; Yilmaz et al. 2006). We established that mTORc1 was active in PTEN$^{-/-}$ T cell lymphoma/leukaemia cells and that this activation was not a direct response to increased AKT signalling resulted from the loss of PTEN. However, we propose that this mTORc1 activation is central for the regulation of metabolism in PTEN$^{-/-}$ T cell lymphoma/leukaemia cells. We found that mTORc1 activity regulated glucose uptake in PTEN$^{-/-}$ T cell lymphoma/leukaemia cells, a process that is the hallmark of the metabolic switch that takes place in rapidly proliferating cells (Vander Heiden et al. 2009). We also showed that PTEN$^{-/-}$ T cell lymphoma/leukaemia cells and not PTEN$^{-/-}$ non-transformed thymocytes expressed Hif1α. Moreover, the expression of Hif1α in PTEN$^{-/-}$ T cell lymphoma/leukaemia cells was controlled by mTORc1. One of the functions of Hif1α is to regulate the expression of glucose transporters and the rate-limiting enzymes of glycolysis (Finlay

et al. 2009). We, thus, thought it was possible that by deleting Hif1α in PTEN$^{-/-}$ T cell lymphoma/leukaemia cells we would be able to block glucose metabolism in these cells and, thereby, block their malignant transformation. Our data did show that Hif1α could regulate the development of T cell lymphoma/leukaemias in PTEN$^{fl/fl}$ x Lck^{Cre+} mice. Hence PTEN$^{fl/fl}$ x Hif1α$^{fl/fl}$ x Lck^{Cre+} mice were able to survive longer than PTEN$^{fl/fl}$ x Lck^{Cre+} animals. The expression of Hif1α in PTEN$^{-/-}$ T cell lymphoma/leukaemia cells was controlled by mTORc1 and the impact of Hif1α on tumour development in our mouse model phenocopied what happens when Raptor is deleted in PTEN null haematopoietic cells (Kalaitzidis et al. 2012). These data argue that Hif1α mediates the effects of mTORc1 in the development of PTEN$^{-/-}$ T cell lymphoma/leukaemias. However, the loss of mTORC1 activity (Kalaitzidis et al. 2012; Tandon et al. 2011) or the loss of Hif1α, only delays tumour progression in these mouse models of T-ALL. There is, thus, an important question that we would like to address in the future. Why do we observe the lag phase in tumour development of PTEN$^{fl/fl}$ x Hif1α$^{fl/fl}$ x Lck^{Cre+} mice? Most probably the lag phase is a result of PTEN$^{-/-}$ x Hif1α$^{-/-}$ T cell lymphoma/leukaemia cells finding alternative mechanisms to re-adjust their metabolic control. As PTEN is a powerful tumour suppressor, early T cell progenitors with PTEN deletion are destined to acquire tumours. We do know that c-Myc is expressed in PTEN$^{-/-}$ x Hif1α$^{-/-}$ T cell lymphoma/leukaemia cells. c-Myc has been described to induce glucose and glutamine uptake in immune activated CD8+ T cells (R. Wang et al. 2011a). In terms of production of biosynthetic precursors that then are used for macromolecules, it is possible that c-Myc mediated glutamine metabolism can in part compensate for the loss in glucose metabolism caused by deletion of Hif1α. One way to test this model is to measure the ability of PTEN$^{-/-}$ x Hif1α$^{-/-}$ T cell lymphoma/leukaemia cells to perform glycolysis and

glutaminolysis. Alternatively, we can measure the relative contribution of glucose and glutamine derivatives by measuring how much radiolabeled carbon from each of the molecules feeds into the TCA pathway.

However, it is also possible that Hif1α loss in PTEN$^{-/-}$ T cell lymphoma/leukaemia cells leads to the generation of new mutations that contribute to tumour development. Therefore, it would be interesting to perform whole genome sequencing of tumours collected from PTEN$^{fl/fl}$ x Hif1α$^{fl/fl}$ x Lck^{Cre+} mice and compare them to tumours isolated from PTEN$^{fl/fl}$ x Lck^{Cre+} mice. A more affordable alternative to the whole genome sequencing would be to sequence exons that are known to carry mutations. However, there is a potential pitfall of this approach. By screening for already existing mutations, there is the possibility that new mutations that occurred as a result of Hif1α deletion would be overlooked. Therefore, the whole genome sequencing should give as better insight into what signalling pathways are deregulated in PTEN$^{-/-}$ x Hif1α$^{-/-}$ T cell lymphoma/leukaemia cells and, hence, contribute to better understanding of this complex disease.

Taken together, we have shown that activation of the PTEN-PI3K-AKT pathway alone does not lead to a robust activation of mTORc1 and nutrient uptake. We also propose that mTORc1 is a central player in metabolism regulation of PTEN$^{-/-}$ T cell lymphoma/leukaemia cells via regulation of Hif1α expression. Lastly, we have shown that loss of Hif1α prolongs the lifespan of PTEN$^{fl/fl}$ x Hif1α$^{fl/fl}$ x Lck^{Cre+} mice but due to unknown mechanisms these mice still develop tumours.

References

Akers, L.J. et al., 2011. Leukemia Research. *Leukemia Research*, 35(6), pp.814–820.

Ali, I.U., Schriml, L.M. & Dean, M., 1999. Mutational spectra of PTEN/MMAC1 gene: a tumor suppressor with lipid phosphatase activity. *Journal of the National Cancer Institute*, 91(22), pp.1922–1932.

Andersson, E.R., Sandberg, R. & Lendahl, U., 2011. Notch signaling: simplicity in design, versatility in function. *Development (Cambridge, England)*, 138(17), pp.3593–3612.

Armstrong, F. et al., 2009. NOTCH is a key regulator of human T-cell acute leukemia initiating cell activity. *Blood*, 113(8), pp.1730–1740.

Atrih, A. et al., 2010. Stoichiometric quantification of Akt phosphorylation using LC-MS/MS. *Journal of proteome research*, 9(2), pp.743–751.

Avellino, R. et al., 2005. Rapamycin stimulates apoptosis of childhood acute lymphoblastic leukemia cells. *Blood*, 106(4), pp.1400–1406.

Bain, J. et al., 2007. The selectivity of protein kinase inhibitors: a further update. *Biochemical Journal*, 408(3), pp.297–315.

Bar-Peled, L. & Sabatini, D.M., 2012. SnapShot: mTORC1 Signaling at the Lysosomal Surface. *Cell*, 151(6), pp.1390–1390.e1.

Bar-Peled, L. et al., 2012. Ragulator Is a GEFfor the Rag GTPases that Signal Amino Acid Levels to mTORC1. *Cell*, 150(6), pp.1196–1208.

Barata, J.T., 2004. Activation of PI3K Is Indispensable for Interleukin 7-mediated Viability, Proliferation, Glucose Use, and Growth of T Cell Acute Lymphoblastic Leukemia Cells. *Journal of Experimental Medicine*, 200(5), pp.659–669.

BEUGNET, A. et al., 2003. Regulation of targets of mTOR (mammalian target of rapamycin) signalling by intracellular amino acid availability. *Biochemical Journal*, 372(2), pp.555–12.

Bhatia, K. et al., 1993. Point mutations in the c-Myc transactivation domain are common in Burkitt's lymphoma and mouse plasmacytomas. *Nature Genetics*, 5(1), pp.56–61.

Biggs, W.H.3. et al., 1999. Protein kinase B/Akt-mediated phosphorylation promotes nuclear exclusion of the winged helix transcription factor FKHR1. *Proceedings of the National Academy of Sciences of the United States of America*, 96(13), pp.7421–7426.

Boag, J.M. et al., 2006. Altered glucose metabolism in childhood pre-B acute lymphoblastic leukaemia. *Leukemia*, 20(10), pp.1731–1737.

Boehmer, von, H. et al., 1999. Pleiotropic changes controlled by the pre-T-cell

receptor. *Current Opinion in Immunology*, 11(2), pp.135–142.

Bonneau, D. & Longy, M., 2000. Mutations of the human PTEN gene. *Human mutation*, 16(2), pp.109–122.

Bonnet, M. et al., 2011. Posttranscriptional deregulation of MYC via PTEN constitutes a major alternative pathway of MYC activation in T-cell acute lymphoblastic leukemia. *Blood*, 117(24), pp.6650–6659.

Boya, P., Reggiori, F. & Codogno, P., 2013. Emerging regulation and functions of autophagy. *Nature Cell Biology*, 15(7), pp.713–720.

Bressanin, D. et al., 2012. Harnessing the PI3K/Akt/mTOR pathway in T-cell acute lymphoblastic leukemia: Eliminating activity by targeting at different levels. *Oncotarget*, 3(8), pp.811–823–13. Available at: http://www.impactjournals.com/oncotarget/index.php?journal=oncotarget&page=article&op=view&path%5B%5D=579&path%5B%5D=923.

Brown, E.J. et al., 1994. A mammalian protein targeted by G1-arresting rapamycin-receptor complex. *Nature*, 369(6483), pp.756–758.

Brunet, A. et al., 1999. Akt promotes cell survival by phosphorylating and inhibiting a Forkhead transcription factor. *Cell*, 96(6), pp.857–868.

Cai, S.-L. et al., 2006. Activity of TSC2 is inhibited by AKT-mediated phosphorylation and membrane partitioning. *The Journal of cell biology*, 173(2), pp.279–289.

Calleja, V. et al., 2007. Intramolecular and intermolecular interactions of protein kinase B define its activation in vivo. *PLoS biology*, 5(4), p.e95.

Calnan, D.R. & Brunet, A., 2008. The FoxO code. *Oncogene*, 27(16), pp.2276–2288.

Cantley, L.C., 2002. The phosphoinositide 3-kinase pathway. *Science*, 296(5573), pp.1655–1657.

Carlson, C.M. et al., 2006. Kruppel-like factor 2 regulates thymocyte and T-cell migration. *Nature*, 442(7100), pp.299–302.

Carr, E.L. et al., 2010. Glutamine uptake and metabolism are coordinately regulated by ERK/MAPK during T lymphocyte activation. *Journal of immunology (Baltimore, Md. : 1950)*, 185(2), pp.1037–1044.

Chen, C. et al., 2001. Regulation of glut1 mRNA by hypoxia-inducible factor-1. Interaction between H-ras and hypoxia. *The Journal of biological chemistry*, 276(12), pp.9519–9525.

Chen, W.-L. et al., 2014. A distinct glucose metabolism signature of acute myeloid leukemia with prognostic value. *Blood*, 124(10), pp.1645–1654.

Ciofani, M. & Zúñiga-Pflücker, J.C., 2005. Notch promotes survival of pre-T cells at the beta-selection checkpoint by regulating cellular metabolism. *Nature*

Immunology, 6(9), pp.881–888.

Ciofani, M. & Zúñiga-Pflücker, J.C., 2007. The thymus as an inductive site for T lymphopoiesis. *Annual review of cell and developmental biology*, 23, pp.463–493.

Cleverley, S., Henning, S. & Cantrell, D., 1999. Inhibition of Rho at different stages of thymocyte development gives different perspectives on Rho function. *Current biology : CB*, 9(12), pp.657–660.

Cornish, G.H., 2006. Differential regulation of T-cell growth by IL-2 and IL-15. *Blood*, 108(2), pp.600–608.

Costello, P.S., Gallagher, M. & Cantrell, D.A., 2002. Sustained and dynamic inositol lipid metabolism inside and outside the immunological synapse. *Nature Immunology*, 3(11), pp.1082–1089.

Cox, J. & Mann, M., 2008. MaxQuant enables high peptide identification rates, individualized p.p.b.-range mass accuracies and proteome-wide protein quantification. *Nature biotechnology*, 26(12), pp.1367–1372.

Cyster, J.G. & Schwab, S.R., 2012. Sphingosine-1-phosphate and lymphocyte egress from lymphoid organs. *Annual Review of Immunology*, 30, pp.69–94.

Dahia, P.L. et al., 1999. PTEN is inversely correlated with the cell survival factor Akt/PKB and is inactivated via multiple mechanismsin haematological malignancies. *Human molecular genetics*, 8(2), pp.185–193.

Dalla-Favera, R. et al., 1982. Human c-myc onc gene is located on the region of chromosome 8 that is translocated in Burkitt lymphoma cells. *Proceedings of the National Academy of Sciences of the United States of America*, 79(24), pp.7824–7827.

Dang, C.V., Le, A. & Gao, P., 2009. MYC-Induced Cancer Cell Energy Metabolism and Therapeutic Opportunities. *Clinical Cancer Research*, 15(21), pp.6479–6483.

Dang, E.V. et al., 2011. Control of T(H)17/T(reg) balance by hypoxia-inducible factor 1. *Cell*, 146(5), pp.772–784.

Daniels, T.R. et al., 2012. The transferrin receptor and the targeted delivery of therapeutic agents against cancer. *Biochimica et biophysica acta*, 1820(3), pp.291–317.

Das, S., Dixon, J.E. & Cho, W., 2003. Membrane-binding and activation mechanism of PTEN. *Proceedings of the National Academy of Sciences of the United States of America*, 100(13), pp.7491–7496.

Demetriades, C., Doumpas, N. & Teleman, A.A., 2014. Regulation of TORC1 in Response to Amino Acid Starvationvia Lysosomal Recruitment of TSC2. *Cell*, 156(4), pp.786–799.

Di Cristofano, A. et al., 1998. Pten is essential for embryonic development and

tumour suppression. *Nature Genetics*, 19(4), pp.348–355.

Dibble, C.C. & Cantley, L.C., 2015. Regulation of mTORC1 by PI3K signaling. *Trends in cell biology*.

Dibble, C.C. et al., 2012. TBC1D7 is a third subunit of the TSC1-TSC2 complex upstream of mTORC1. *Molecular cell*, 47(4), pp.535–546.

Duran, R.V. et al., 2012. Glutaminolysis activates Rag-mTORC1 signaling. *Molecular cell*, 47(3), pp.349–358.

Eng, C., 2003. PTEN: one gene, many syndromes. *Human mutation*, 22(3), pp.183–198.

Erikson, J. et al., 1986. Deregulation of c-myc by translocation of the alpha-locus of the T-cell receptor in T-cell leukemias. *Science*, 232(4752), pp.884–886.

Evangelisti, C. et al., 2011. Targeted inhibition of mTORC1 and mTORC2 by active-site mTOR inhibitors has cytotoxic effects in T-cell acute lymphoblastic leukemia. *Leukemia*, 25(5), pp.781–791.

Feyerabend, T.B. et al., 2009. Deletion of Notch1 converts pro-T cells to dendritic cells and promotes thymic B cells by cell-extrinsic and cell-intrinsic mechanisms. *Immunity*, 30(1), pp.67–79.

Finlay, D.K., 2012. Regulation of glucose metabolism in T cells: new insight into the role of phosphoinositide 3-kinases. pp.1–7.

Finlay, D.K. et al., 2012. Phosphoinositide (3,4,5)-Triphosphate Binding to Phosphoinositide-Dependent Kinase 1 Regulates a Protein Kinase B/Akt Signaling Threshold That Dictates T-Cell Migration, Not Proliferation. *Journal of Experimental Medicine*, 209(13), pp.2441–2453.

Finlay, D.K. et al., 2009. Phosphoinositide-dependent kinase 1 controls migration and malignant transformation but not cell growth and proliferation in PTEN-null lymphocytes. *Journal of Experimental Medicine*, 206(11), pp.2441–2454.

Fox, C.J., Hammerman, P.S. & Thompson, C.B., 2005. Fuel feeds function: energy metabolism and the T-cell response. *Nature reviews. Immunology*, 5(11), pp.844–852.

Frauwirth, K.A. et al., 2002. The CD28 signaling pathway regulates glucose metabolism. *Immunity*, 16(6), pp.769–777.

Fukuda, R. et al., 2002. Insulin-like growth factor 1 induces hypoxia-inducible factor 1-mediated vascular endothelial growth factor expression, which is dependent on MAP kinase and phosphatidylinositol 3-kinase signaling in colon cancer cells. *The Journal of biological chemistry*, 277(41), pp.38205–38211.

Furnari, F.B., Huang, H.J. & Cavenee, W.K., 1998. The phosphoinositol phosphatase activity of PTEN mediates a serum-sensitive G1 growth arrest in glioma cells. *Cancer Research*, 58(22), pp.5002–5008.

Ganley, I.G. et al., 2009. ULK1.ATG13.FIP200 complex mediates mTOR signaling and is essential for autophagy. *The Journal of biological chemistry*, 284(18), pp.12297–12305.

Gao, X. et al., 2012. Pyruvate kinase M2 regulates gene transcription by acting as a protein kinase. *Molecular cell*, 45(5), pp.598–609.

Garcon, F. et al., 2008. CD28 provides T-cell costimulation and enhances PI3K activity at the immune synapse independently of its capacity to interact with the p85/p110 heterodimer. *Blood*, 111(3), pp.1464–1471.

Georgescu, M.M. et al., 1999. The tumor-suppressor activity of PTEN is regulated by its carboxyl-terminal region. *Proceedings of the National Academy of Sciences of the United States of America*, 96(18), pp.10182–10187.

Germain, R.N., 2002. T-cell development and the CD4-CD8 lineage decision. *Nature reviews. Immunology*, 2(5), pp.309–322.

Gharbi, S.I. et al., 2007. Exploring the specificity of the PI3K family inhibitor LY294002. *Biochemical Journal*, 404(1), pp.15–21.

Giambra, V. et al., 2015. Leukemia stem cells in T-ALL require active Hif1 and Wnt signaling. *Blood*.

González-García, S. et al., 2012. Notch1 and IL-7 Receptor Signalling in Early T-cell Development and Leukaemia. In *Current Topics in Microbiology and Immunology*. Current Topics in Microbiology and Immunology. Berlin, Heidelberg: Springer Berlin Heidelberg, pp. 47–73.

Green, C.J. et al., 2008. Use of Akt inhibitor and a drug-resistant mutant validates a critical role for protein kinase B/Akt in the insulin-dependent regulation of glucose and system A amino acid uptake. *The Journal of biological chemistry*, 283(41), pp.27653–27667.

Gu, H. et al., 1994. Deletion of a DNA polymerase beta gene segment in T cells using cell type-specific gene targeting. *Science*, 265(5168), pp.103–106.

Guertin, D.A. & Sabatini, D.M., 2007. Defining the Role of mTOR in Cancer. *Cancer Cell*, 12(1), pp.9–22.

Guo, W. et al., 2008. Multi-genetic events collaboratively contribute to Pten-null leukaemia stem-cell formation. *Nature*, 453(7194), pp.529–533.

Guo, W. et al., 2011. Suppression of leukemia development caused by PTEN loss. *Proceedings of the National Academy of Sciences of the United States of America*, 108(4), pp.1409–1414.

Gutierrez, A. et al., 2009. High frequency of PTEN, PI3K, and AKT abnormalities in T-cell acute lymphoblastic leukemia. *Blood*, 114(3), pp.647–650.

Hagenbeek, T.J. & Spits, H., 2007. T-cell lymphomas in T-cell-specific Pten-deficient mice originate in the thymus. *Leukemia*, 22(3), pp.608–619.

Hagenbeek, T.J. et al., 2014. Cancer Letters. *Cancer Letters*, 346(2), pp.237–248.

Hagenbeek, T.J. et al., 2004. The loss of PTEN allows TCR alphabeta lineage thymocytes to bypass IL-7 and Pre-TCR-mediated signaling. *The Journal of experimental medicine*, 200(7), pp.883–894.

Hajduch, E., Litherland, G.J. & Hundal, H.S., 2001. Protein kinase B (PKB/Akt)--a key regulator of glucose transport? *FEBS Letters*, 492(3), pp.199–203.

Hale, L.P. et al., 2002. Hypoxia in the thymus: role of oxygen tension in thymocyte survival. *American journal of physiology. Heart and circulatory physiology*, 282(4), pp.H1467–77.

Hanahan, D. & Weinberg, R.A., 2011. Hallmarks of Cancer: The Next Generation. *Cell*, 144(5), pp.646–674.

Harriague, J. & Bismuth, G., 2002. Imaging antigen-induced PI3K activation in T cells. *Nature Immunology*, 3(11), pp.1090–1096.

Hawkins, P.T. et al., 2006. Signalling through Class I PI3Ks in mammalian cells. *Biochemical Society Transactions*, 34(Pt 5), pp.647–662.

Hedrick, S.M. et al., 2012. FOXO transcription factors throughout T cell biology. *Nature reviews. Immunology*, 12(9), pp.649–661.

Herranz, D. et al., 2014. A NOTCH1-driven MYC enhancer promotes T cell development, transformation and acute lymphoblastic leukemia. *Nature Medicine*, 20(10), pp.1130–1137.

Hinton, H.J., Alessi, D.R. & Cantrell, D.A., 2004. The serine kinase phosphoinositide-dependent kinase 1 (PDK1) regulates T cell development. *Nature Immunology*, 5(5), pp.539–545.

Hinton, H.J., Clarke, R.G. & Cantrell, D.A., 2006. Antigen receptor regulation of phosphoinositide-dependent kinase 1 pathways during thymocyte development. *FEBS Letters*, 580(25), pp.5845–5850.

Hosokawa, N. et al., 2009. Nutrient-dependent mTORC1 association with the ULK1-Atg13-FIP200 complex required for autophagy. *Molecular biology of the cell*, 20(7), pp.1981–1991.

Huang, Jianhe et al., 2002. Sequence determinants in hypoxia-inducible factor-1alpha for hydroxylation by the prolyl hydroxylases PHD1, PHD2, and PHD3. *The Journal of biological chemistry*, 277(42), pp.39792–39800.

Huang, Jingxiang & Manning, B.D., 2009. A complex interplay between Akt, TSC2 and the two mTOR complexes. *Biochemical Society Transactions*, 37(1), p.217.

Hudson, C.C. et al., 2002. Regulation of hypoxia-inducible factor 1alpha expression and function by the mammalian target of rapamycin. *Molecular and Cellular Biology*, 22(20), pp.7004–7014.

Hukelmann, J.L. et al., 2015. The cytotoxic T cell proteome and its shaping by the kinase mTOR. *Nature Immunology*.

Hulleman, E. et al., 2009. Inhibition of glycolysis modulates prednisolone resistance in acute lymphoblastic leukemia cells. *Blood*, 113(9), pp.2014–2021.

Huppa, J.B. et al., 2003. Continuous T cell receptor signaling required for synapse maintenance and full effector potential. *Nature Immunology*, 4(8), pp.749–755.

Im, S.-H. & Rao, A., 2004. Activation and deactivation of gene expression by Ca2+/calcineurin-NFAT-mediated signaling. *Molecules and cells*, 18(1), pp.1–9.

Inoki, K. et al., 2002. TSC2 is phosphorylated and inhibited by Akt and suppresses mTOR signalling. *Nature Cell Biology*, 4(9), pp.648–657.

Ivan, M. et al., 2001. HIFalpha targeted for VHL-mediated destruction by proline hydroxylation: implications for O2 sensing. *Science*, 292(5516), pp.464–468.

Iyer, N.V. et al., 1998. Cellular and developmental control of O2 homeostasis by hypoxia-inducible factor 1 alpha. *Genes & development*, 12(2), pp.149–162.

Jiang, B.H. et al., 1996. Dimerization, DNA binding, and transactivation properties of hypoxia-inducible factor 1. *The Journal of biological chemistry*, 271(30), pp.17771–17778.

Josko, J. et al., 2000. Vascular endothelial growth factor (VEGF) and its effect on angiogenesis. *Medical science monitor : international medical journal of experimental and clinical research*, 6(5), pp.1047–1052.

Jotta, P.Y. et al., 2010. Negative prognostic impact of PTEN mutation in pediatric T-cell acute lymphoblastic leukemia. *Leukemia*, 24(1), pp.239–242.

Juntilla, M.M. & Koretzky, G.A., 2008. Critical roles of the PI3K/Akt signaling pathway in T cell development. *Immunology Letters*, 116(2), pp.104–110.

Juntilla, M.M. et al., 2007. Akt1 and Akt2 are required for alphabeta thymocyte survival and differentiation. *Proceedings of the National Academy of Sciences of the United States of America*, 104(29), pp.12105–12110.

Kalaitzidis, D. et al., 2012. mTOR Complex 1 Plays Critical Roles in Hematopoiesis and Pten-Loss-Evoked Leukemogenesis. *Cell Stem Cell*, 11(3), pp.429–439.

Kelly, A.P. et al., 2007. Notch-induced T cell development requires phosphoinositide-dependent kinase 1. *The EMBO Journal*, 26(14), pp.3441–3450.

Kemp, J.D. et al., 1995. Inhibition of lymphoma growth in vivo by combined treatment with hydroxyethyl starch deferoxamine conjugate and IgG monoclonal antibodies against the transferrin receptor. *Cancer Research*, 55(17), pp.3817–3824.

Kenneth, N.S. & Rocha, S., 2008. Regulation of gene expression by hypoxia.

Biochemical Journal, 414(1), pp.19–29.

Kerdiles, Y.M. et al., 2009. Foxo1 links homing and survival of naive T cells by regulating L-selectin, CCR7 and interleukin 7 receptor. *Nature Immunology*, 10(2), pp.176–184.

Kim, E. et al., 2008. Regulation of TORC1 by Rag GTPases in nutrient response. *Nature*, 10(8), pp.935–945.

Kim, J.E. & Chen, J., 2004. regulation of peroxisome proliferator-activated receptor-gamma activity by mammalian target of rapamycin and amino acids in adipogenesis. *Diabetes*, 53(11), pp.2748–2756.

Kim, K. et al., 1998. The trophic action of IL-7 on pro-T cells: inhibition of apoptosis of pro-T1, -T2, and -T3 cells correlates with Bcl-2 and Bax levels and is independent of Fas and p53 pathways. *Journal of immunology (Baltimore, Md. : 1950)*, 160(12), pp.5735–5741.

Kline, D.D. et al., 2002. Defective carotid body function and impaired ventilatory responses to chronic hypoxia in mice partially deficient for hypoxia-inducible factor 1 alpha. *Proceedings of the National Academy of Sciences of the United States of America*, 99(2), pp.821–826.

Korolchuk, V.I. et al., 2011. Lysosomal positioning coordinates cellular nutrient responses. *Nature Cell Biology*, 13(4), pp.453–460.

Kotch, L.E. et al., 1999. Defective vascularization of HIF-1alpha-null embryos is not associated with VEGF deficiency but with mesenchymal cell death. *Developmental biology*, 209(2), pp.254–267.

Lacalle, R.A. et al., 2004. PTEN regulates motility but not directionality during leukocyte chemotaxis. *Journal of Cell Science*, 117(Pt 25), pp.6207–6215.

Laplante, M. & Sabatini, D.M., 2012. mTOR Signaling in Growth Control and Disease. *Cell*, 149(2), pp.274–293.

Laplante, M. & Sabatini, D.M., 2013. Regulation of mTORC1 and its impact on gene expression at a glance. *Journal of Cell Science*, 126(Pt 8), pp.1713–1719.

Lee, J.O. et al., 1999. Crystal structure of the PTEN tumor suppressor: implications for its phosphoinositide phosphatase activity and membrane association. *Cell*, 99(3), pp.323–334.

Lee, K. et al., 2010. Mammalian target of rapamycin protein complex 2 regulates differentiation of Th1 and Th2 cell subsets via distinct signaling pathways. *Immunity*, 32(6), pp.743–753.

Lempiainen, H. & Halazonetis, T.D., 2009. Emerging common themes in regulation of PIKKs and PI3Ks. *The EMBO Journal*, 28(20), pp.3067–3073.

Leslie, N.R. & Downes, C.P., 2004. PTEN function: how normal cells control it and tumour cells lose it. *Biochemical Journal*, 382(Pt 1), pp.1–11.

Leslie, N.R. et al., 2007. PtdIns(3,4,5)P(3)-dependent and -independent roles for PTEN in the control of cell migration. *Current biology : CB*, 17(2), pp.115–125.

Leslie, N.R. et al., 2009. The significance of PTEN's protein phosphatase activity. *Advances in enzyme regulation*, 49(1), pp.190–196.

Li, D.M. & Sun, H., 1997. TEP1, encoded by a candidate tumor suppressor locus, is a novel protein tyrosine phosphatase regulated by transforming growth factor beta. *Cancer Research*, 57(11), pp.2124–2129.

Li, J. et al., 1997. PTEN, a putative protein tyrosine phosphatase gene mutated in human brain, breast, and prostate cancer. *Science*, 275(5308), pp.1943–1947.

Li, Y. et al., 2002. Regulation of TSC2 by 14-3-3 binding. *The Journal of biological chemistry*, 277(47), pp.44593–44596.

Liliental, J. et al., 2000. Genetic deletion of the Pten tumor suppressor gene promotes cell motility by activation of Rac1 and Cdc42 GTPases. *Current biology : CB*, 10(7), pp.401–404.

Liu, Q. et al., 2014. Significance of CD71 expression by flow cytometry in diagnosis of acute leukemia. *Leukemia & lymphoma*, 55(4), pp.892–898.

Liu, X. et al., 2010. Distinct roles for PTEN in prevention of T cell lymphoma and autoimmunity in mice. *Journal of Clinical Investigation*, 120(7), pp.2497–2507.

Lukashev, D. et al., 2006. Cutting edge: hypoxia-inducible factor 1alpha and its activation-inducible short isoform I.1 negatively regulate functions of CD4+ and CD8+ T lymphocytes. *Journal of immunology (Baltimore, Md. : 1950)*, 177(8), pp.4962–4965.

Lukashev, D. et al., 2001. Differential regulation of two alternatively spliced isoforms of hypoxia-inducible factor-1 alpha in activated T lymphocytes. *The Journal of biological chemistry*, 276(52), pp.48754–48763.

Lunt, S.Y. & Vander Heiden, M.G., 2011. Aerobic glycolysis: meeting the metabolic requirements of cell proliferation. *Annual review of cell and developmental biology*, 27, pp.441–464.

Luo, W. et al., 2011. Pyruvate kinase M2 is a PHD3-stimulated coactivator for hypoxia-inducible factor 1. *Cell*, 145(5), pp.732–744.

Ly, T. et al., 2014. A proteomic chronology of gene expression through the cell cycle in human myeloid leukemia cells. *eLife*, 3, p.e01630.

Ma, L. et al., 2005. Phosphorylation and functional inactivation of TSC2 by Erk implications for tuberous sclerosis and cancer pathogenesis. *Cell*, 121(2), pp.179–193.

Ma, X.M. & Blenis, J., 2009. Molecular mechanisms of mTOR-mediated translational control. *Nature Reviews Molecular Cell Biology*, 10(5), pp.307–318.

Macintyre, A.N. et al., 2011. Protein Kinase B Controls Transcriptional Programs that Direct Cytotoxic T Cell Fate but Is Dispensable for T Cell Metabolism. *Immunity*, 34(2), pp.224–236.

Maciver, N.J. et al., 2008. Glucose metabolism in lymphocytes is a regulated process with significant effects on immune cell function and survival. *Journal of leukocyte biology*, 84(4), pp.949–957.

Maehama, T. & Dixon, J.E., 1998. The tumor suppressor, PTEN/MMAC1, dephosphorylates the lipid second messenger, phosphatidylinositol 3,4,5-trisphosphate. *The Journal of biological chemistry*, 273(22), pp.13375–13378.

Mahfouz, R. et al., 2014. Characterising the inhibitory actions of ceramide upon insulin signaling in different skeletal muscle cell models: a mechanistic insight. *PLoS ONE*, 9(7), p.e101865.

Maki, K., Sunaga, S. & Ikuta, K., 1996. The V-J recombination of T cell receptor-gamma genes is blocked in interleukin-7 receptor-deficient mice. *The Journal of experimental medicine*, 184(6), pp.2423–2427.

Makino, Y. et al., 2003. Hypoxia-inducible factor regulates survival of antigen receptor-driven T cells. *Journal of immunology (Baltimore, Md. : 1950)*, 171(12), pp.6534–6540.

Manning, B.D. & Cantley, L.C., 2003. Rheb fills a GAP between TSC and TOR. *Trends in biochemical sciences*, 28(11), pp.573–576.

Manning, B.D. et al., 2002. Identification of the tuberous sclerosis complex-2 tumor suppressor gene product tuberin as a target of the phosphoinositide 3-kinase/akt pathway. *Molecular cell*, 10(1), pp.151–162.

Mariathasan, S., Jones, R.G. & Ohashi, P.S., 1999. Signals involved in thymocyte positive and negative selection. *Seminars in immunology*, 11(4), pp.263–272.

Maxwell, P.H. et al., 1999. The tumour suppressor protein VHL targets hypoxia-inducible factors for oxygen-dependent proteolysis. *Nature*, 399(6733), pp.271–275.

Mazurek, S. et al., 2005. Pyruvate kinase type M2 and its role in tumor growth and spreading. *Seminars in cancer biology*, 15(4), pp.300–308.

McConnachie, G. et al., 2003. Interfacial kinetic analysis of the tumour suppressor phosphatase, PTEN: evidence for activation by anionic phospholipids. *Biochemical Journal*, 371(Pt 3), pp.947–955.

Medyouf, H. et al., 2010. Acute T-cell leukemias remain dependent on Notch signaling despite PTEN and INK4A/ARF loss. *Blood*, 115(6), pp.1175–1184.

Menon, S. et al., 2014. Spatial Control of the TSC Complex Integrates Insulin and Nutrient Regulation of mTORC1 at the Lysosome. *Cell*, 156(4), pp.771–785.

Michie, A.M. & Zúñiga-Pflücker, J.C., 2002. Regulation of thymocyte

differentiation: pre-TCR signals and beta-selection. *Seminars in immunology*, 14(5), pp.311–323.

Mikalsen, S.O. & Kaalhus, O., 1998. Properties of pervanadate and permolybdate. Connexin43, phosphatase inhibition, and thiol reactivity as model systems. *The Journal of biological chemistry*, 273(16), pp.10036–10045.

Mora, A. et al., 2004. PDK1, the master regulator of AGC kinase signal transduction. *Seminars in cell & developmental biology*, 15(2), pp.161–170.

Mullin, M. et al., 2007. The RhoA transcriptional program in pre-T cells. *FEBS Letters*, 581(22), pp.4309–4317.

Myers, M.P. et al., 1997. P-TEN, the tumor suppressor from human chromosome 10q23, is a dual-specificity phosphatase. *Proceedings of the National Academy of Sciences of the United States of America*, 94(17), pp.9052–9057.

Myers, M.P. et al., 1998. The lipid phosphatase activity of PTEN is critical for its tumor supressor function. *Proceedings of the National Academy of Sciences of the United States of America*, 95(23), pp.13513–13518.

Nakaya, M. et al., 2014. Inflammatory T cell responses rely on amino acid transporter ASCT2 facilitation of glutamine uptake and mTORC1 kinase activation. *Immunity*, 40(5), pp.692–705.

Neshat, M.S. et al., 2001. Enhanced sensitivity of PTEN-deficient tumors to inhibition of FRAP/mTOR. *Proceedings of the National Academy of Sciences of the United States of America*, 98(18), pp.10314–10319.

Nicklin, P. et al., 2009. Bidirectional transport of amino acids regulates mTOR and autophagy. *Cell*, 136(3), pp.521–534.

O'Donnell, K.A. et al., 2006. Activation of transferrin receptor 1 by c-Myc enhances cellular proliferation and tumorigenesis. *Molecular and Cellular Biology*, 26(6), pp.2373–2386.

O'Neil, J. et al., 2007. FBW7 mutations in leukemic cells mediate NOTCH pathway activation and resistance to gamma-secretase inhibitors. *The Journal of experimental medicine*, 204(8), pp.1813–1824.

Ogg, S. & Ruvkun, G., 1998. The C. elegans PTEN homolog, DAF-18, acts in the insulin receptor-like metabolic signaling pathway. *Molecular cell*, 2(6), pp.887–893.

Okkenhaug, K., 2013. Signaling by the phosphoinositide 3-kinase family in immune cells. *Annual Review of Immunology*, 31, pp.675–704.

Okkenhaug, K. & Fruman, D.A., 2010. PI3Ks in lymphocyte signaling and development. *Current topics in microbiology and immunology*, 346, pp.57–85.

Okkenhaug, K. & Vanhaesebroeck, B., 2003. PI3K-signalling in B- and T-cells: insights from gene-targeted mice. *Biochemical Society Transactions*, 31(Pt 1),

pp.270–274.

Okkenhaug, K. et al., 2002. Impaired B and T cell antigen receptor signaling in p110delta PI 3-kinase mutant mice. *Science*, 297(5583), pp.1031–1034.

Okkenhaug, K. et al., 2006. The p110delta isoform of phosphoinositide 3-kinase controls clonal expansion and differentiation of Th cells. *Journal of immunology (Baltimore, Md. : 1950)*, 177(8), pp.5122–5128.

Palomero, T. & Ferrando, A., 2008. Oncogenic NOTCH1 Control of MYC and PI3K: Challenges and Opportunities for Anti-NOTCH1 Therapy in T-Cell Acute Lymphoblastic Leukemias and Lymphomas. *Clinical Cancer Research*, 14(17), pp.5314–5317.

Palomero, T. et al., 2006. NOTCH1 directly regulates c-MYC and activates a feed-forward-loop transcriptional network promoting leukemic cell growth. *Proceedings of the National Academy of Sciences of the United States of America*, 103(48), pp.18261–18266.

Papa, A. et al., 2014. Cancer-associated PTEN mutants act in a dominant-negative manner to suppress PTEN protein function. *Cell*, 157(3), pp.595–610.

Patel, S.A. & Simon, M.C., 2008. Biology of hypoxia-inducible factor-2alpha in development and disease. *Cell death and differentiation*, 15(4), pp.628–634.

Patton, D.T. et al., 2011. The PI3K p110delta regulates expression of CD38 on regulatory T cells. *PLoS ONE*, 6(3), p.e17359.

Pearce, L.R., Komander, D. & Alessi, D.R., 2010. The nuts and bolts of AGC protein kinases. *Nature Reviews Molecular Cell Biology*, 11(1), pp.9–22.

Peschon, J.J. et al., 1994. Early lymphocyte expansion is severely impaired in interleukin 7 receptor-deficient mice. *The Journal of experimental medicine*, 180(5), pp.1955–1960.

Podsypanina, K. et al., 2001. An inhibitor of mTOR reduces neoplasia and normalizes p70/S6 kinase activity in Pten+/- mice. *Proceedings of the National Academy of Sciences of the United States of America*, 98(18), pp.10320–10325.

Podsypanina, K. et al., 1999. Mutation of Pten/Mmac1 in mice causes neoplasia in multiple organ systems. *Proceedings of the National Academy of Sciences of the United States of America*, 96(4), pp.1563–1568.

Pollizzi, K.N. et al., 2015. mTORC1 and mTORC2 selectively regulate CD8(+) T cell differentiation. *Journal of Clinical Investigation*, 125(5), pp.2090–2108.

Ponka, P. & Lok, C.N., 1999. The transferrin receptor: role in health and disease. *The international journal of biochemistry & cell biology*, 31(10), pp.1111–1137.

Porstmann, T. et al., 2008. SREBP activity is regulated by mTORC1 and contributes to Akt-dependent cell growth. *Cell Metabolism*, 8(3), pp.224–236.

Preston, G.C. et al., 2015. Single cell tuning of Myc expression by antigen receptor signal strength and interleukin-2 in T lymphocytes. *The EMBO Journal*.

Preston, G.C. et al., 2013. The Impact of KLF2 Modulation on the Transcriptional Program and Function of CD8 T Cells J. Alberola-Ila, ed. *PLoS ONE*, 8(10), pp.e77537–17.

Proud, C.G., 2007. Amino acids and mTOR signalling in anabolic function. *Biochemical Society Transactions*, 35(Pt 5), pp.1187–1190.

Pui, C.-H., Robison, L.L. & Look, A.T., 2008. Acute lymphoblastic leukaemia. *Lancet (London, England)*, 371(9617), pp.1030–1043.

Radtke, F. et al., 1999. Deficient T cell fate specification in mice with an induced inactivation of Notch1. *Immunity*, 10(5), pp.547–558.

Recher, C. et al., 2005. Antileukemic activity of rapamycin in acute myeloid leukemia. *Blood*, 105(6), pp.2527–2534.

Ribeiro, D., Melão, A. & Barata, J.T., 2013. Advances in Biological Regulation. *Advances in Biological Regulation*, 53(2), pp.211–222.

Richardson, D.R. & Ponka, P., 1997. The molecular mechanisms of the metabolism and transport of iron in normal and neoplastic cells. *Biochimica et biophysica acta*, 1331(1), pp.1–40.

Robbins, E. & Pederson, T., 1970. Iron: its intracellular localization and possible role in cell division. *Proceedings of the National Academy of Sciences of the United States of America*, 66(4), pp.1244–1251.

Roderick, J.E. et al., 2014. c-Myc inhibition prevents leukemia initiation in mice and impairs the growth of relapsed and induction failure pediatric T-ALL cells. *Blood*, 123(7), pp.1040–1050.

Rodewald, H.R., Waskow, C. & Haller, C., 2001. Essential requirement for c-kit and common gamma chain in thymocyte development cannot be overruled by enforced expression of Bcl-2. *The Journal of experimental medicine*, 193(12), pp.1431–1437.

Rolf, J. et al., 2013. AMPKalpha1: a glucose sensor that controls CD8 T-cell memory. *European Journal of Immunology*, 43(4), pp.889–896.

Rolf, J. et al., 2010. Phosphoinositide 3-kinase activity in T cells regulates the magnitude of the germinal center reaction. *Journal of immunology (Baltimore, Md. : 1950)*, 185(7), pp.4042–4052.

Rosilio, C. et al., 2014. Accepted Article Preview: Published ahead of advance online publication. pp.1–38.

Ryan, H.E. et al., 2000. Hypoxia-inducible factor-1alpha is a positive factor in solid tumor growth. *Cancer Research*, 60(15), pp.4010–4015.

Ryan, H.E., Lo, J. & Johnson, R.S., 1998. HIF-1 alpha is required for solid tumor formation and embryonic vascularization. *The EMBO Journal*, 17(11), pp.3005–3015.

Salceda, S., Beck, I. & Caro, J., 1996. Absolute requirement of aryl hydrocarbon receptor nuclear translocator protein for gene activation by hypoxia. *Archives of biochemistry and biophysics*, 334(2), pp.389–394.

Sancak, Y. et al., 2007. PRAS40 is an insulin-regulated inhibitor of the mTORC1 protein kinase. *Molecular cell*, 25(6), pp.903–915.

Sancak, Y. et al., 2010. Ragulator-Rag Complex Targets mTORC1 to the Lysosomal Surface and Is Necessaryfor Its Activation by Amino Acids. *Cell*, 141(2), pp.290–303.

Sancak, Y. et al., 2008. The Rag GTPases Bind Raptor and Mediate Amino Acid Signaling to mTORC1. *Science*, 320(5882), pp.1496–1501.

Sang, N. et al., 2002. Carboxyl-terminal transactivation activity of hypoxia-inducible factor 1 alpha is governed by a von Hippel-Lindau protein-independent, hydroxylation-regulated association with p300/CBP. *Molecular and Cellular Biology*, 22(9), pp.2984–2992.

Sarbassov, D.D. et al., 2005. Phosphorylation and regulation of Akt/PKB by the rictor-mTOR complex. *Science*, 307(5712), pp.1098–1101.

Sasaki, T. et al., 2000. Function of PI3Kgamma in thymocyte development, T cell activation, and neutrophil migration. *Science*, 287(5455), pp.1040–1046.

Saucedo, L.J. et al., 2003. Rheb promotes cell growth as a component of the insulin/TOR signalling network. *Nature Cell Biology*, 5(6), pp.566–571.

Saunders, R.N., Metcalfe, M.S. & Nicholson, M.L., 2001. Rapamycin in transplantation: a review of the evidence. *Kidney international*, 59(1), pp.3–16.

Scharenberg, A.M. & Kinet, J.P., 1998. PtdIns-3,4,5-P3: a regulatory nexus between tyrosine kinases and sustained calcium signals. *Cell*, 94(1), pp.5–8.

Schmelzle, T. & Hall, M.N., 2000. TOR, a central controller of cell growth. *Cell*, 103(2), pp.253–262.

Schriever, S.C. et al., 2013. Cellular signaling of amino acids towards mTORC1 activation in impaired human leucine catabolism. *The Journal of nutritional biochemistry*, 24(5), pp.824–831.

Schubbert, S. et al., 2014. Targeting the MYC and PI3K Pathways Eliminates Leukemia-Initiating Cells in T-cell Acute Lymphoblastic Leukemia. *Cancer Research*, 74(23), pp.7048–7059.

Schwarzer, A. et al., 2014. Hyperactivation of mTORC1 and mTORC2 by multipleoncogenic events causes addiction to eIF4E-dependent mRNAtranslation in T-cell leukemia. 0, pp.1–12.

Semenza, G.L., 2001. HIF-1 and mechanisms of hypoxia sensing. *Current opinion in cell biology*, 13(2), pp.167–171.

Semenza, G.L. & Wang, G.L., 1992. A nuclear factor induced by hypoxia via de novo protein synthesis binds to the human erythropoietin gene enhancer at a site required for transcriptional activation. *Molecular and Cellular Biology*, 12(12), pp.5447–5454.

Shah, D.K. & Zuniga-Pflucker, J.C., 2014. An Overview of the Intrathymic Intricacies of T Cell Development. *The Journal of Immunology*, 192(9), pp.4017–4023.

Shen, W.H. et al., 2007. Essential role for nuclear PTEN in maintaining chromosomal integrity. *Cell*, 128(1), pp.157–170.

Shi, L.Z. et al., 2011. HIF1alpha-dependent glycolytic pathway orchestrates a metabolic checkpoint for the differentiation of TH17 and Treg cells. *The Journal of experimental medicine*, 208(7), pp.1367–1376.

Shima, E.A. et al., 1986. Gene encoding the alpha chain of the T-cell receptor is moved immediately downstream of c-myc in a chromosomal 8;14 translocation in a cell line from a human T-cell leukemia. *Proceedings of the National Academy of Sciences of the United States of America*, 83(10), pp.3439–3443.

Shinkai, Y. et al., 1992. RAG-2-deficient mice lack mature lymphocytes owing to inability to initiate V(D)J rearrangement. *Cell*, 68(5), pp.855–867.

Shochat, C. et al., 2011. Gain-of-function mutations in interleukin-7 receptor- (IL7R) in childhood acute lymphoblastic leukemias. *Journal of Experimental Medicine*, 208(5), pp.901–908.

Shrestha, S. et al., 2014. Tsc1 promotes the differentiation of memory CD8+ T cells via orchestrating the transcriptional and metabolic programs. *Proceedings of the National Academy of Sciences of the United States of America*, 111(41), pp.14858–14863.

Silva, A. et al., 2011. IL-7 contributes to the progression of human T-cell acute lymphoblastic leukemias. *Cancer Research*, 71(14), pp.4780–4789.

Silva, A. et al., 2008. PTEN posttranslational inactivation and hyperactivation of the PI3K/Akt pathway sustain primary T cell leukemia viability. *Journal of Clinical Investigation*, 118(11), pp.3762–3774.

Simpson, I.A. et al., 2008. The facilitative glucose transporter GLUT3: 20 years of distinction. *American journal of physiology. Endocrinology and metabolism*, 295(2), pp.E242–53.

Sinclair, L.V. et al., 2013. Control of amino-acid transport by antigen receptors coordinates the metabolic reprogramming essential for T cell differentiation. *Nature Publishing Group*, 14(5), pp.500–508.

Sinclair, L.V. et al., 2008. Phosphatidylinositol-3-OH kinase and nutrient-sensing

mTOR pathways control T lymphocyte trafficking. *Nature Immunology*, 9(5), pp.513–521.

Soond, D.R. et al., 2010. PI3K p110delta regulates T-cell cytokine production during primary and secondary immune responses in mice and humans. *Blood*, 115(11), pp.2203–2213.

Soond, D.R. et al., 2012. Pten Loss in CD4 T Cells Enhances Their Helper Function but Does Not Lead to Autoimmunity or Lymphoma. *The Journal of Immunology*, 188(12), pp.5935–5943.

Sparks, C.A. & Guertin, D.A., 2010. Targeting mTOR: prospects for mTOR complex 2 inhibitors in cancer therapy. *Oncogene*, 29(26), pp.3733–3744.

Stambolic, V. et al., 1998. Negative regulation of PKB/Akt-dependent cell survival by the tumor suppressor PTEN. *Cell*, 95(1), pp.29–39.

Steck, P.A. et al., 1997. Identification of a candidate tumour suppressor gene, MMAC1, at chromosome 10q23.3 that is mutated in multiple advanced cancers. *Nature Genetics*, 15(4), pp.356–362.

Stiles, B. et al., 2004. Liver-specific deletion of negative regulator Pten results in fatty liver and insulin hypersensitivity [corrected]. *Proceedings of the National Academy of Sciences of the United States of America*, 101(7), pp.2082–2087.

Sulis, M.L. et al., 2008. NOTCH1 extracellular juxtamembrane expansion mutations in T-ALL. *Blood*, 112(3), pp.733–740.

Suzuki, A. et al., 1998. High cancer susceptibility and embryonic lethality associated with mutation of the PTEN tumor suppressor gene in mice. *Current Biology*, 8(21), pp.1169–1178.

Suzuki, A. et al., 2008. Portrait of PTEN: Messages from mutant mice. *Cancer Science*, 99(2), pp.209–213.

Suzuki, A. et al., 2001. T cell-specific loss of Pten leads to defects in central and peripheral tolerance. *Immunity*, 14(5), pp.523–534.

Swat, W. et al., 2006. Essential role of PI3Kdelta and PI3Kgamma in thymocyte survival. *Blood*, 107(6), pp.2415–2422.

Tandon, P. et al., 2011. Requirement for ribosomal protein S6 kinase 1 to mediate glycolysis and apoptosis resistance induced by Pten deficiency. *Proceedings of the National Academy of Sciences of the United States of America*, 108(6), pp.2361–2365.

Taub, R. et al., 1982. Translocation of the c-myc gene into the immunoglobulin heavy chain locus in human Burkitt lymphoma and murine plasmacytoma cells. *Proceedings of the National Academy of Sciences of the United States of America*, 79(24), pp.7837–7841.

Teng, D.H. et al., 1997. MMAC1/PTEN mutations in primary tumor specimens and

tumor cell lines. *Cancer Research*, 57(23), pp.5221–5225.

Thoreen, C.C. et al., 2012. A unifying model for mTORC1-mediated regulation of mRNA translation. *Nature*, 485(7396), pp.109–113.

Tibarewal, P. et al., 2012. PTEN protein phosphatase activity correlates with control of gene expression and invasion, a tumor-suppressing phenotype, but not with AKT activity. *Science Signaling*, 5(213), p.ra18.

Tonks, N.K., 2006. Protein tyrosine phosphatases: from genes, to function, to disease. *Nature Reviews Molecular Cell Biology*, 7(11), pp.833–846.

van der Windt, G.J.W. & Pearce, E.L., 2012. Metabolic switching and fuel choice during T-cell differentiation and memory development. *Immunological reviews*, 249(1), pp.27–42.

Vander Heiden, M.G., Cantley, L.C. & Thompson, C.B., 2009. Understanding the Warburg Effect: The Metabolic Requirements of Cell Proliferation. *Science*, 324(5930), pp.1029–1033.

Vanhaesebroeck, B. & Waterfield, M.D., 1999. Signaling by distinct classes of phosphoinositide 3-kinases. *Experimental cell research*, 253(1), pp.239–254.

Vanhaesebroeck, B. et al., 2010. The emerging mechanisms of isoform-specific PI3K signalling. *Nature Reviews Molecular Cell Biology*, 11(5), pp.329–341.

Vazquez, F. & Sellers, W.R., 2000. The PTEN tumor suppressor protein: an antagonist of phosphoinositide 3-kinase signaling. *Biochimica et biophysica acta*, 1470(1), pp.M21–35.

Verrey, F. et al., 2004. CATs and HATs: the SLC7 family of amino acid transporters. *Pflugers Archiv : European journal of physiology*, 447(5), pp.532–542.

Waickman, A.T. & Powell, J.D., 2012. mTOR, metabolism, and the regulation of T-cell differentiation and function. *Immunological reviews*, 249(1), pp.43–58.

Walker, S.M. et al., 2004. The tumour-suppressor function of PTEN requires an N-terminal lipid-binding motif. *Biochemical Journal*, 379(Pt 2), pp.301–307.

Walsh, S.T.R., 2012. Structural insights into the common gamma-chain family of cytokines and receptors from the interleukin-7 pathway. *Immunological reviews*, 250(1), pp.303–316.

Wang, G.L. et al., 1995. Hypoxia-inducible factor 1 is a basic-helix-loop-helix-PAS heterodimer regulated by cellular O2 tension. *Proceedings of the National Academy of Sciences of the United States of America*, 92(12), pp.5510–5514.

Wang, H. et al., 2012. Proline-rich Akt substrate of 40kDa (PRAS40): a novel downstream target of PI3k/Akt signaling pathway. *Cellular Signalling*, 24(1), pp.17–24.

Wang, R. & Green, D.R., 2012. Metabolic checkpoints in activated T cells. *Nature*

Immunology, 13(10), pp.907–915.

Wang, R. et al., 2011a. The Transcription Factor Myc Controls Metabolic Reprogramming upon T Lymphocyte Activation. *Immunity*, 35(6), pp.871–882.

Wang, Y. et al., 2011b. Targeting HIF1alpha eliminates cancer stem cells in hematological malignancies. *Cell Stem Cell*, 8(4), pp.399–411.

Watson, J.V., Chambers, S.H. & Smith, P.J., 1987. A pragmatic approach to the analysis of DNA histograms with a definable G1 peak. *Cytometry*, 8(1), pp.1–8.

Waugh, C. et al., 2009. Phosphoinositide (3,4,5)-Triphosphate Binding to Phosphoinositide-Dependent Kinase 1 Regulates a Protein Kinase B/Akt Signaling Threshold That Dictates T-Cell Migration, Not Proliferation. *Molecular and Cellular Biology*, 29(21), pp.5952–5962.

Webb, L.M.C. et al., 2005. Cutting edge: T cell development requires the combined activities of the p110gamma and p110delta catalytic isoforms of phosphatidylinositol 3-kinase. *Journal of immunology (Baltimore, Md. : 1950)*, 175(5), pp.2783–2787.

Welcker, M., Orian, A., Grim, J.E., et al., 2004a. A nucleolar isoform of the Fbw7 ubiquitin ligase regulates c-Myc and cell size. *Current biology : CB*, 14(20), pp.1852–1857.

Welcker, M., Orian, A., Jin, J., et al., 2004b. The Fbw7 tumor suppressor regulates glycogen synthase kinase 3 phosphorylation-dependent c-Myc protein degradation. *Proceedings of the National Academy of Sciences of the United States of America*, 101(24), pp.9085–9090.

Weng, A.P. et al., 2004. Activating mutations of NOTCH1 in human T cell acute lymphoblastic leukemia. *Science*, 306(5694), pp.269–271.

Weng, A.P. et al., 2006. c-Myc is an important direct target of Notch1 in T-cell acute lymphoblastic leukemia/lymphoma. *Genes & development*, 20(15), pp.2096–2109.

Wenger, R.H., 2002. Cellular adaptation to hypoxia: O2-sensing protein hydroxylases, hypoxia-inducible transcription factors, and O2-regulated gene expression. *FASEB journal : official publication of the Federation of American Societies for Experimental Biology*, 16(10), pp.1151–1162.

White, S. et al., 1990. Combinations of anti-transferrin receptor monoclonal antibodies inhibit human tumor cell growth in vitro and in vivo: evidence for synergistic antiproliferative effects. *Cancer Research*, 50(19), pp.6295–6301.

Wiesener, M.S. et al., 2003. Widespread hypoxia-inducible expression of HIF-2alpha in distinct cell populations of different organs. *FASEB journal : official publication of the Federation of American Societies for Experimental Biology*, 17(2), pp.271–273.

Wijesekara, N. et al., 2005. Muscle-specific Pten deletion protects against insulin

resistance and diabetes. *Molecular and Cellular Biology*, 25(3), pp.1135–1145.

Wilson, J.E., 2003. Isozymes of mammalian hexokinase: structure, subcellular localization and metabolic function. *The Journal of experimental biology*, 206(Pt 12), pp.2049–2057.

Winslow, M.M., Neilson, J.R. & Crabtree, G.R., 2003. Calcium signalling in lymphocytes. *Current Opinion in Immunology*, 15(3), pp.299–307.

Wise, D.R. & Thompson, C.B., 2010. Glutamine addiction: a new therapeutic target in cancer. *Trends in biochemical sciences*, 35(8), pp.427–433.

Wise, D.R. et al., 2008. Myc regulates a transcriptional program that stimulates mitochondrial glutaminolysis and leads to glutamine addiction. *Proceedings of the National Academy of Sciences of the United States of America*, 105(48), pp.18782–18787.

Wisniewski, J.R. et al., 2014. A "proteomic ruler" for protein copy number and concentration estimation without spike-in standards. *Molecular & cellular proteomics : MCP*, 13(12), pp.3497–3506.

Xue, L. et al., 2008. Normal development is an integral part oftumorigenesis in T cell-specificPTEN-deficient mice. pp.1–6.

Yang, Z. & Klionsky, D.J., 2010. Eaten alive: a history of macroautophagy. *Nature Cell Biology*, 12(9), pp.814–822.

Yecies, J.L. & Manning, B.D., 2011. mTOR links oncogenic signaling to tumor cell metabolism. *Journal of molecular medicine (Berlin, Germany)*, 89(3), pp.221–228.

Yee, W.M. & Worley, P.F., 1997. Rheb interacts with Raf-1 kinase and may function to integrate growth factor- and protein kinase A-dependent signals. *Molecular and Cellular Biology*, 17(2), pp.921–933.

Yilmaz, Ö.H. et al., 2006. Pten dependence distinguishes haematopoietic stem cells from leukaemia-initiating cells. *Nature*, 441(7092), pp.475–482.

Yu, L. et al., 2010. Termination of autophagy and reformation of lysosomes regulated by mTOR. *Nature*, 465(7300), pp.942–946.

Zenatti, P.P. et al., 2011. Oncogenic IL7R gain-of-function mutations in childhood T-cell acute lymphoblastic leukemia. *Nature Genetics*, 43(10), pp.932–939.

Zhang, J et al., 2011. Differential requirements for c-Myc in chronic hematopoietic hyperplasia and acute hematopoietic malignancies in Pten-null mice. *Leukemia*, 25(12), pp.1857–1868.

Zhang, Jinghui et al., 2012. The genetic basis of early T-cell precursor acute lymphoblastic leukaemia. *Nature*, 481(7380), pp.157–163.

Zhang, Jiwang et al., 2006. PTEN maintains haematopoietic stem cells and acts in

lineage choice and leukaemia prevention. *Nature*, 441(7092), pp.518–522.

Zhou, G. et al., 1994. The catalytic role of Cys124 in the dual specificity phosphatase VHR. *The Journal of biological chemistry*, 269(45), pp.28084–28090.

Zoncu, R. et al., 2011. mTORC1 senses lysosomal amino acids through an inside-out mechanism that requires the vacuolar H(+)-ATPase. *Science*, 334(6056), pp.678–683.